A COMPARISON OF THE DESULFURIZATION AND DENITROGENATION ACTIVITIES OF MONOLITH ALUMINA IMPREGNATED WITH COBALT AND MOLYBDENUM AND NALCOMO 474 CATALYST

By

DALIP SINGH SONI

Bachelor of Science
Punjab University
Chandigarh, India
1963

Bachelor of Science in Chemical Engineering
Punjab University
Chandigarh, India
1974

Submitted to the Faculty of the Graduate College
of the Oklahoma State University
in partial fulfillment of the requirements
for the Degree of
MASTER OF SCIENCE
July, 1977

A COMPARISON OF THE DESULFURIZATION AND DENITROGENATION ACTIVITIES OF MONOLITH ALUMINA IMPREGNATED WITH COBALT AND MOLYBDENUM AND NALCOMO 474 CATALYST

Thesis Approved:

Billy L. Haynes
Thesis Adviser

Robert T. Robinson Jr.

Jerald D. Parker

Norman N. Durham
Dean of the Graduate College

PREFACE

The desulfurization and denitrogenation activities of two cobalt molybdenum-alumina catalysts were tested on two coal-derived liquids, a Synthoil liquid (a high-boiling stock), and raw anthracene oil (a low-boiling stock). One of the two catalysts was prepared in the laboratory by impregnating cobalt and molybdenum on a monolith alumina support received from Corning Glass Company. The other catalyst used was Nalcomo 474 (a commercial preparation) received from Nalco Chemical Company. Three reactor experiment runs were conducted with space time, temperature and pressure variations to study the effect of these parameters on sulfur and nitrogen removal. The pressures and temperatures employed were 500, 1000 and 1500 psig; and 650, 700 and 800 F (320, 371 and 426 C) respectively. The three volume hourly space times used were around 0.6 hours, 1.1 hours and 1.6 hours. The nominal hydrogen flow rate was 1500 scf/bbl of oil in all the runs. The activities of the two catalysts, on two feedstocks, were compared on volume, weight and surface area bases.

I am highly grateful to my thesis adviser, Professor B. L. Crynes, for his guidance and help in completion of this study. My special appreciation and thanks are due to him for his inspiration, support and patience during difficult stages of this project. I would, also, like to thank Dr. Steven D. Hottman, R. Sivasubramanian, M. Mustaq Ahmed, and Jan W. Wells for their help in conducting the experiments and

providing useful ideas which greatly helped in the completion of this work. I am also thankful to the undergraduate students who helped me carry out reactor runs and analyze the product samples. Special thanks are due to Professor Z. Al Zhaieb of the Geology Department who spent much of his valuable time in analyzing the catalyst samples for me.

Financial support for this work was gratefully received from the School of Chemical Engineering and the United States Energy Research and Development Administration.

Finally, I thank my parents and other members of my family for their support and encouragement in making all this possible.

TABLE OF CONTENTS

LIST OF TABLES

LIST OF FIGURES

CHAPTER I

INTRODUCTION

For the United States to maintain its strength, economy and leadership of the industrial world, a continuous supply of cheap and abundant energy is essential. Oil and natural gas account for 75% of this country's energy needs. Of this, about 25% is imported. But, dwindling oil and natural gas reserves, high prices of imported oil and the necessity to shed dependence on others for this vital commodity, has made it imperative to look for alternate sources of energy within the country.

The abundance of coal in the United States provides one answer. Coal lost its ground in the face of oil and natural gas because of its not being environmentally clean and convenient fuel. But, coal can substitute for oil and natural gas if it can be liquefied and gasified. One of the problems in making liquid and gaseous fuels from coal is that the coal contains high percentages of sulfur and nitrogen. These appear in the liquids and gases obtained from coal. If these fuels are burned as such, oxides of sulfur and nitrogen would be emitted causing pollution of the atmosphere. Moreover, the sulfur and nitrogen present in coal liquids would poison the catalysts which will be used to treat these liquids for upgrading them to better fuels. Therefore, removal of sulfur and nitrogen from liquids or gases obtained from coal is necessary. This study is concerned with desulfurization and denitrogenation of liquids derived from coal. Therefore, it falls under the

larger purview of coal liquefaction.

The objectives of this study were:

(1) To try to hydroprocess heavier coal liquids.

(2) To study the ability of a novel monolith catalyst to remove sulfur and nitrogen from heavier liquids. This catalyst had a large pore size, small surface area and an entirely different geometric configuration than the reference catalyst (a commercially available catalyst) used in these studies.

(3) To study the activity or effectiveness of the standard or reference catalyst towards these heavier feedstocks and compare it with the activity of the monolith catalyst.

(4) To compare the activities of these two catalysts on a lighter feedstock, raw anthracene oil.

CHAPTER II

LITERATURE REVIEW

Pertinent literature on the following aspects will be reviewed:

(1) Catalysts

(2) Reactor Engineering

(3) Kinetics of hydrodesulfurization and hydrodenitrogenation

(4) Operational parameters

(5) Monolith structures

Material covered in this chapter will form the basis for discussion of the results in Chapter V.

Catalysts

Sulfided $CoO-MoO_3-\gamma Al_2O_3$ catalysts have been used for hydrodesulfurization of petroleum feedstocks for a long time. Since the coal-derived liquids are somewhat analogous to those derived from petroleum, the same type of catalysts are being assessed for removing sulfur and nitrogen from coal liquids.

In the above catalyst, molybdenum is believed to be the active constituent, taking part in the reaction in the following way (23).

$$2\ S^{2-} + 2\ Mo^{4+} + H_2 \longrightarrow 2\ (SH)^- + 2\ Mo^{3+}$$

$$4\ Mo^{3+} + 2\ (SH)^- + R\ S \longrightarrow R + 4\ Mo^{4+} + 3\ S^{2-}$$

The first reaction takes place during sulfiding of the $CoO-MoO_3-\gamma Al_2O_3$ catalyst with a mixture of H_2S/H_2. The organo-sulfur compound (RS) then reacts with the active spieces Mo^{+3} and $(SH)^-$ resulting in desulfurization of RS.

Cobalt is considered to promote the activity of the molybdenum. As to how it does, that is not clear. The concentration of cobalt with respect to molybdenum is seen to have important bearing on catalyst activity. Both of these points will be reviewed here.

Studies (1,3,14,17,23) show that there is an optimum bulk ratio of cobalt to molybdenum at which activity of the catalyst is maximum. However, this optimum ratio has quite a wide range (0.1 - 0.4) and is a function of the specific surface area of the catalyst (2). The proven catalyst used in industry has a bulk Co/Mo ratio of about 0.28. The existence of this ratio would be more clear when the mechanism of cobalt promoting the activity of the molybdenum is discussed later in this chapter. But, a simple explanation can be that at very low values of Co/Mo ratio, cobalt is not sufficient to activate all molybdenum, while at values of Co/Mo ratio higher than optimum, cobalt would block the active sites meant for molybdenum (4).

The rate of reaction catalysed by a solid also depends on the properties of the surface of the solid. Therefore, surface composition of cobalt and molybdenum is more important than the bulk composition. This poses problems in trying to relate composition of the catalyst with its activity. However, based on surface enrichment studies by Van Santen and Boerma (15), Phillips and Fote (2) have derived two models to explain dependence of catalytic activity on the bulk promoter concentration. These are:

A. Surface complex model

$$\Delta k = \gamma_A C_A + \gamma_{AP} C_{AP} - \left[\gamma_A C_A\right]^o,$$

where

Δk = difference in first order reaction rate constant between promoted and unpromoted catalyst

C_A = number of sites of Mo per unit surface area

C_{AP} = number of sites of Mo-Co complex per unit surface area

γ_A = specific rate constant per site for Mo

γ_{AP} = specific rate constant per site for Mo-Co complex

$\left[\gamma_A C_A\right]^o$ = refers to the unpromoted catalyst.

Assumptions made in this model are:

(1) Surface has higher promoter concentration than the bulk.

(2) Two phases exist at the surface for a given bulk composition. One is the promoter-active spieces complex and the second is a phase that either contains no catalyst or no promoter. The relative concentration of these two phases can be determined from the studies of Van Santen and Boerma (15).

(3) Desulfurization activity of the promoter is zero ($\gamma_p=0$) and activity of promoter-active spieces complex is more than the active spieces ($\gamma_{AP}<\gamma_A$).

B. Boundary Model

$$k = \gamma_A C_A + \gamma_G L_{AP}$$

where

k = rate constant

C_A = number of sites of Mo per unit surface area.

C_{AP} = number of sites of Mo-Co complex per unit surface area.

L_{AP} = number of sites on the grain boundary per unit area.

γ_G = specific catalytic rate constant per site at the Mo-Co grain boundary.

L_{AP} can be determined by microscopic examination of the surface.

Assumptions in this model are:

(1) Surface is richer in promoter atoms than the bulk.

(2) Only two phases exist at the surface. One is a compound containing no promoter atoms and the second, a compound containing no atoms of the active species.

(3) The specific catalytic rate constant per site at the promoter active species grain boundary, γ_G, is very high. This means $\gamma_G >> \gamma_A$ and γ_p is again zero.

To what accuracy these models predict the rate constant is not known. But these models do show that the rate constant depends on sum of two terms, one of which decreases as the bulk concentration of the promoter increases. The other term shows a maximum for some ratio of promoter to the active species. Hence, such models suggest why the activity of the catalyst peaks at a particular concentration of the promoter.

Regarding mechanism of the promoting effect of cobalt, three models have been proposed. These are, monolayer model, intercalcation model and synergy model. Of these, the synergy model, proposed by Hagenbach, Courtly, and Delmon (1) is based on their studies of the effect of Co/(Co+Mo) on physical properties such as surface area, density, crystalline parameters, and sulfur content of the catalyst. Addition of very small amounts of cobalt resulted in considerable decrease in the activity but the crystallinity of MoS_2 improved markedly. This showed that there was strong interaction of Co with the MoS_2 lattice. X-ray studies of MoS_2 lattice showed that Co atoms can enter lattice structure of MoS_2. As the cobalt concentration was increased, the authors found that the crystalline parameters of MoS_2 tried to recover to their original values. They hypothesized that as

more Co was added, nucleation of Co as Co_9S_8 was easier. Therefore, the Co dissolved or interacted with MoS_2 got progressively segregated as Co_9S_8. Thus, the maximum activity, they observed at Co/Co+Mo of 0.3-0.4, could not be attributed to changes in the structure of MoS_2 (2). They proposed that there was a synergetic effect between the two phases, MoS_2 and Co_9S_8. This involves transfer of electrons between them. As cobalt is seen to facilitate perfect crystallization of MoS_2, it would be present near the growth defects of MoS_2 crystals. This arrangement between Co and Mo would help the transfer of electrons. But, Furinsky and Amberg (17) do not agree with the above view. They maintain that within a Co/(Co+Mo) ratio of 0.4, there is no evidence of the presence of Co_9S_8. Their X-ray studies showed that only at higher ratio, a second phase becomes detectable and has lattice parameters identical with that of Co_9S_8.

In the monolayer model, Mo is considered to be chemically bonded to the surface of γ-Al_2O_3, and O^{2-} ions are present in the capping layer (3). Addition of CoO results in location of Co^{2+} ions in the solid. These ions are tetrahedrally surrounded. The accompanying O^{2-} ions remain in the capping layer. As Co^{2+} ions go into γ-Al_2O_3, Al^{3+} ions are forced out of the solid and come to the monolayer containing Mo. The presence of Al^{3+} ions enhances stability of the monolayer. On sulfiding, the O^{2-} ions in the capping layer are replaced by S^{2-} ions. On reduction with H_2, these S^{2-} ions are removed and leave behind Mo^{3+} ions. As seen earlier, these ions are supposed to be catalytically active.

A detailed study of the intercalcation model has been done by Voorhoeve and Stuiver (33), Voorhoeve (34), and Farragher and Cosec (35).

During intercalcation, Co^{2+} ions occupy empty spaces in double layers of MoS_2. This would occur only at the edges of the sulfide crystals so that a minimum amount of energy is expended. This intercalcation frees or exposes a greater number of Mo^{3+} ions to the reactants.

Based on the above models the extent to which Co^{2+} ions can get into the γ-Al_2O_3 or intercalcate with MoS_2, can be assessed and the ratio Co/Mo approximately known. Studies (1,3) have shown that the ratio calculated this way corresponds to that used in industry.

Physical Properties of the Catalysts

Specific surface area affects catalyst activity in a direct way. Higher surface area would mean a greater number of active sites and hence higher overall activity of the catalyst provided the sites can be contacted. Other physical properties like, size, shape, pore size, and pore volume influence catalyst activity somewhat indirectly. The size and shape have a bearing on the surface area of the catalyst, the dynamics of the liquid flow through the reactor, and the mass transfer limitations on conversion. Smaller particle size of the catalyst would give better liquid distribution and reduce the effect of mass transfer on conversion. These two points will be discussed in detail later in this chapter. The shape of the particle affects the external surface area of the catalyst. Certain shapes provide more of this area per unit volume than others. But this is not very important or significant because outer area may account for only about ten percent of total area (68). Generally, catalyst particles of 8 - 10 mesh size and spherical in shape are used in industry for hydrodesulfurization and hydrodenitrogenation.

The pore size and pore volume affect catalyst activity by influencing intraparticle diffusion (refer page 16). Higher pore size would enable heavier or larger molecules to reach the active sites. Moreover catalyst deactivation due to pore plugging (refer page 10) would be slower for catalyst of larger pores and pore volume. Mineav, et al. (36) in their studies of three Co-Mo-γAl_2O_3 catalysts, with residual fuel oil from West Siberian crude as the feedstock, observed that the catalyst with larger pores and pore volume had higher activity and stability than the catalyst with smaller pores and pore volume. But increasing pore size to $1000^{o}A$ or so (macropores) can adversely affect catalyst selectivity.

Catalyst Deactivation

Catalysts can deactivate or lose their effectiveness due to the following reasons (41):

(1) Chemisorption of impurities present in reactants, poisoning.

(2) Reactants or products degrading on the catalyst surface, coking.

(3) Deactivation due to ash deposition on the catalyst.

(4) Decrease of active surface, sintering.

Besides these, catalyst may lose its activity because of some mechanical causes like wear, disintegration or loss of mechanical strength. But these problems are not frequent and are usually taken care of during manufacture of the catalyst particles.

Sintering is caused by the exposure of catalyst to excessively high temperatures. At high temperatures, the crystalline structure of the catalyst can change resulting in the decrease of surface area (41).

McIver, et al. (42), show that there is no change in surface area of γ-Al_2O_3 up to 932 F (500 C). But when the temperature is increased from 932 F (500 C) to 1472 F (800 C) surface area (and activity) decreases by 25%. Since such high temperatures are not employed in hydrodesulfurization and hydrodenitrogenation, sintering would normally not occur unless there should be a localized "hot-spot."

Poisoning assumes added importance while treating heavy feedstocks because more organometallic compounds are present in high molecular weight fractions. On hydroprocessing, these metal bearing compounds decompose and metals deposit on the active surface of the catalyst. This is known as demetallization. Deposits of these metals plug the pores of the catalyst and thus reduce the effective diffusitivity of the catalyst particles to the reactants (37). This would reduce the effectiveness factor (refer page 17) and hence the rate of the reaction. Johnson, et al. (43), reported that the second order rate constant for desulfurization of a Venezuelan atm. residuum containing 320 ppm V and 30 ppm Ni reduced from 0.25 to 0.05 compared to reduction from 0.2 to 0.155 in case of a Kuwait atm. residuum containing only 36 ppm V and 15 ppm Ni. The nature of metals present in coal liquids will depend on the type of coal from which liquids are derived. Typically, iron, silicon, aluminum, sodium, potassium would be the main impurities (45). These refer to a liquid obtained from the Synthoil process. However, the presence of these metals instead of Ni and V does not alleviate the problem of catalyst poisoning. Therefore, larger size of the pores and smaller size of the catalyst particles would slow down catalyst deactivation by helping reactants to diffuse into the catalyst particle. However, the desulfurization and demetallization reactions being

parallel and competitive (37), the above parameters will have to be such that the catalyst remains selective to desulfurization.

Fouling or coking in processing of heavy feedstocks is caused by deposition of carbonaceous material on the catalyst. This is a consequence of easily condensed polycyclic compounds, which may be present initially and of secondary reaction products and intermediates (47). The extent of coking depends upon the process conditions; severe process conditions usually produce more coking. But when a certain amount of coke has deposited, further deposition slows down or stops completely. This is an equilibrium stage between the rate of coke formation and coke hydrogenation (46). Coking deactivates the catalyst in the same way as demetallization, i.e., by plugging the pores and covering the active sites.

Ash which is composed of inorganic metallic compounds, also adversely affects catalyst activity by depositing on the catalyst surface. In most cases, the catalyst bed acts as a filter and the ash is retained on and within the catalyst particle.

Reactor Engineering

Trickle bed reactors have been successfully employed in industry for hydrodesulfurization of petroleum feedstocks. In trickle bed reactors, liquid and gas flow co-currently down a fixed bed of catalyst. Advantages of this system over slurry or ebullient bed reactors have been discussed by Satterfield (5).

The basic purpose of a packed bed is to bring the reactants in contact with each other and provide a surface where these can react. Evidently, conversion efficiency, under a given set of conditions,

would be maximum if all the surface offered by the packed bed is utilized by the reactants. This will depend on the way the liquid and gas flow through the reactor. While the gas can easily get distributed within the reactor, the distribution of the liquid can be a problem. The material on this aspect is reviewed below.

Liquid Dynamics

Ross (12) found that the conversion efficiency of a commercial trickle flow reactor was lower than that of pilot plant units operated under identical conditions. Since all other parameters were same, he attributed this to liquid maldistribution in the commercial reactor.

Satterfield and Ozel (13) have observed that inspite of excellent initial liquid distribution, the liquid tries to flow downwards as rivulets. This would leave some of the catalyst uncontacted with the liquid. In the narrow diameter trickle bed reactors, the liquid would also tend to migrate toward the wall (5). This is because the solid catalyst particles mesh with each other better than they would mesh with the walls of the reactor. Thus, resistance to flow along the wall is less than that through the bed. The migration of liquid toward the wall results in by-passing of some of the catalyst.

To account for the above phenomena, a term liquid hold-up has been proposed as a measure of the effectiveness of contacting between the liquid and the solid (5). Liquid hold-up is defined as the volume of the liquid present in the reactor per unit volume of the empty reactor. Ross (12) defined it as the volume of the liquid present in the reactor per unit volume of the catalyst. When he applied this

correction to his results from commercial and pilot plant reactors, the results could be brought in agreement (5).

The liquid present in the reactor consists of two types: 1) that which is held in the pores of the catalyst, and 2) that which is flowing downward outside the catalyst particle. This second type of hold-up called the external or dynamic hold-up is important in the present context. Satterfield and Way (11) have found that the external hold-up, H, can be represented by

$$H = AU_l^{1/3} \mu^{1/4} + B$$

where U_l is superficial velocity and μ is viscosity of the liquid. A and B are constants depending on the characteristics of the particle i.e., its size and shape. Thus, liquid hold-up is a function of the viscosity of the liquid and particle size and shape.

Henry and Gilbert (20) gave the following conversion model based on the postulate that reaction rate is proportional to the liquid hold-up and this hold-up is proportional to $L_V^{1/3}$.

$$\ln \frac{C_{out}}{C_{in}} \propto \frac{k_V h^{1/3}}{(LHSV)^{2/3}}$$

where

C_{in}, C_{out} = initial and final concentrations of the reactants in the feedstock, gm mole/cm^3

k_V = volumetric rate constant, $(sec)^{-1}$

h = height of the packed bed, cms

LHSV = liquid hourly space velocity, $(hour)^{-1}$

L_V = liquid superficial velocity, cms./sec.

They verified this model with two sets of data and found good agreement.

Mears (6) suggested that instead of liquid hold-up, effective catalyst wetting may be a better criteria to assess the effect of these dynamic conditions in the reactor. Satterfield and Ozel (13) have provided visual evidence to show that the catalyst in packed bed is not uniformly wetted. Mears (6) therefore assumes that reaction rate is proportional to the fraction of the catalyst surface that is effectively and freshly wetted. Based on the correlation between wetted area and total area given by Puranic and Vogelpohl (18) and incorporating the effectiveness factor, Mears proposed the following correlation for conversion efficiency.

$$\log \frac{C_{in}}{C_{out}} \propto (h)^{0.32} (LHSV)^{-0.68} (d_p)^{0.18} \nu^{-0.05} \left(\frac{\sigma c}{\sigma}\right)^{0.21} \eta$$

where

C_{in}, C_{out} = initial and final concentrations of the reactant, gram moles/cm^3

h = bed height, cm

LHSV = liquid hourly space velocity

$$\frac{\text{volume of liquid fed to the reactor}}{(\text{volume of the reactor})(\text{hr})}$$

d_p = catalyst particle diameter, cm

ν = kinematic viscosity, cm^2/sec

σ = surface tension, dynes/cm

σc = critical surface tension, dynes/cm

η = effectiveness factor, unitless

Axial Dispersion

Another factor that can be important in the study of flow pattern in the trickle bed reactors is the axial dispersion. Plug flow is the most ideal way in which liquid can flow through the reactor. The definition of plug flow implies that there is no mixing or eddy diffusion in the direction of the flow, i.e., the axial direction and the velocity across the radius is uniform. This would require that residence time for each portion of the liquid be the same and constant (19). But this ideal situation is not generally achieved in practice. Liquid back mixing and eddy diffusion in the axial direction occur and can adversely affect conversion.

Results derived by assuming an ideal plug flow reactor and a completely stirred reactor can give some idea of the magnitude of effect caused by axial dispersion. According to Smith (19), the effect of axial dispersion is more pronounced at high conversions. He has found that for a first order reaction, when $k\theta$ (rate constant times residence time) is four, the conversion in a stirred tank reactor is 80%, while in the plug flow reactor, it is 98%. For higher order reactions this difference would be even larger (19).

The phenomena of axial dispersion has been seen to be more prevalent in shallow reactors. Its effect decreases with increase in bed depth. Mears (8) has given the following correlation for finding the minimum bed height for negligible axial dispersion.

$$h/d_p = \frac{20m}{Pe_L} \ln \frac{C_{in}}{C_{out}}$$

where

h = minimum bed height, cm

d_p = particle diameter, cm

Pe_L = $U_\ell d_p / D_\ell$

U_ℓ = liquid superficial velocity, cm/sec.

D_ℓ = diffusivity of the liquid, cm^2/sec

m = order of reaction, unitless

C_{in}, C_{out} = concentrations of the reactants in the feed and product, gm $mole/cm^3$.

Using the above model, Mears obtained good agreement between experimental and calculated values.

All of the above three models have been recently tested by Montagna, and Shah (21) for their applicability to data obtained on desulfurization of a 36% reduced Kuwait crude and a 53% reduced Kuwait crude. Their conclusion is that all three models, i.e., hold-up, effective wetting, and axial dispersion explain the data equally well. Note that these factors are strongly dependent on catalyst particle size and viscosity of the feedstock. Their results also indicated that beyond the minimum bed depth defined by Mears, these parameters were not important.

Mass Transfer Effects

For the solid catalyst to be effective, the reactants must diffuse through the bulk of the fluid, reach the active sites on the catalyst, and the products of the reaction get transported back into the main body of the fluid. These requirements of hetrogeneous catalysis may impose mass transfer limitations on the kinetics of the reaction.

The study of mass transfer in the above case can be split into two parts. One concerns diffusion through the bulk phase of the fluid up to the external surface of the catalyst particle. This may be called external phase mass transfer. The second concerns the diffusion from the particle surface to the active internal surface of the porous solid. This may be called the internal mass transfer or intraparticle mass transfer.

The external phase mass transfer resistance will depend on the degree of turbulence in the fluid and hence on the type of the fluid and its mass velocity. Using pilot plant trickle bed reactors for hydrodesulfurization of various petroleum fractions, Cecil et al. (22) reported that changing liquid mass velocities from 0.013 to 0.056 $g/(cm)^2(sec)$, did not affect the rate of the reaction. This shows that external phase mass transfer resistance was negligible over the region studied. Studies of Satterfield (5) also support this.

But mass transfer resistance within the catalyst pores can be significant (23). This is accounted for by means of a variable called the "effectiveness factor," η, defined as the ratio of observed rate of reaction to that which would occur if pellet interior were all exposed to reactants at the same concentration and temperature as that existing at the outside of the pellet (24). A lower effectiveness factor signifies higher intraparticle resistance. The effectiveness factor will depend on the type of reactant molecule (reactivity), their diffusivity through the liquid filled pores, pore size, size of the catalyst particle and diffusion length. Adlington and Thompson (25) estimated effectiveness factor of 0.6 for a Mo catalyst of particle size 0.125 inch (0.318 cm) when processing gas oil at 780 F (416 C)

and 1500 psig. Sooter (26) found that decreasing particle size from 0.079 inch (0.2 cm) to 0.0127 inch (0.03 cm) had no significant effect on hydrodesulfurization of raw anthracene oil with Co-Mo-γAl_2O_3 catalyst. This means that effectiveness factor was nearly one. Van Deemter (41) studied desulfurization of gas oil with $CoO-MoO_3-\gamma Al_2O_3$ and observed that the effectiveness factor increased from 0.36 to 0.97 when particle size was reduced from 0.196 inch (0.5 cm) to 0.137 inch (0.348 cm).

Studies on effectiveness factor for hydrodenitrogenation also differ widely. Studies by Satchell (27) on denitrogenation of raw anthracene oil, a coal derived liquid, with Co-Mo-γAl_2O_3 catalyst gave effectiveness factor of one at 650 F (343 C) and of 0.95 at 700 F (371 C). The reactor operating pressure was 1000 psig. Jones and Friedman (32) observed that hydrodenitrogenation of a coal-derived liquid increases four times when catalyst particle size was decreased by a factor of three. The studies were conducted at 770 F (410 C) and 3000 psig. This showed that under these conditions the effectiveness factor was very low. Van Zoonen and Douwes (31) found an effectiveness factor of one for hydrodenitrogenation of a straight run gasoline.

Thus, from these studies one cannot conclude about the expected effectiveness factor and hence intraparticle diffusion. The widely differing results are due to different feedstocks and different conditions of reactor operation.

While dealing with heavier feedstock, the effects of catalyst aging and demetallization reactions on the effectiveness factor also become important. These have been discussed already.

Kinetics of Hydrodesulfurization and Hydrodenitrogenation

Desulfurization: Frye and Mosby (48) studied kinetics of hydrodesulfurization of light catalytic oil feedstocks from petroleum. From gas chromatograph analyses of the oil before and after desulfurization, they observed that the rate of reaction was first order with respect to each of the three compounds they labelled A, B and C. Studies by Hoog (49) and Ohtsuka (50) also show that desulfurization in trickle flow reactors is first order in concentration of each sulfur compound. Schuit and Gates (23) in their review of studies on pure sulfur compounds give similar kinetic behavior. These studies also illustrate that low molecular weight compounds are more easily desulfurized than high molecular weight compounds.

But the study of kinetics of industrial feedstocks gets complicated because the feeds contain a large number of sulfur compounds which have different rates of reaction. A large amount of published work indicates that the rate of hydrodesulfurization declines with increasing boiling range of the feed (14). Works of Beuther and Schmidt (52) and Cecil, et al. (22) suggest that a second order rate expression best describes the desulfurization data for wide boiling range petroleum stocks. Work done at Chevron Research (51) also supports the above contention. Sooter (26) during his studies on desulfurization of raw anthracene oil observed that the reaction rate could be described better by the sum of two first order reactions; one for lower boiling and the other for the higher boiling fractions. He found that this model fitted his data better than a simple overall second order model. Johnson, et al. (43) showed second order reaction for desulfurization of Kuwait atmospheric residua.

However, a true picture is, probably, a multitude of first order reactions of varying rates, with the heaviest (asphaltenes) molecules the least reactive. Therefore, overall rate of reaction will very much depend on composition of feed.

Hydrodenitrogenation: Satchell (27) observed second order reaction during his study on denitrogenation of raw anthracene oil. Another study (54) showed first order rate expression while hydrodenitrogenating a coal-derived liquid. Sivasubramanian (40) in a recent study on raw anthracene oil observed that his results could be best explained by a pseudo first order model which takes into account catalyst wetting effects. The model developed by him was of the following form.

$$\ln \frac{C_{out}}{C_{in}} = k\ (LHSV)^{-x}$$

where

LHSV = liquid hourly space velocity, $(hour)^{-1}$

k = first order reaction constant, $(hour)^{-x}$

x = empirical constant

Reaction rate constants predicted from this model agreed with the observed behavior of the catalysts. Values of x varied from 0.306 to 0.92. Flinn, et al. (53) have shown that denitrogenation was first order reaction for a Kuwait heavy gas oil. Some of the qualitative observations of Flinn, et al. are worth noting. These are:

(1) Reaction proceeds rapidly with low boiling stocks but becomes much slower as boiling range increases.

(2) Denitrogenation of residua is very difficult.

(3) Nitrogen compounds containing aromatic-type hetrocyclic ring are the most difficult to denitrogenate.

(4) As the denitrogenation level increases, rate of removal falls off.

(5) In some cases, at least five hydrogenation and hydrocracking steps are required before nitrogen is finally removed as ammonia.

(6) Side reactions may produce some resonance stabilized structures which may be difficult to hydrogenate and hence difficult to denitrogenate.

Besides the reactivity of sulfur and nitrogen species in the feed, some other factors would influence the order or rate of the reaction. Effect of reactor performance or fluid dynamics and mass transfer limitations have already been reviewed. Other factors of importance can be the presence of hydrogen sulfide and interaction between sulfur and nitrogen compounds in the feed. Hydrogen sulfide inhibits the removal of sulfur while it favors denitrogenation. This is because during desulfurization, H_2S is one of the products of reaction. Schuit and Gates (23) in their review of hydrodesulfurization report Metcalfe's expression to account for the inhibitive effect of H_2S.

$$k_{effective} = k \frac{1}{1+21(P_{H_2S}/P_{total})}$$

where

k = pseudo first order rate constant, $(hour)^{-1}$

$k_{effective}$ = corrected rate constant, $(hour)^{-1}$

P_{H_2S} = partial pressure of H_2S, mm Hg

P_{total} = total system pressure, mm Hg

Cecil, et al. (22) also reported a similar relation.

Gaurdiaan, et al. (55) studied denitrogenation of pyridine with a Co-Mo-γAl_2O_3 catalyst in the presence of hydrogen sulfide and observed that for the same conversion, a temperature of 108 F (60 C) less could

be used when H_2S was present than when H_2S was not present. This is because the hydrogen sulfide has a beneficial effect on the hydrocracking activity of the catalyst.

Satterfield, et al. (56) studied the interaction between hydrodesulfurization of thiophene and hydrodenitrogenation of pyridine. Their findings indicate that the presence of small amounts of pyridine has severe inhibiting effects on the hydrodesulfurization and it changes the order of the reaction. Larger additions of pyridine may not increase these effects further. They also observed that the presence of thiophene inhibited hydrodenitrogenation of pyridine below 325 C but above this temperature it enhanced hydrodenitrogenation.

Operational Parameters

Operational parameters or the conditions under which hydrotreatment of the petroleum feedstocks or coal derived liquids is usually conducted, include the following:

(1) Space time

(2) Temperature

(3) Pressure

(4) Hydrogen flow rate

Space Time: The studies (26,57) done on hydrodesulfurization of raw anthracene oil with Co-Mo-γAl_2O_3 catalyst show that sulfur removal increases with increase in volume hourly space time in the range 0.216 - 1.802 hours. Jones, et al. (69) observed that desulfurization of a coal-derived liquid, from an FMC process, increased when weight hourly space time was increased from 1.3 to 5 hours. However, there is general agreement in literature that kinetics of hydrodesulfurization

of petroleum feedstocks is second order in sulfur concentration (refer page 18). This shows that dependence of sulfur removal on space time reduces in the higher ranges of space time.

In the petroleum industry a wide range of space time is employed for desulfurization. Typical range would be 0.1 to 2.0 hours (24). This is because feedstocks with wide difference in boiling ranges have to be processed. A high boiling fraction would generally contain less reactive species and, therefore, would require higher space times than required by lighter fractions.

Though denitrogenation has also been observed to increase with increase in space time, the literature does not agree on the order of denitrogenation reaction and hence on the effect of space time (refer to page 19). The first order kinetics, observed by Jones and Friedman (54) from their studies on denitrogenation of COED process coal-derived liquid, suggested that the dependence of hydrodenitrogenation on space time remained the same over their range of study, i.e., 0.77 to 3.3 weight hourly space time. Satchell (27) studied hydrodenitrogenation of raw anthracene oil and observed second order kinetics. This showed that though nitrogen removal increased with increase in space time, the effect of space time reduced in higher ranges of space time.

Temperature: Temperature dependence of the rate constant, k, is best described by the Arrhenius law (61).

$$k = k_o e^{-E/RT}$$

where, k_o is a frequency factor and E is the activation energy. However, this is true only for elementary reactions. But, evidentally rate of any typical reaction should increase with increase in

temperature. For hydrodesulfurization of petroleum feedstocks, temperatures of 650 F (343 C) to 800 F (426 C) are employed. The choice of operating temperature will depend on the properties of the feedstock and the severity of treatment required. For hydrodesulfurization of coal-derived liquids, the temperatures being studied are in the range of 600 F (319 C) to 930 F (499 C).

Sooter (26) observed that the desulfurization of raw anthracene oil, with Co-Mo-γAl_2O_3 catalyst and at 1000 psig, increased from 48% to 84% when temperature was increased from 600 F (319 C) to 700 F (371 C). He calculated the activation energy of the high boiling fraction to be 44.65 kcal/g.mole and of low boiling fraction to be 5.4 kcal/g.mole. This shows how much the effect of temperature on the desulfurization of heavy feedstocks will differ from that on the desulfurization of very light feedstocks. The hydrotreating studies carried out at Chevron Research Company (51) show that activation energy, for desulfurization of atmospheric residuum from Arabian heavy crude, is 30 kcal/g.mole. Qader, et al. (60) observed more than 90% removal of sulfur from a coal derived liquid when the reactor operating temperature was 788 F (420 C). Ahmed (28) reported more than 94% removal of sulfur from an FMC oil at reactor conditions of 800 F (426 C), 1500 psig and volume hourly space time of 3.0 hours. Chirakaparambil (58) studied uncatalysed desulfurization of a PAMCO oil. He observed higher sulfur removal at 700 F (371 C) than at 800 F (426 C). He said that at 800 F, cracking instead of desulfurization was more predominant and this concentrated the sulfur in the product oil. This indicates that in certain situations increase in temperature may have more favorable effect on some of the side reactions than on the desired reaction.

Denitrogenation also increases with increase in temperature. Satchell (27) conducted studies on denitrogenation of raw anthracene oil at 1000 psig and observed increase in nitrogen removal from 16.5% to 71% with increase in temperature from 600 F (316 C) to 800 F (426 C). Qader and Hill (60) observed that nitrogen removal from coal tar increased from 32% to 99% with increase in temperature from 662 F (350 C) to 932 F (500 C) at a pressure of 1500 psig. Flinn, et al. (53) while denitrogenating cracked heavy naphtha observed that increasing temperature beyond 700 F (371 C) does not greatly increase denitrogenation rate because of equilibrium limitations.

Pressure: The studies of Sooter (26) and Wan (57) on desulfurization of raw anthracene oil show that increase in sulfur removal was rather sharp with increase in pressure from 500 to 1000 psig. But the pressure increase from 1000 to 1500 psig caused only marginal increase in sulfur removal. Qader and Hill (60) observed that sulfur removal, from a coal tar, increases from 90% to 99% when pressure is increased from 1000 to 3000 psig. Scotti (70) observed 96% sulfur removal from a COED process coal-derived liquid at reactor pressures between 1800 and 2400 psig.

Denitrogenation also increases with increase in pressure. Satchell (27) in his studies on denitrogenation of raw anthracene oil observed increase in nitrogen removal with increase in pressure from 500 to 1500 psig. He reported that if the rate constant is related to pressure by the following equation

$$k \propto P^b$$

then values of b would be 0.76 and 0.84 at temperatures of 650 F

(343 C) and 700 F (371 C) respectively. From the studies of Jones and Friedmann (54) on pressure effect on denitrogenation of COED process coal-derived liquid, Satchell calculated the value of b as 1.1. Qader and Hill (60) reported 30% increase in nitrogen removal from coal tar, with increase in pressure from 1000 to 3000 psig.

Hydrogen Flow Rate: Hydrogen flow rate can affect conversion in two ways. One, it will increase hydrogen partial pressure and thus affect rate of the reaction. Schuit and Gates (23) have reported on the work of Phillipson wherein the rate of reaction has been found to be proportional to the square root of the hydrogen partial pressure. Second, a high hydrogen flow rate will create more turbulence in the reactor and thereby reduce mass transfer resistance which may be important while dealing with heavy liquids having a large viscosity.

Sooter (26) found no significant effect on sulfur removal, from raw anthracene oil, by increasing the hydrogen flow rate from 1500 to 20,000 scf/bbl of oil at reactor operating conditions of 1000 psig, 650 F (343 C) and volume hourly space time of 1.5 hours. Wan (57) in his studies on the same feedstock, also observed no effect on desulfurization when flow rate was increased by tenfold, i.e., from 3980 to 39800 scf/bbl of oil. The reactor operating conditions in this study were 800 F (426 C), 1000 psig and 0.9 hour as volume hourly space time. However, in this study, some effect of increase in hydrogen flow rate on denitrogenation was observed. The nitrogen removal increased from 61.2 to 69.2%. But Satchell (27) in his studies on denitrogenation of the same feedstock observed that variation in hydrogen flow rate from 1500 to 20,000 scf/bbl of oil had no effect on the nitrogen removal at

reactor operating conditions of 700 F (371 C), 1000 psig and volume hourly space time of 1.5 hours.

The above review on reactor operating conditions shows that properties of the feedstock and severity of the treatment required would determine as to which combination of variables would achieve the desired results. Also, most of the studies reviewed indicate that there is no equilibrium limitation to the removal of sulfur or nitrogen from petroleum feedstocks or coal-derived liquids.

Monolith Structures

Monolith supports are cylindrical in shape and have many parallel and longitudinal channels along their length. Figure 1 shows a cross-section of the monolith, from Corning Glass Company, used in this study. Monoliths are being widely used for catalytic conversion of auto-exhaust because they fulfill the requirement of low pressure drop even at very high velocities at which auto exhaust is emitted.

The potential use of monoliths for petroleum industry has not been assessed as yet. Therefore, little is available in the literature from which inferences can be drawn regarding utility of monoliths for this study. However, the geometry of the catalyst offers some advantages for their use in trickle bed reactors. These stem from the fact that 60 to 80 percent of the cross-sectional area of the monolith is open and available for liquid to flow through it. This would give less pressure drop than that encountered in packed beds. Moreover, a stacked bed of monoliths would guide the liquid through regular channels. Therefore, the task of analyzing the flow pattern and its impact

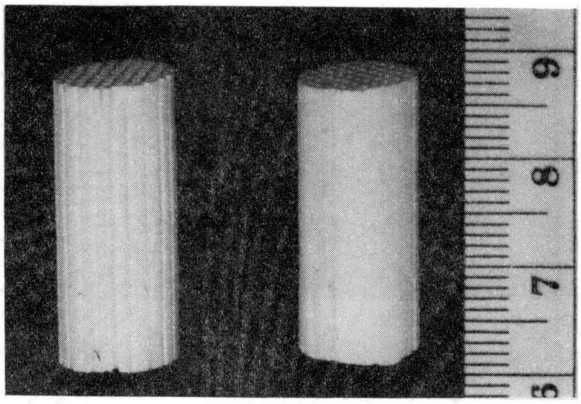

Monolith Alumina Segments

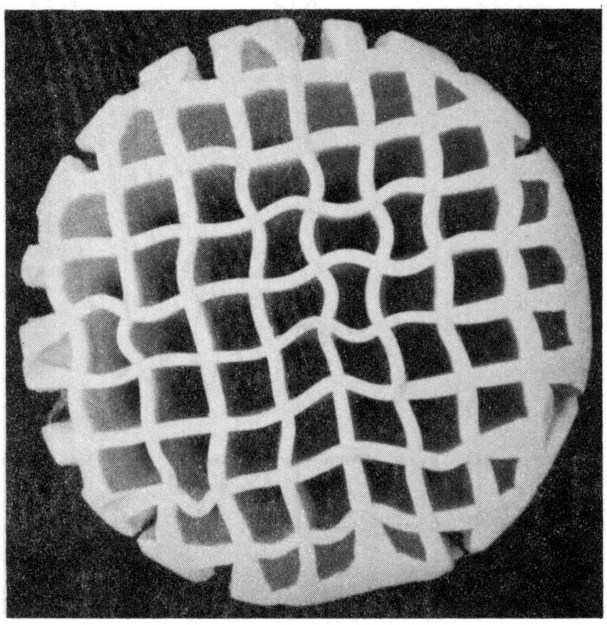

Cross Section of a Monolith Alumina

Figure 1. Monolith Structure

on reaction rate would be much easier in the case of a bed of monoliths than in the case of a randomly packed catalyst bed.

Satterfield and Ozel (39) in a very recent study observed significantly lower pressure drop for two phase flow (water-air system) in monoliths than in conventional packed beds. Some of the other advantages listed are:

(1) High compressive strength of monoliths may permit deep beds to be constructed without the necessity of using intermediate supports and gas-liquid redistributors.

(2) Controlled channeling may provide better gas liquid contacting and better liquid distribution than obtained in conventional trickle bed reactors.

(3) Uniformity of passage ways may minimize axial dispersion.

(4) With liquids containing fine solids such as those derived from liquefaction of coal, bed plugging may be minimized or avoided.

(5) There is no net migration of liquid to the vessel wall and liquid distribution improves with distance.

(6) Wetting of solids may be considerably more effective than that occuring with conventional packing, especially at relatively low liquid flow rates.

(7) Pressure drop limitations in conventional packed beds may not permit reduction of catalyst particle size to increase effectiveness factor. Use of monoliths in such situations can give higher effectiveness factors.

Literature Summary

The following items summarize the literature reviewed for this study.

(1) There is an optimum ratio of Co to Mo at which the activity of the Co-Mo-γAl_2O_3 catalyst is maximum. This ratio depends on the surface area of the catalyst.

However, the mechanism of cobalt promoting the activity of molybdenum is not well understood.

(2) Catalyst deactivation depends on the nature of the feedstock and hydroprocessing conditions. Liquids of high ash content and organometalic compounds would irreversibly deactivate the catalyst.

(3) Maldistribution of the reactant liquid in the trickle bed can affect reactor efficiency. Liquid hold-up and contacting efficiency can predict this effect reasonably well. Correlations of Henry, et al. (2) and Mears (6) take into consideration the above factors.

Problems of liquid distribution may not be as severe in laboratory reactors as in industrial reactors.

(4) Intraparticle mass transfer resistances may be important in desulfurization and denitrogenation. These would depend on the catalyst particle size, pore size, and feedstock properties.

(5) The orders of the desulfurization and denitrogenation reactions depend on the composition of the feedstock. Differences in the spectrum of compounds present in different feedstocks, may change the order of the reaction. However, for desulfurization a second order or a combination of first order reactions generally holds good. Denitrogenation has been observed to be first order or second order. A recent study (40) has even shown fractional order with respect to total nitrogen concentration.

(6) Desulfurization and denitrogenation of residua or heavier feedstocks is more difficult than that of lighter feedstocks.

(7) The presence of H_2S would retard desulfurization, but would help denitrogenation.

(8) The presence of certain basic nitrogen compounds (like pyridine) may inhibit desulfurization.

(9) Desulfurization and denitrogenation generally increased with space time.

(10) Increase in pressure increases sulfur and nitrogen removal but the effect of pressure reduces in higher ranges of operating pressure.

(11) An increase in temperature increases desulfurization. But increase in temperature beyond a certain level may catalyze cracking more than the desired reaction.

(12) Hydrogen flow rate can affect desulfurization and denitrogenation. Flow rate higher than 1500 scf/bbl of oil was not found to increase desulfurization or denitrogenation of raw anthracene oil. But for heavier feedstocks, higher flow rates may be desirable.

(13) A stacked bed of monolith catalyst could provide more ideal flow conditions in the trickle bed reactors than conventional packed bed. However, utility of monoliths for hydroprocessing petroleum feedstocks or coal-derived liquids has not been assessed yet.

CHAPTER III

EXPERIMENTAL SET UP AND PROCEDURE

Schematic diagram of the experimental set up employed in this study is given in Figure 2. This system was designed and constructed much earlier and a number of studies (28,57,58) on hydrodesulfurization and hydrodenitrogenation of coal derived liquids have been successfully carried out using this set up. The list of various equipment and instruments, which constitute the total set up, is given in Table I. The number of items on the list corresponds to the number of the same equipment on the diagram.

A Ruska metering pump, 26, feeds oil at the top of the reactor at the desired rate. Hydrogen gas also enters at the top of the reactor. Both the oil and the hydrogen gas flow down co-currently through the reactor packed with the catalyst. Hydrogen pressure is maintained at the desired level by the backpressure regulator, 24. Hydrogen flow rate is adjusted, as desired, by the micro-valve, 3, and is measured with the help of a bubble flow meter installed at the hydrogen off-gas line. The outlet gas is vented after scrubbing with caustic soda solution to remove H_2S. The oil coming out of the reactor is sampled periodically with the help of two sampling bombs 22 and 23. A trap, 28, is installed in the gas exit line for taking gas samples. This trap is shown in Figure 8. The salient features of the above experimental set up, henceforth called Reactor-System I, are:

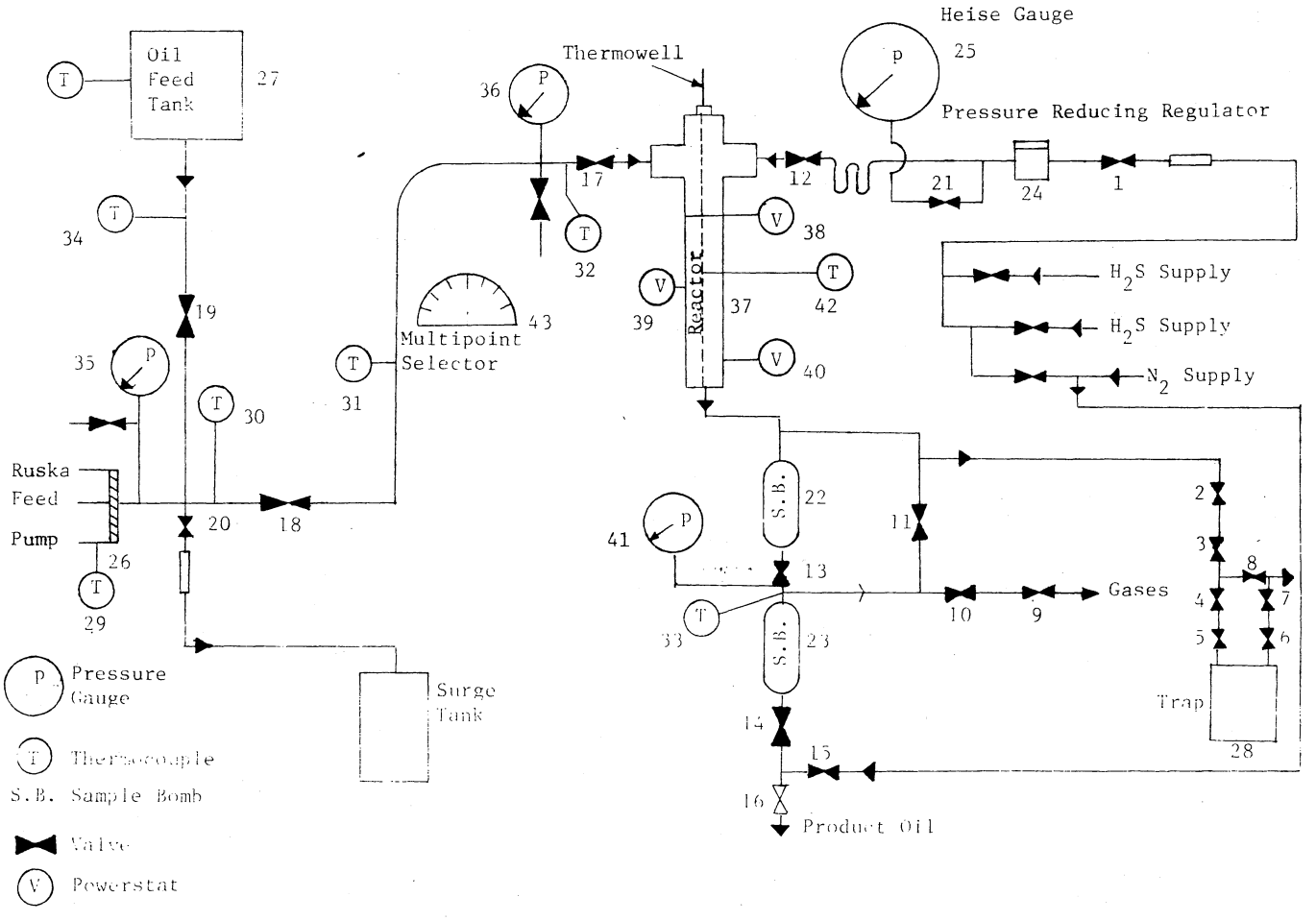

Figure 2. Reactor-System I

TABLE I

EQUIPMENT ITEMS

Tubing	1/4 inch O.D., stainless steel, 316
Valves 1,3,9	1/4 inch stainless steel, micro-metering, 3000 psi, Whitley Model #22S4
Valves 4,5,6,7,8	1/4 inch Parker Hannifin 4Z-V4LK Staninless Steel Valves
Valves 10,11,12,13,14	1/4 inch gate valves, 316 stainless steel, 3000 psi, Whitley Model #IRS4
Valves 2,15,16	1/4 inch gate valves, 316 stainless steel, Autoclave Engineers Model #6V-71U8
Valves 17,18,20	1/4 inch gate valves, 316 stainless steel, Whitley Model #6VS4
Valve 19	1/4 inch gate valve, 316 stainless steel, Autoclave Engineers Model #6V-71U8
Valve 21	1/8 inch needle valve, 11000 psi, Autoclave Engineers, Model #10V-2001
Sample Bombs 22,23	300 c.c., 1800 psig, 304 stainless steel, Matheson Model #6-645-232
Pressure Regulator, 24	Mitey-Mite Model 94
Pressure Gauge, 25	Heise-Bourden tube gauge, 3000 psig
Feed Pump, 26	Ruska Pump Model #2242 BI
Feed Tank, 27	8.5 inch O.D., 7.5 inches high, stainless steel tank.
Thermocouples 29,30,31, 32,33,34	Iron-constantan, 0.04 inch O.D. 304 stainless steel sheath bare sensor tip, 1/2 inch, conax.
Pressure Gauges 35,36,41	Crosby pressure gauge, 3000 psig
Reactor, 37	0.5 inch O.D., 0.035 inch thick, 2 feet long, 316 stainless steel tube
Powerstats, 38,40	Curtin type 316

TABLE I (Continued)

Temperature Programmer, 39	Hewlett-Packard Model 240M-2
Thermocouple, 42	Iron-constantan, 0.04 inch O.D., 304 stainless steel sheath, grounded sensor tip, 1/2 inch

(1) The reactor can be operated isothermally up to temperature of 850 F and pressure of 1500 psig.

(2) The catalyst portion of the reactor can be kept at uniform temperature along its length.

(3) The liquid samples can be drawn without interfering with normal operation of the reactor.

(4) The pump and all the oil lines can be kept heated to facilitate pumping of heavier feedstocks. All the heated lines have thermocouples connected to them and their temperatures can be read with the help of a multipoint selector, 25.

In one of the three runs conducted for this study, another but similar experimental set up, henceforth called Reactor-System II, was employed. This was because a lighter oil (raw anthracene oil) was used in this run and the Reactor-System II was best suited for lighter feedstocks. All the previous studies (26,27,29) on desulfurization and denitrogenation of the raw anthracene oil were conducted on this system. Since this Reactor-System had 36 inches (91.5 cm) long reactor, modifications were done to accommodate 24 inches (61 cm) long reactor which was used in other runs of this study. Reactor-System II set up is shown in Figure 3. Method of operation given in this chapter will apply to both the reactor systems

A detailed description of the main components of the system follows.

Reactor

The Reactor consists of a 24 inch (62 cm) long, 1/2 inch (1.27 cm) O.D., and 0.045 inches (0.114 cm) thick stainless steel tube packed with the catalyst. Figure 4 shows Reactor-I used in the runs ADA and

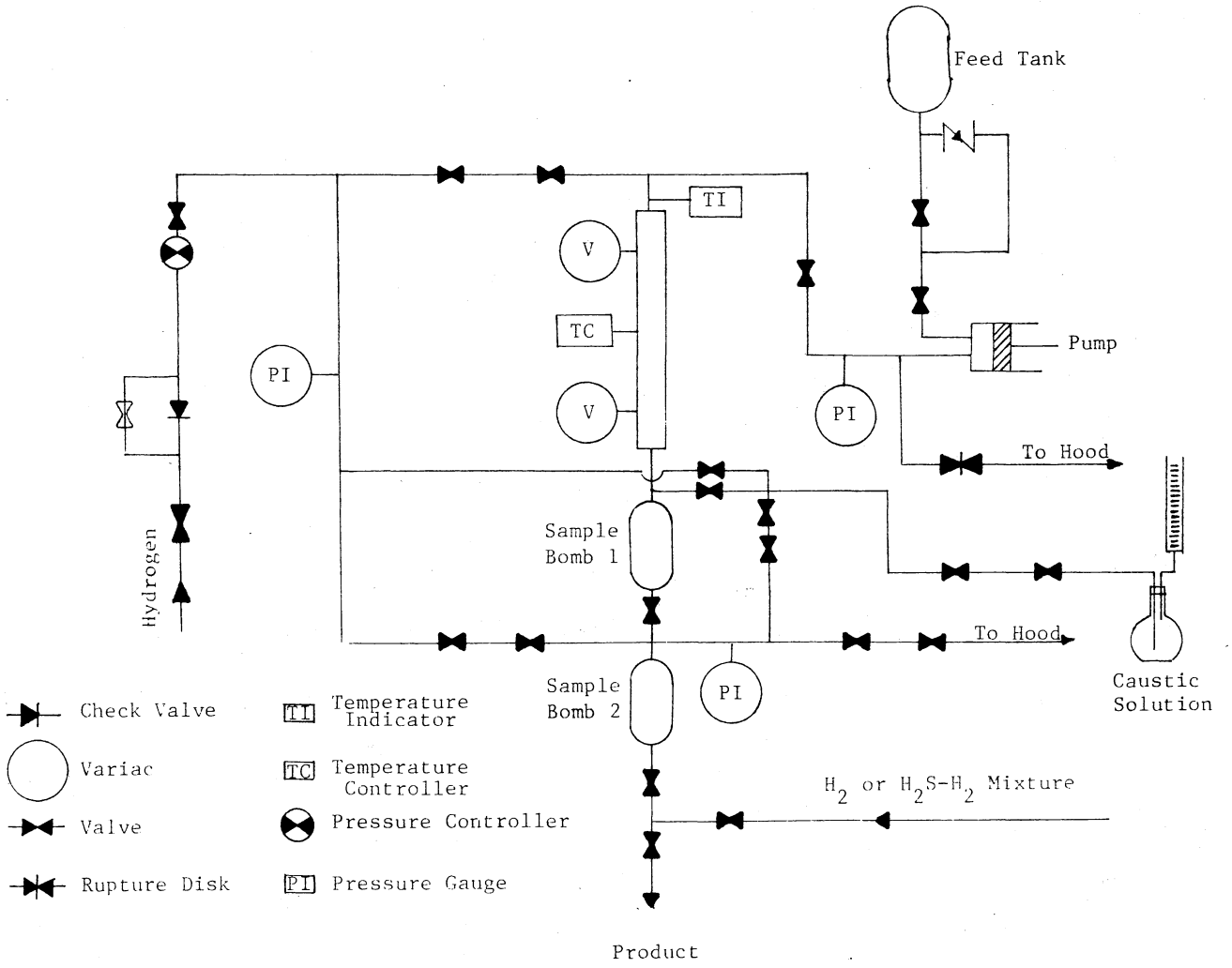

Figure 3. Reactor-System II

ADB, while Figure 5 shows Reactor-II used in the run ADC. The only difference in the two Reactors is the placing of the 1/8 inch (0.317 cm) O.D. stainless steel tube which acts as the thermowell. Reactor-I has only one thermowell running along its outside. Reactor-II has another thermowell running down through its center. Longitudinal cross-sections of the two Reactors packed with catalysts are shown in Figures 9 and 10 respectively.

Reactor Heating System

To maintain the reactor at desired temperature, electrical heating, by three specially designed aluminum blocks, is employed. A typical block is shown in Figure 6. The blocks have 1/2 inch (1.27 cm) diameter holes through their centers, for enclosing the reactor. This provides a tight and uniform contact between the blocks and the reactor. The grooves in the blocks provide space for electrical resistance heaters. Three blocks are used for better heat distribution and control.

After keeping the blocks in place and making all the necessary electrical connections, the blocks are thoroughly insulated by felt fabric and fiber-glass insulations. The heating to the middle block is controlled by Hewlett-Packard 240 temperature programmer. The heating to the top and bottom blocks is controlled by powerstats. With the heating arrangement described above, the reactor could be maintained at nearly isothermal conditions.

Temperature Measurements

An iron-constantan thermocouple is used for sensing the

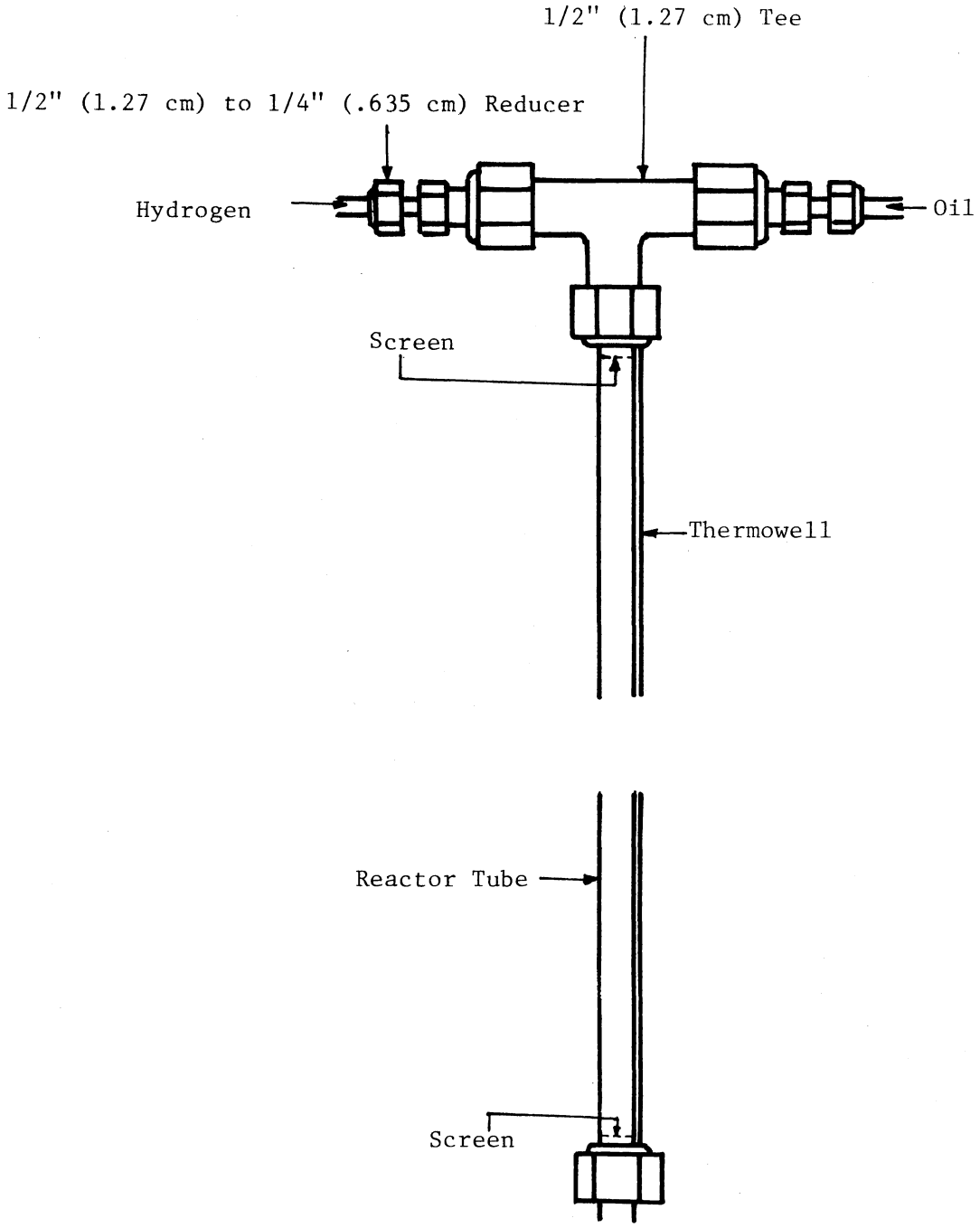

Figure 4. Reactor-I Design

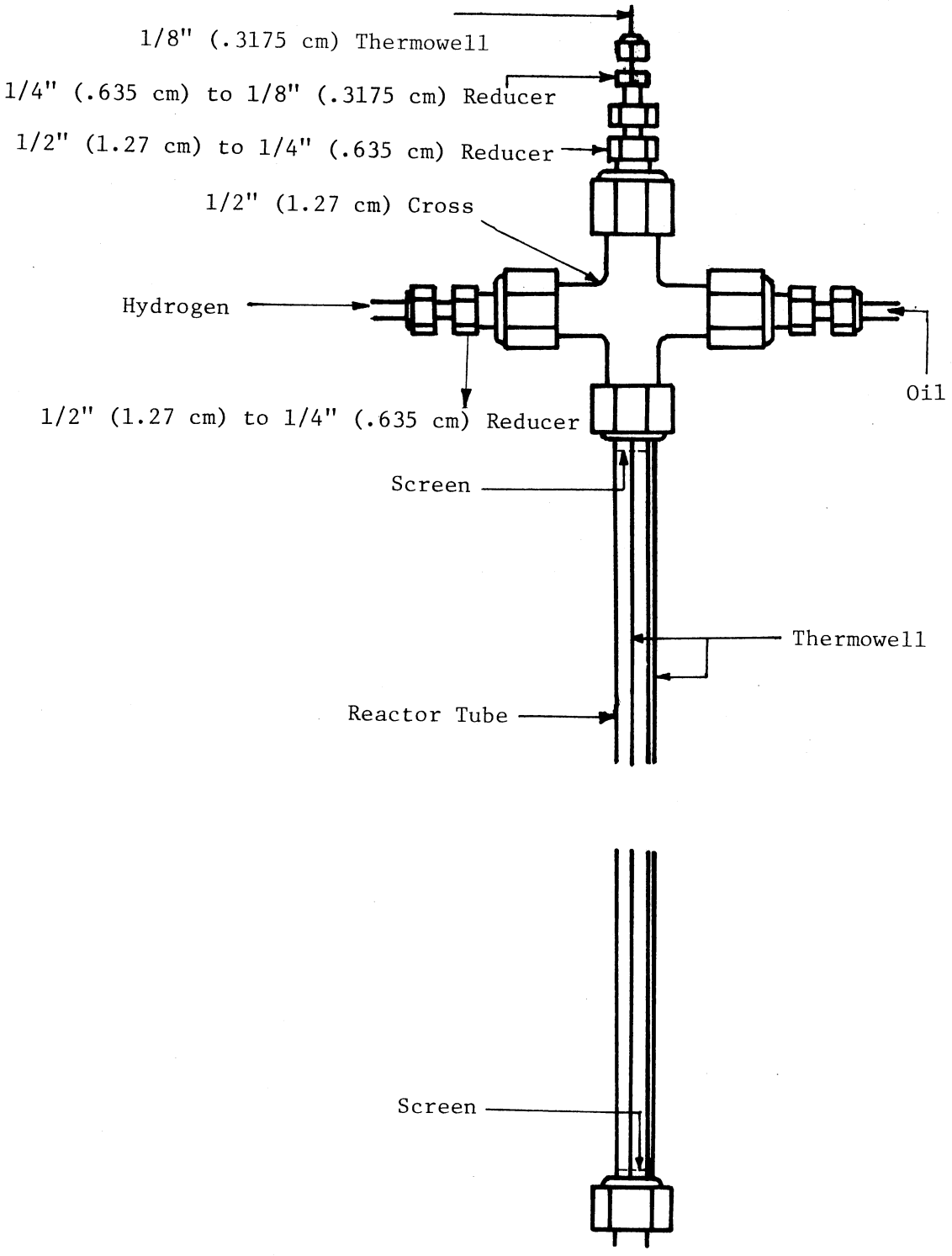

Figure 5. Reactor-II Design

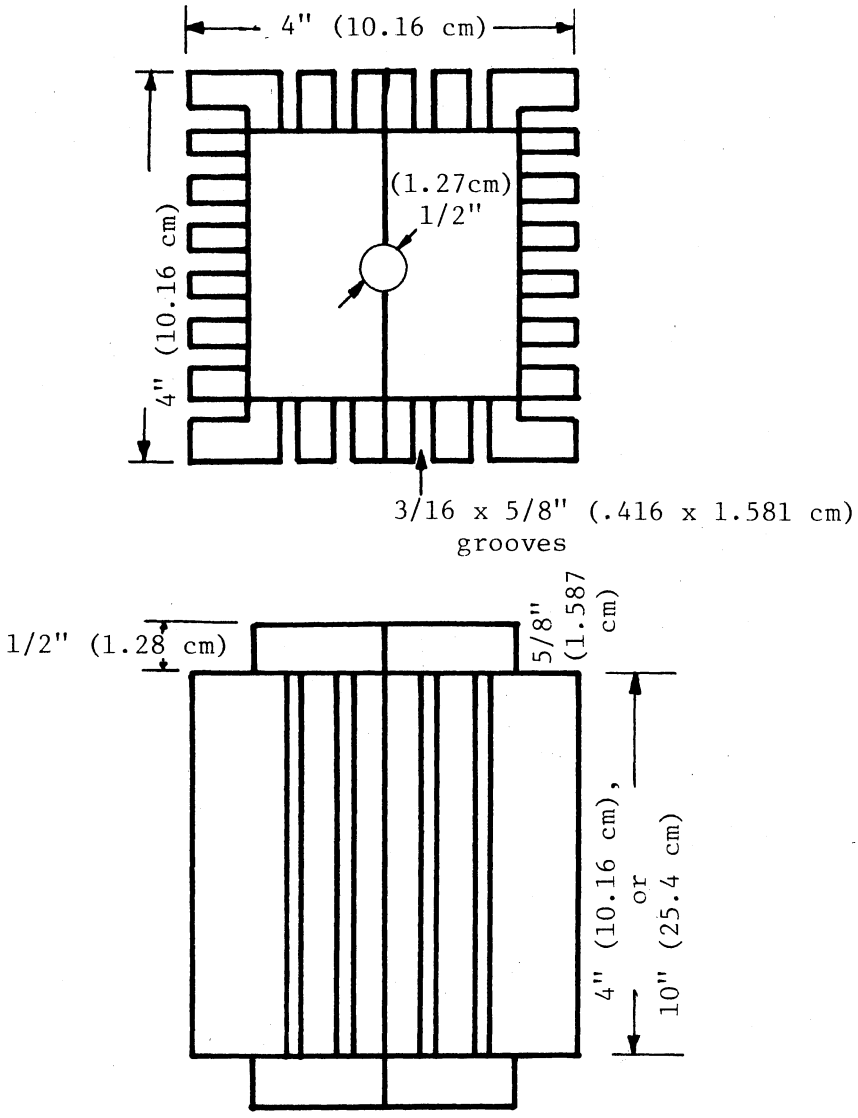

Figure 6. Reactor Heater Block

temperature of the reactor. This thermocouple and those in the heated oil lines, are connected to a multipoint selector, 43. This selector can accept output of nine thermocouples and by switching it to any one of them, the output signal can be fed to a digital read out which is a Doric DS-300-T3 thermocouple indicator. The reactor temperature is measured at every inch of the reactor (except a small portion, at the top and bottom, containing inerts) by moving the thermocouple in the thermowell at that position, letting the thermocouple to come to equilibrium with the reactor, and then noting the temperature on the digital read out. There is another thermocouple which also gives an idea of the temperature of the reactor. This is the control thermocouple of the temperature programmer which is used to control heat to the middle heating block and is 19/16 inch (3.00 cm) deep.

Pressure and Flow Control

The system pressure is measured by Heise Gauge, 25, connected in the hydrogen feed line. This pressure is controlled by means of Mitey Mite Pressure Controller, 24. The pressure on the upstream of this controller is adjusted by the hydrogen manifold regulator. The gas flow rate is controlled by Whitley Microvalve, 3, connected in the off-gas flow line of the reactor. A bubble flow meter is used to measure the flow rate of the gas.

Oil and Hydrogen Feed System

The oil feed system consists of a stainless steel feed tank, 27, and a Ruska positive displacement pump, 26. The feed tank, the oil pump, and the oil lines to the reactor are all wrapped with heating

tapes which, in turn, are insulated with fiberglass. The temperatures of the oil lines are controlled by means of powerstats to which the heating tapes are connected. The temperatures are read with the help of six thermocouples, 29, 30, 31, 32, 33 and 34, connected to oil lines at different places. A rupture disk rated at 2200 psig is connected in the oil line as a safety measure against excessive pressure build-up due to plugging of oil line. The Bourden pressure gauges, 35 and 36, measure the oil pressure at the pump outlet and reactor inlet respectively. Appreciable difference in pressures shown by these two gauges would indicate restriction to flow of oil through the tube.

The hydrogen gas is fed directly from the bottles. The bottles are connected to a manifold which allows changing of bottles without any interruption of the run. As a safety measure, an excess flow valve is installed upstream of Mity-Mite pressure controller, 24. This valve will shut down the system in event of excess flow. A quarter-turn valve is placed upstream of the excess flow valve so that in case of emergency, hydrogen supply can be cut off very rapidly. Another safety device is the hydrogen detectors which will give an alarm when hydrogen concentration in the room reached 50 percent of the lower explosion limit.

Sampling System

Liquid Sampling: The liquid sampling system consists of two sampling bombs, 22 and 23, connected, one after another, at the outlet of the Reactor. The bombs are 300 cc stainless steel cylinders rated up to 1800 psig. Figure 7 shows design of the sample bomb. At the top of the bomb a 1/2 inch (0.27 cm) to 1/4 inch (0.635 cm) reducer is connected so as to allow a 1/4 inch (0.635 cm) tube to pass through

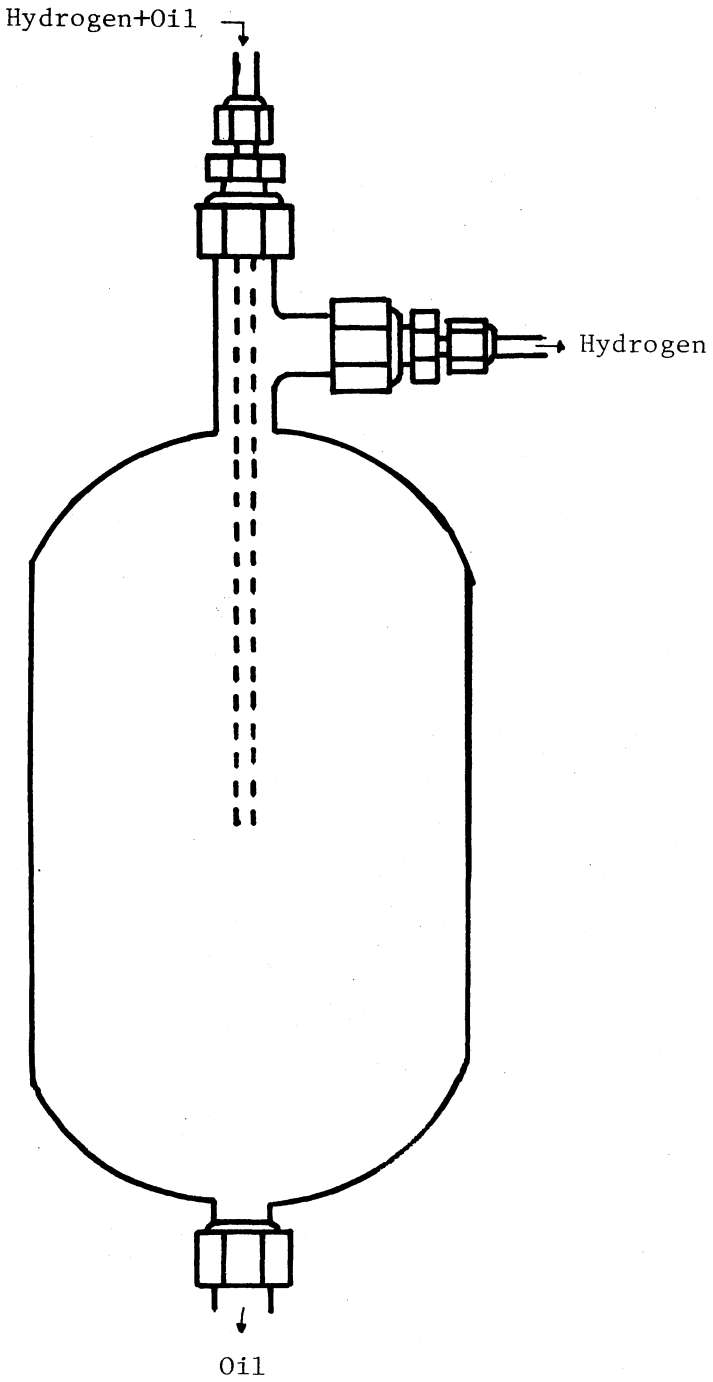

Figure 7. Sample Bomb

it. This 1/4 inch (0.635 cm) tube extends into the bomb. The liquid and gas enter the sampling bomb through this tube and separate into two phases. The liquid collects at the bottom of the bomb and gases go to the vent.

Gas Sampling: The gas sampling system consists of a coil made out of 1/4 inch stainless steel tube and connected in the off-gas line. The coil is enclosed in a Dewar flask in which liquid nitrogen can be put. This arrangement is shown in Figure 8. The coil is in two parts connected to each other by means of a 1/4 inch (0.365 cm) stainless steel Tee-joint. The third end of the Tee is connected to the vent line. The coil is kept immersed in liquid nitrogen during the time sample is being taken. The gases coming out of the reactor will condense (except hydrogen) as they pass through the coil. The condensate will collect at the lower part of the coil and uncondensed gases will escape through the vent line. The condensed gases are then transferred to 300 cc gas bottles.

Experimental Procedure

A step-wise description of the experimental procedure follows. The sequence in which steps are given is the same as involved in conducting actual experimentation.

Catalyst Preparation: One of the three reactor runs for this study was conducted with Nalcomo 474 catalyst which was a vendor preparation and available commercially. For the other two runs, the catalyst was prepared according to the procedure suggested by Bruce E. Leach, Research Chemist at Conoco in Ponca City, Oklahoma. In this method, weighed amount of MoO_3 is dissolved in ammonia and distilled water.

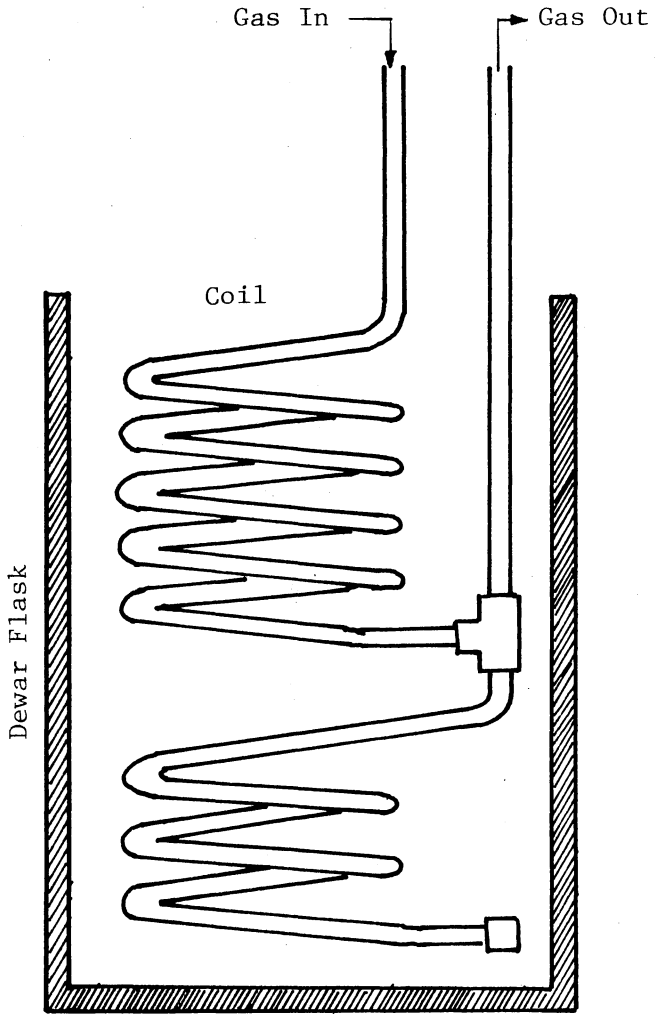

Figure 8. Gas Sampling Trap

The pH of the solution is adjusted to 5.5 with HNO_3, and a weighed quantity of $Co(NO_3)_2$, is then dissolved in it. The solution is diluted with distilled water and poured over weighed amount of alumina support. This is allowed to set overnight and then dried and calcined. The complete details of the method are given in Appendix A.

Loading the Reactor and Making the Experimental Set up Ready: The catalyst loading in the Run ADC, which used commercial Nalcomo 474 catalyst in the form of 1/8 inch (0.31 cm) pellets, was done by first crushing and screening the pellets to obtain 8-10 mesh (0.2 cm) particles. A few porcelain Berl saddles were also reduced to the same size. Then a fifty mesh size stainless steel screen was put between the top of the reactor and the 1/2 inch (1.27 cm) Swagelock cross. The reactor was held vertical with the screen end down, and the thermowell positioned centrally in the reactor. The 8-10 mesh (0.2 cm) Berl saddles were poured in the reactor. The reactor was tapped vigorously so that particles distribute uniformly around the thermowell. The Berl saddles were filled in the reactor up to a height of 6 inches (15.2 cm). Then 8-10 mesh (0.2 cm) catalyst particles were packed, in the same way, up to a height of 14 inches (35.5 cm). The 4 inches (10 cm) height of the reactor, left at the bottom, was again packed with 8-10 mesh (0.2 cm) size Berl saddles. Finally, the bottom end of the reactor was covered with a 50 mesh stainless steel screen and a 1/2 inch (1.27 cm) union was screwed on it. Figures 4 and 5 show the reactors with all the necessary fittings and Figures 9 and 10 show the reactors packed with the catalysts.

The reactor was then installed in the experimental set up (Figure 2) by connecting it with the 1/4 inch (0.635 cm) oil and

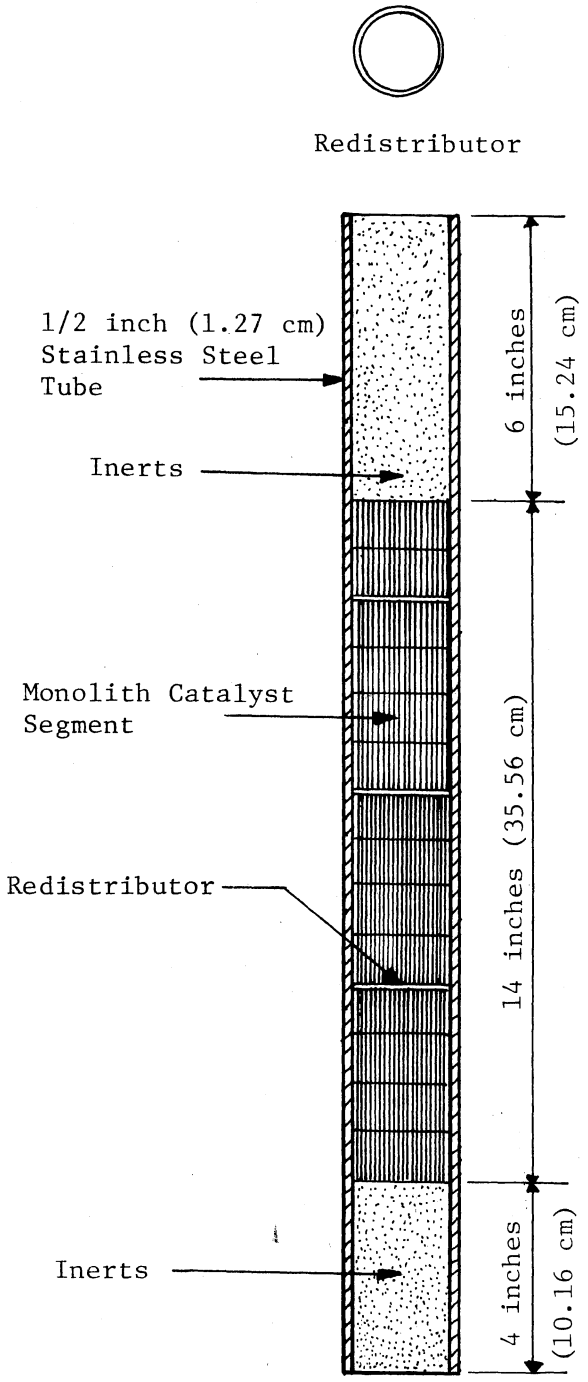

Figure 9. Cross Section of Reactor-I

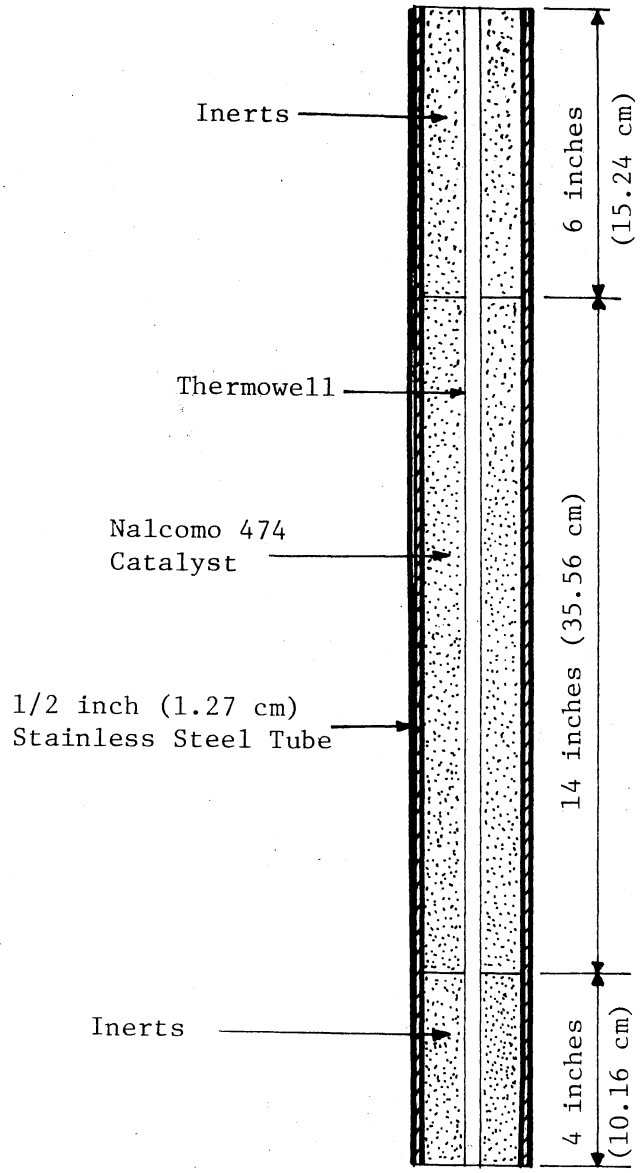

Figure 10. Cross Section of Reactor-II

hydrogen lines at the top and 1/4 inch (0.635 cm) reactor outlet line at the bottom. After the reactor was secured in the system, the whole set-up was pressure tested up to 1700 psig with nitrogen. All the fittings were tested for leaks with soap solution. The system was kept in this pressurized condition for 10-12 hours and drop in pressure was observed. A pressure drop of less than 20 psig was considered to indicate no leakage. The heating blocks were then put around the reactor and electrical connections made. Finally, the insulation was installed and heater circuits checked for any short circuiting or discontinuity.

The above steps for runs ADA and ADB were also carried out in the same way except that no tapping of the reactor was done while packing it with the monolith catalyst. Each monolith segment was slipped into the reactor. Also, three redistributors, in the form of rings, as shown in Figure 9, were put at intervals of 4 inches each for sealing clearance between the catalyst segments and reactor tube. Figures 9 and 10 show the cross-sectional views of the packed reactors in both the cases.

Activation of the Catalyst: This was done in two steps given below:

(1) Calcination: The reactor was gradually heated to 450 F (232 C) and kept at this temperature for 12 hours. During this time nitrogen was passed through the reactor at a rate of 3.1 cc/sec. This calcination step was meant to remove absorbed water from the catalyst.

(2) Sulfiding: After calcination the Heise pressure gauge was disconnected and the catalyst was treated for 90 minutes with a mixture of 5.14 percent H_2S in H_2. The flow rate of this mixture through the reactor was maintained at 3.1 cc/sec. After sulfiding the system was

flushed with nitrogen for about 10 minutes and the Heise Gauge reconnected.

Start Up: After activation of the catalyst, heating of the reactor was started to bring it to the operating temperature. In the meantime, the feed tank, 27, was filled with the oil and heating of oil lines started and their temperatures raised to 250 ± 20 F. The heating of oil lines was not involved while using Reactor-System II for conducting run ADB with raw anthracene oil as the feedstock. After heating the oil feed system, the Ruska Pump, 26, was filled with the oil. When the reactor reached the operating temperature to start with, the system was pressurized with hydrogen to the operating pressure. The hydrogen flow rate was then adjusted. The pump was then set at the desired flow rate and the pressure on the oil side was built-up to the reactor operating pressure by manually moving forward the plunger of the pump. The pump was then switched on and the oil inlet valve, 17, to the reactor was opened.

Normal Operation: After temperature and pressure had stabilized, the reactor was considered to operate normally. A maximum variation of ± 3 F in temperature and ± 20 psig in pressure was considered to be within the stabilized limits of these parameters. During normal operation, the temperature profile, pressure gauge reading, setting of temperature controllers, gas flow rate, pump reading, and oil flow rate were recorded every hour.

Table XXVIII in Appendix A gives the position of the various valves during normal operation.

Sampling Procedure: After the reactor was on oil for 32 hours, sampling of the reactor products was started. The line out time of

32 hours was given for the catalyst activity to stablize. Sampling was done in such a way as not to disturb the normal operation of the reactor. Complete details of the sampling procedure for the liquid and the gaseous products are given in Appendix A.

Reactor Shut Down: Reactor was shut down by carrying out the following steps.

(1) Hydrogen supply was cut off by closing the valve 12.

(2) Pump, 26, and all the heating system was switched off.

(3) Valve, 17, in oil line was closed.

(4) The system pressure was allowed to fall to 250 psig.

(5) The oil lines were depressurized by running the pump in reverse direction.

(6) The system was then purged with N_2 for 30 mintues.

(7) After the reactor had cooled down to room temperature, insulation was removed, heating blocks taken out and the reactor disconnected from the system.

Sample Analysis: The product samples from the reactor were analyzed for their sulfur and nitrogen contents. Some of the samples were subjected to ASTM distillation. The analytical procedures are described below in brief. Appendix A contains their complete details.

Sulfur Analysis: The sulfur content was determined by means of a Leco Automatic Sulfur Analyzer, consisting of a Model 321-500 Induction Furnace, a Model 532-000 Automatic Titrator, and an oxygen purifying train. The general procedure for operation of these machines and finding sulfur content is given in the Leco Bulletin (63). In this system, the induction furnace is used to burn the sample in an atmosphere of purified oxygen. The SO_2 obtained passes through the automatic

titrator, along with other products of combustion. The SO_2 is automatically titrated against standard KIO_3 solution using starch as the indicator.

Nitrogen Analysis: The complete analytical system consisted of a Model 24 Perkin-Elmer Elemental Analyzer, a Model AD-2 Perkin-Elmer Autobalance, a Leeds and Northrup Recorder, and a Model 04-1280 Perkin-Elmer Sealer. The elemental analyzer could analyze for three elements, carbon, hydrogen and nitrogen, simultaneously. The working of this analyzer would be described below briefly.

A combustion tube, a reduction tube, and a detector system are major components of the analyzer. Figure 11 shows packed combustion and reduction tubes. These tubes are put in furnaces at temperatures of 650 to 700 C and 950 to 1000 C respectively. The weighed sample burns in an atmosphere of purified oxygen in the combustion zone. The gases so produced are carried, by high grade purity helium, through packings of combustion tube which would remove sulfur oxides and halogens from the gases. The gases then pass through reduction tube where nitrogen oxides are reduced to molecular nitrogen. The exit gases from combustion tube now consist of water vapor, carbon dioxide, nitrogen and helium diluent. These collect in a 300 ml capacity glass vessel. The pressure in glass vessel is allowed to rise to 2 atmospheres and the temperature is held constant. After equilibrium has reached, the gas mixture is expanded into an elongated sampling system and then passed through detectors which consist of a series of thermal conductivity cells. Before gases reach the first cell, they pass through a trap containing magnesium percolate. This removes water through the gas stream. The difference between the thermal conductivity

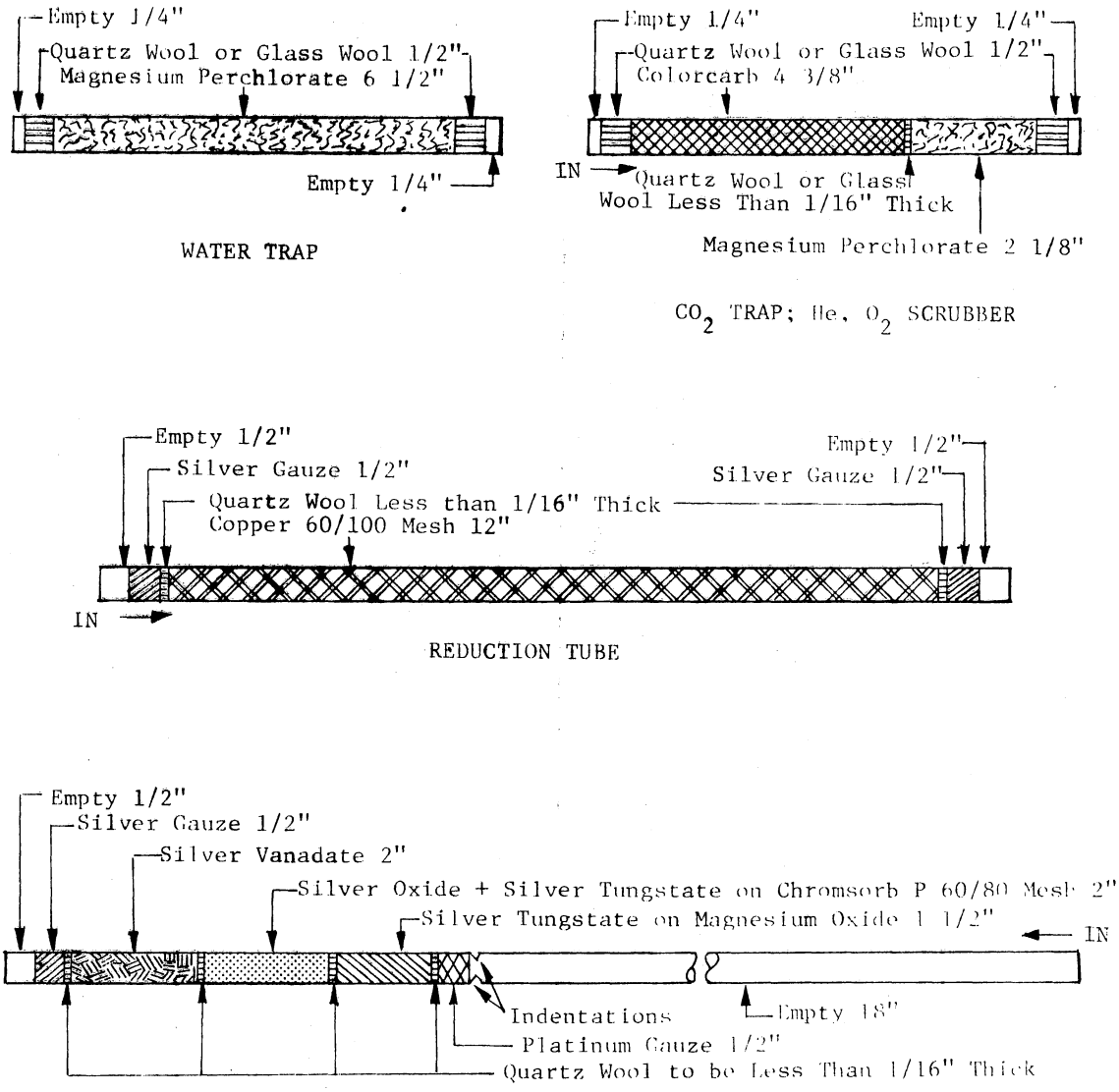

Figure 11. Recommended Make Up for Combustion, Reduction Tubes, Traps and Scrubbers (64)

of the gas before and after the trap indicates the water and hence the hydrogen concentration in the original sample. Next the gases pass through a CO_2 trap and a similar measurement of the thermal conductivity gives the carbon dioxide and hence the carbon in the original sample. Figure 11 shows the H_2O and CO_2 traps. The gas that remains now consists of helium and nitrogen. This gas passes through a thermal conductivity cell, the output of which is compared to that of a reference cell through which only pure helium flows. The difference in thermal conductivities would give the nitrogen concentration. Figure 12 shows the schematic diagram of the elemental analyser.

Appendix A gives complete details of the procedure for nitrogen analysis.

Ash Analysis: The Synthoil-1 was analyzed for its ash content by ASTM standard method. The method, essentially, involves careful combustion of a known amount of the sample. The residue left after complete combustion gives the amount of the ash. The ASTM method suggests that after taking the sample in a weighed crucible, it should be heated until the contents can be ignited with a flame. The sample should be allowed to burn and then it should be put in the furnace after burning ceases. However, Synthoil-1 could not be ignited this way. So, the initial combustion of the sample was done in the furnace itself. To ensure that the combustion takes place at uniform and moderate rate, temperature of the furnace was kept low in the beginning. The complete details of the procedure employed are given in Appendix A.

ASTM Distillation: A few samples from run ADC were subjected to ASTM distillation. The method used was the same as established by Wells (29). Appendix A contains a copy of his method.

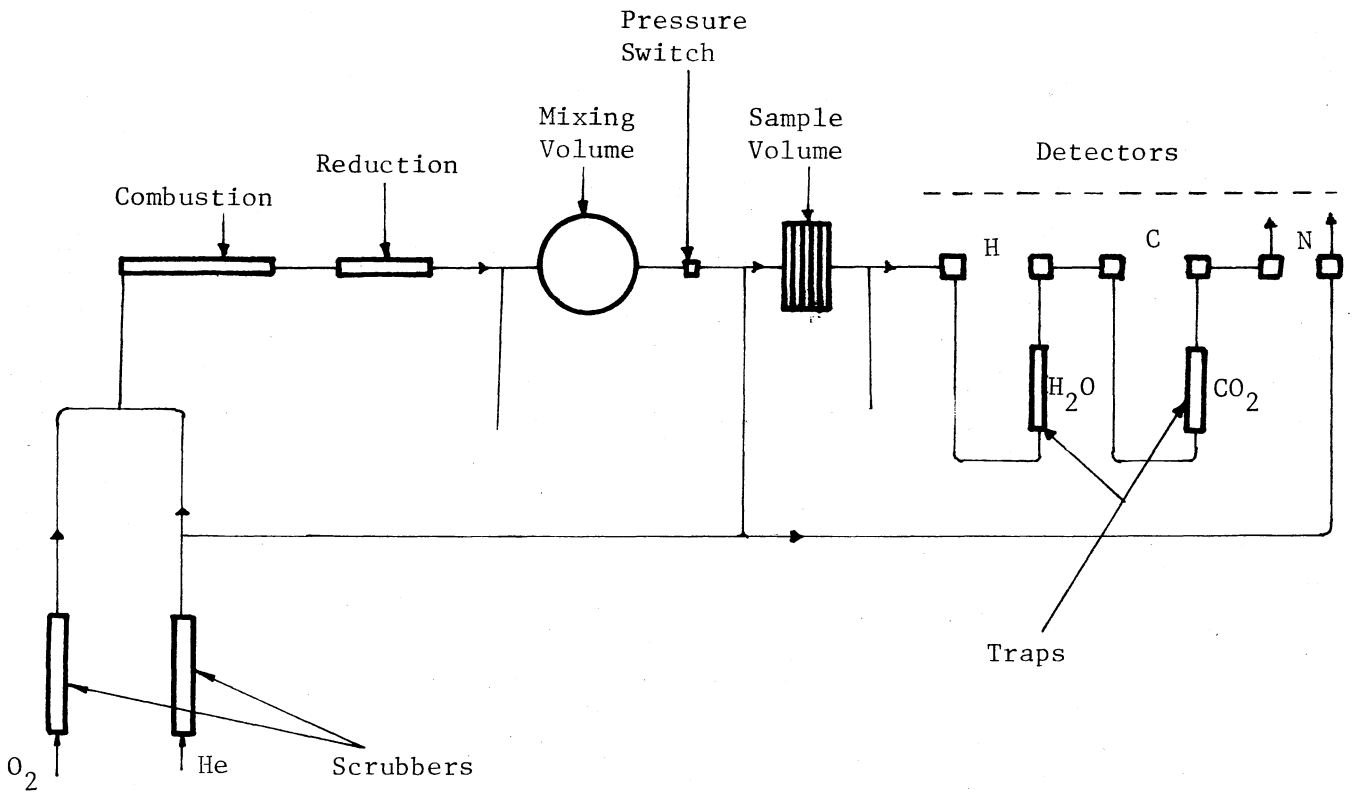

Figure 12. Schematic Diagram of the Analytical System (64)

Feedstock and Catalyst Characterization

Feedstock: Two feedstocks were used in this study. One was Synthoil-I supplied by Pittsburg Energy Research Center of Energy Research and Development Administration. This oil was produced from Western Kentucky Bituminous Coal containing 5.3 percent sulfur. The 1/2 ton per day coal liquefaction unit had 28 feet long reactor and a 35% solid slurry was fed at a rate of 25 lbs. per hour. The reactor conditions were 4000 psig and 232 F (450 C).

Analysis of this feedstock, done in the laboratory here, is given in Table II. The analysis were not available from the vendor.

The second feedstock used was a raw anthracene oil obtained from Reilly Tar and Chemical Corporation. This feedstock has been extensively studied here and is used as a reference liquid. Table III gives properties of this feedstock. The nitrogen content differs somewhat from the values reported in previous studies (26,27,29).

Catalyst: Two types of catalyst were used in this study. One of the catalysts was prepared in the laboratory, here, by impregnating the monolith alumina support, recieved from Corning Glass Company, with molybdenum and cobalt. The procedure used is described in Appendix A. The properties of the support and the prepared catalyst are given in Table IV. The second catalyst was Nalcomo 474, a vendor preparation, received from Nalco Chemical Corporation. It was in the form of 1/8 inch (0.317 cm) pellets. Table V gives properties of this catalyst.

Figures 48 and 49 given in Appendix E, show pore size distribution and pore volume of both the catalysts.

TABLE II

PROPERTIES OF RAW ANTHRACENE OIL

Carbon*	90.28 wt. %
Hydrogen*	5.57 wt. %
Sulfur	0.47 wt. %
Nitrogen	1.035 wt %
Oxygen	2.62 wt. % (Diff.)
Ash*	Nil wt. %
API Gravity	-7

Boiling Range*

Volume Distilled, Percent	Vapor Temperature, F, at 50 mm Hg	Vapor Temperature, F, at 760 mm Hg
10	282	445
20	337	507
30	367	542
40	397	576
50	419	600
60	441	628
70	465	653
80	493	685
90	534	730

* Determined by Wells (29).

TABLE III

PROPERTIES OF SYNTHOIL-1

Carbon	80.5 wt. %
Hydrogen	7.72 wt. %
Sulfur	1.02 wt. %
Nitrogen	1.19 wt. %
Ash	3.4 wt. %
Specific Gravity	1.12 gram/cc

Boiling Range

Volume Percent Distilled	Vapor Temperature, F at 50 mmHg	Weight % S
10	339	0.2
20	413	0.242
30	500	0.232
33	530	0.366
Bottoms	-	1.7

TABLE IV

PROPERTIES OF MONOLITH CATALYST AND SUPPORT

	Monolith Alumina	Monolith Alumina Impregnated with Co and Mo
CoO	--	3.37* wt. %
MoO_3	--	7.25* wt. %
Support	Alumina	Alumina
Surface Area, m^2/gram	73**	66***
Pore Volume, cc/gram	9.613**	0.55***
Most Frequent Pore Radius, ^oA	80**	80***

* Analyzed by Atomic Mass Spectrograph in Geology Department of Oklahoma State University.

** Data received from Corning Glass Company

*** Calculated from the support properties and according to the findings of Mamidi (71).

Note: Later determinations at Oklahoma State University showed that surface area of monolith alumina impregnated with Co and Mo was 92 m^2/gram.

TABLE V

PROPERTIES OF THE NALCOMO 474 CATALYST

Alumina	82.39 wt. %
MoO_3	12.5 wt. %
CoO	3.5 wt. %
Na_2O	0.08 wt. %
Fe	0.03 wt. %
SiO_2	1.5 wt. %
Surface Area, m^2/gram	270*(240)**
Pore Volume, cc/gram	0.51*(0.46)**
Most Frequent Pore Radius, ^oA	33**

* Determined by Nalco Chemical Company
** Measured by American Instrument Company

CHAPTER IV

EXPERIMENTAL RESULTS

This chapter contains results of the experimental work performed for this study. All the results are presented here in the form of graphs, and Appendix C gives the results in tabular form. The abscissas of the graphs given in this chapter would either be space time or pressure, and the ordinates would either be weight percent sulfur or nitrogen in product oil from the reactor. Low sulfur or nitrogen in the product oil corresponds to higher removal, and hence, higher activity of the catalyst under consideration.

Since this study is a comparison of two catalysts on two different feedstocks, some of the figures in this section have duplicate curves showing the comparison between the results of two different experimental runs. The curve drawn with a solid line represents the results of the run under review; the curve drawn with a broken line shows results of another similar run but with different feedstock or catalyst.

Run ADB

This run was conducted to evaluate the activity of the monolith catalyst for removal of sulfur and nitrogen from the reference feedstock, the raw anthracene oil. Properties of raw anthracene oil and the monolith catalyst are given on pages 58 and 60. The catalyst preparation, reactor packing, and start up were done according to the

respective procedures explained in Chapter III. The reactor was operated continuously for 132.5 hours and the reactor conditions at start up were repeated in the end to check for loss, if any, of the catalyst activity. During this 132.5 hours of reactor operation, space time, temperature and pressure were varied to study their effect on catalyst performance. Figures 13 through 18 show the results obtained in this run together with the results of Sooter's work (26) and Satchell's work (27) who did a similar study using the reference catalyst, Nalcomo 474. Properties of this catalyst are given on page 61.

Figures 13 and 14 show the effect of pressure on desulfurization and denitrogenation respectively. As is evident, the pressure effect in both the studies is similar. However, overall activity of Nalcomo 474 is more than that of the monolith catalyst. Effect of pressure is marked up to 500 psig, but thereafter, it is marginal. Beyond 1000 psig, the effect is almost negligible. Similar shape of the curves in both the studies might indicate that the pressure effect does not depend on what catalyst is used and is a function only of the feedstock which was the same in both the studies.

Figure 15 shows the effect of space time on desulfurization at three different temperatures. At all these temperatures, increasing space time beyond 1.0 hour results in negligible decrease in sulfur content of the product.

The relative position of the three curves gives the effect of temperature on sulfur removal. The Figure 15 shows that increase in sulfur removal is more between 650 F (343 C) and 700 F (371 C) than between 700 F (371 C) and 800 F (426 C). This might indicate that for

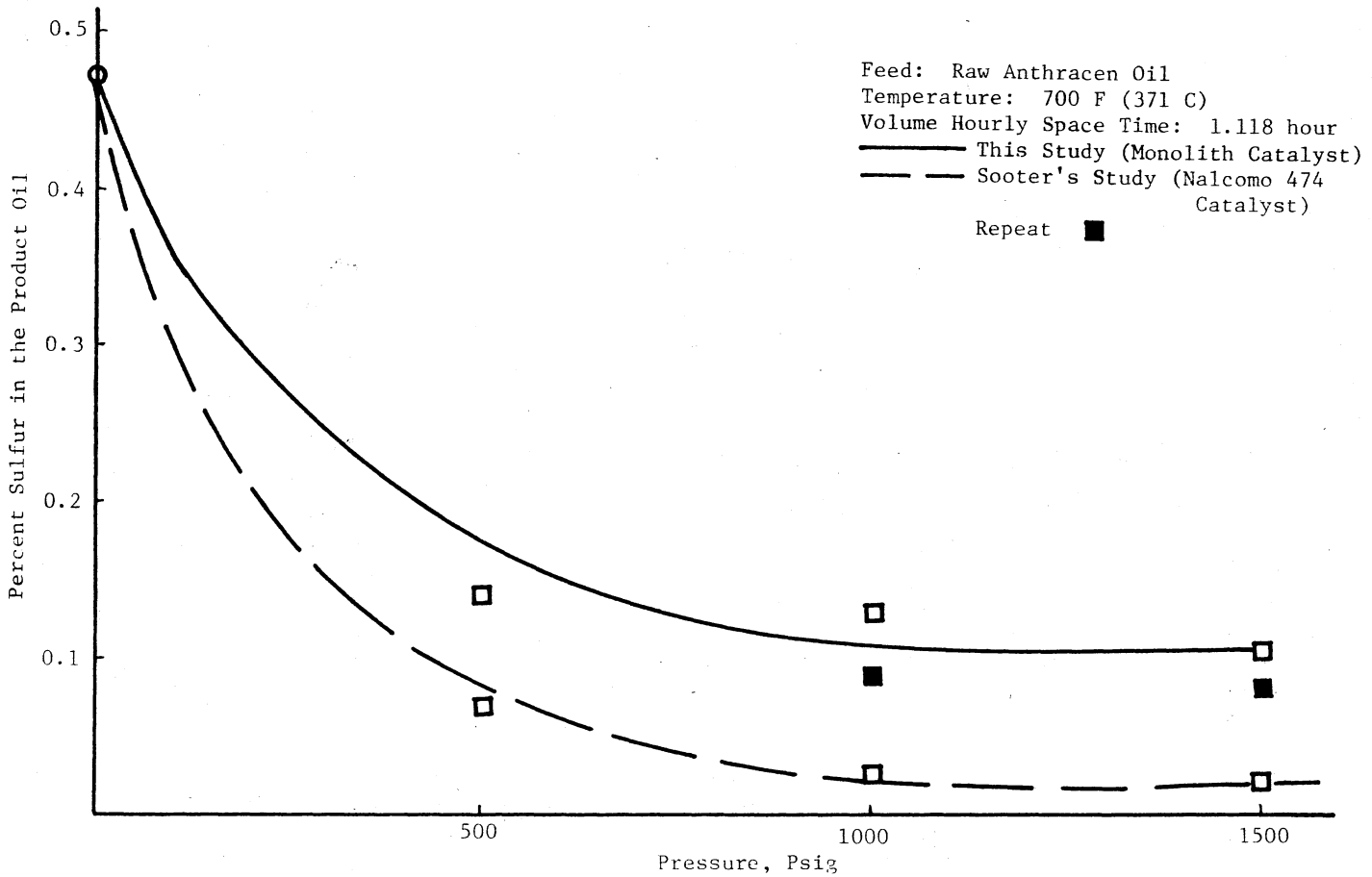

Figure 13. Raw Anthracene Oil Desulfurization, Response to Change in Pressure and Comparison of Nalcomo 474 and Monolith Catalysts

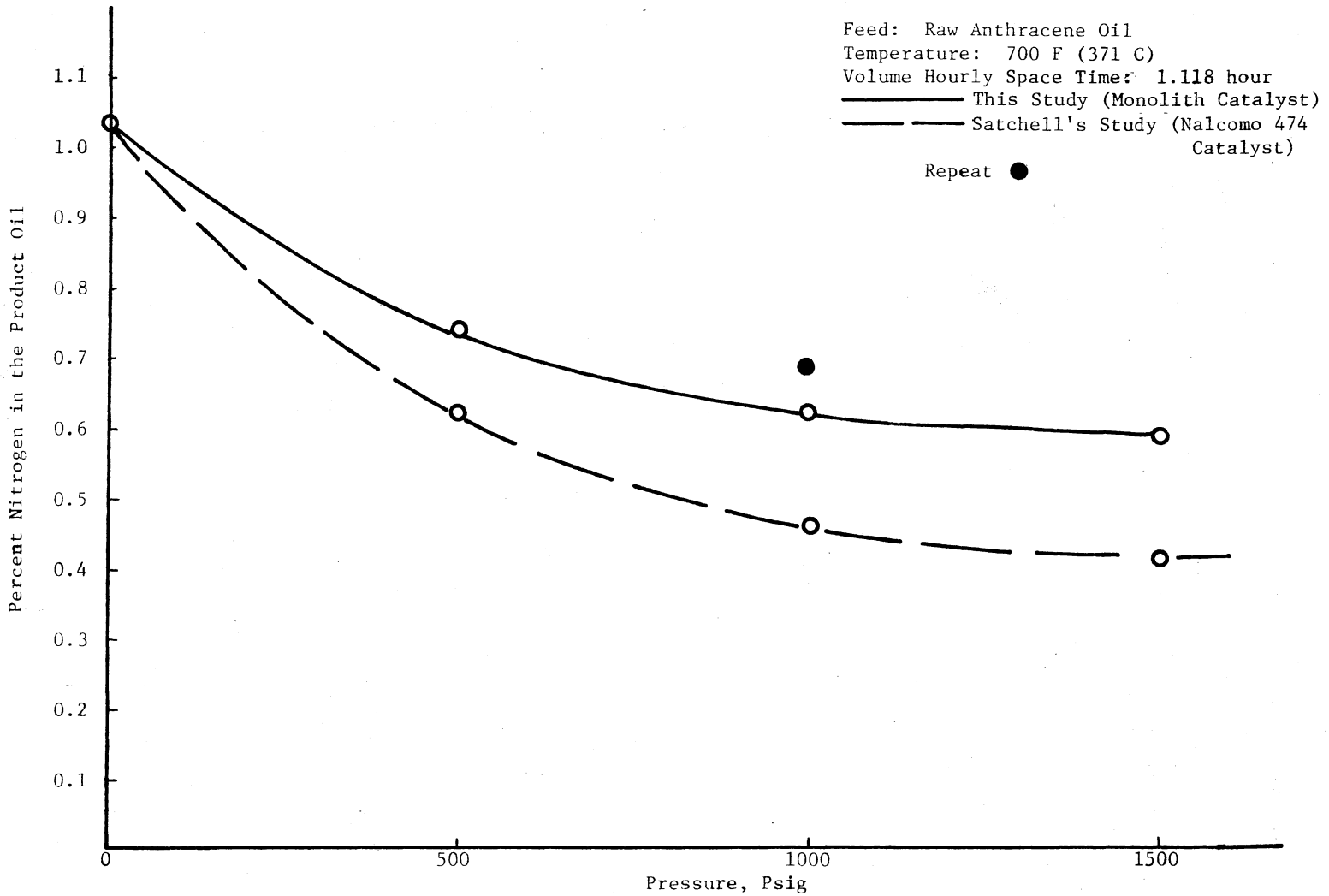

Figure 14. Raw Anthracene Oil Denitrogenation, Response to Change in Pressure and Comparison of Nalcomo 474 and Monolith Catalysts.

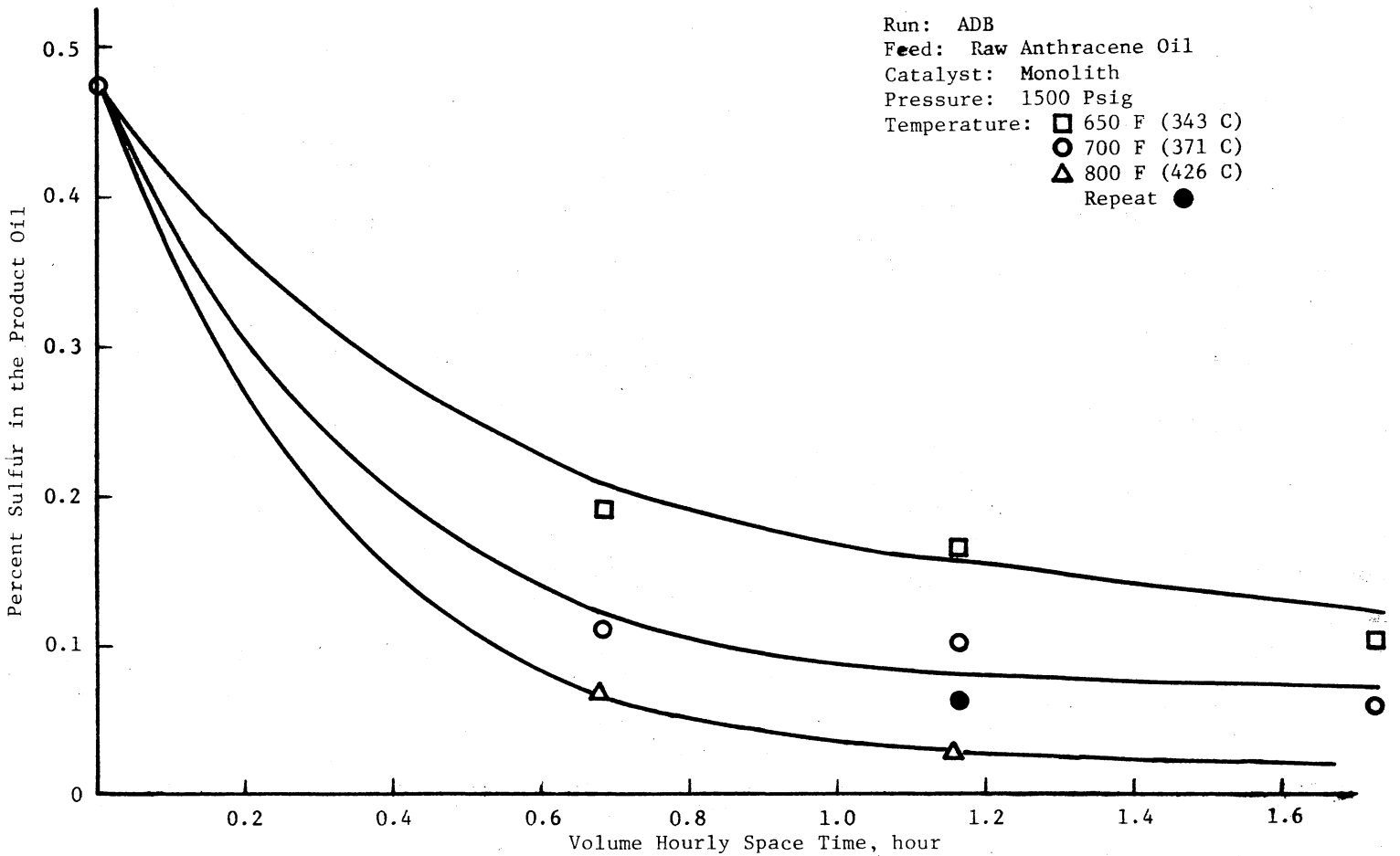

Figure 15. Raw Anthracene Oil Desulfurization Response to Changes in Space Time and Temperature

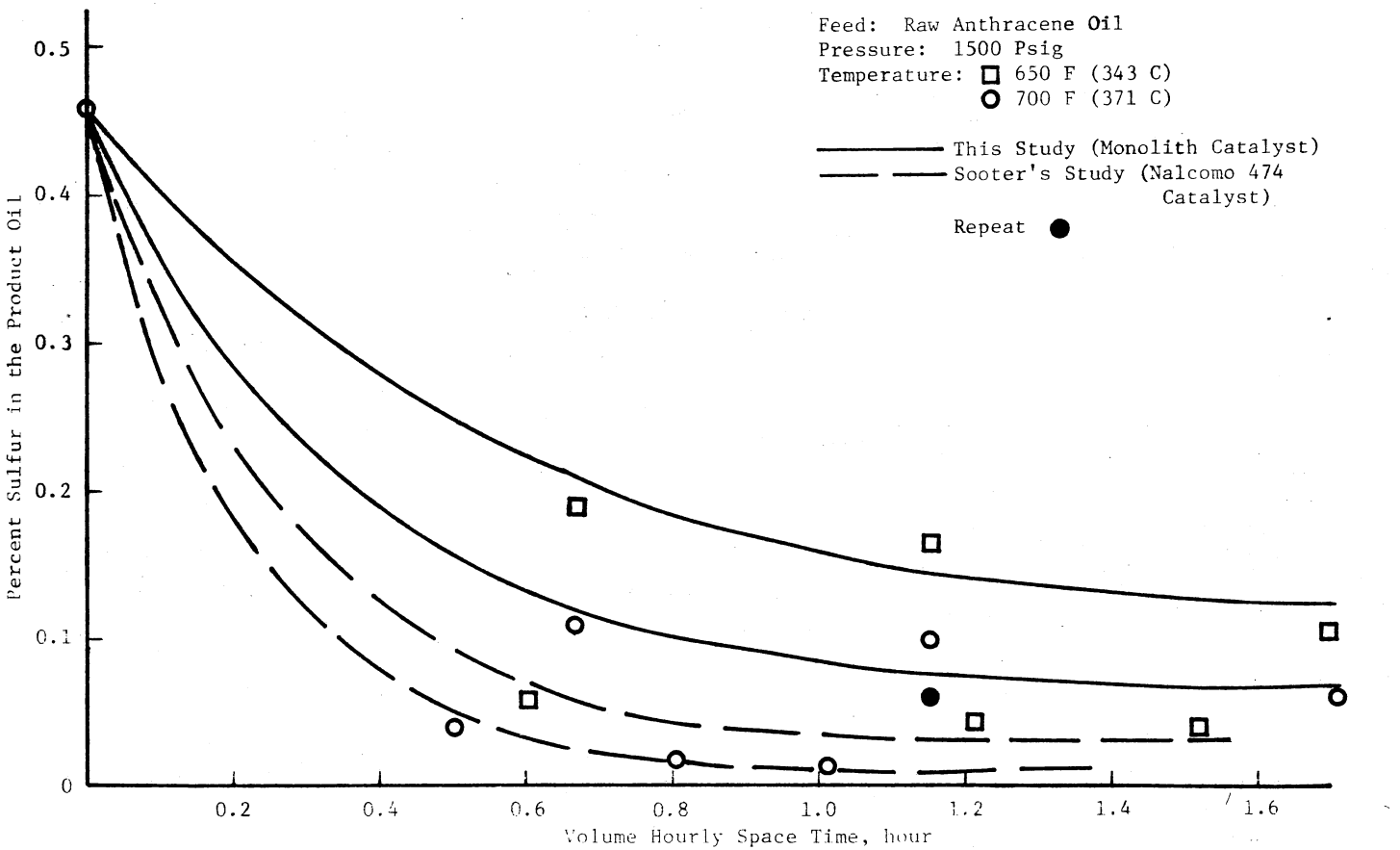

Figure 16. Raw Anthracene Oil Desulfurization, Comparison of Nalcomo 474 and Monolith Catalysts on Volume Hourly Space Time Basis

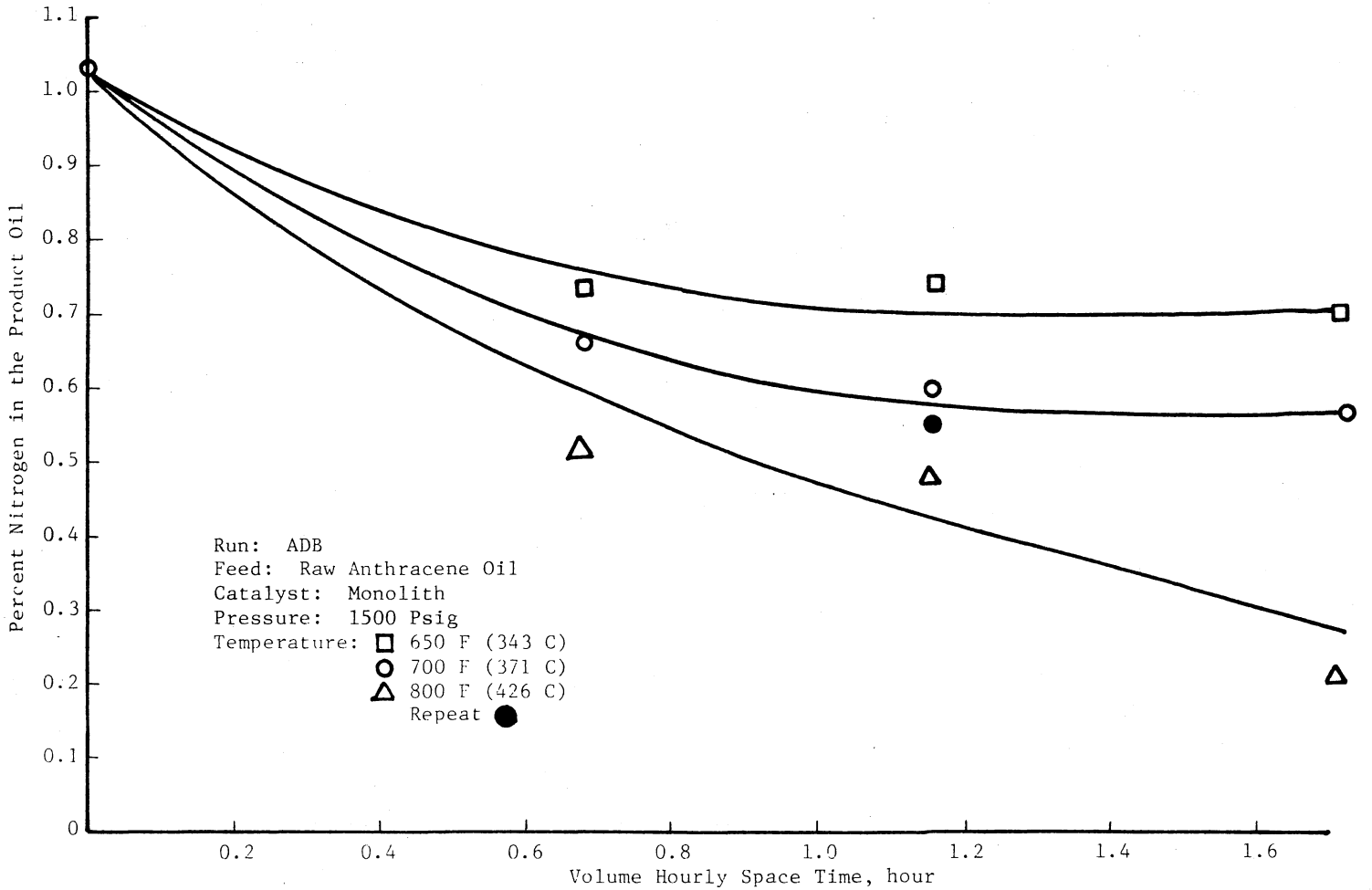

Figure 17. Raw Anthracene Oil Denitrogenation Response to Changes in Space Time and Temperature

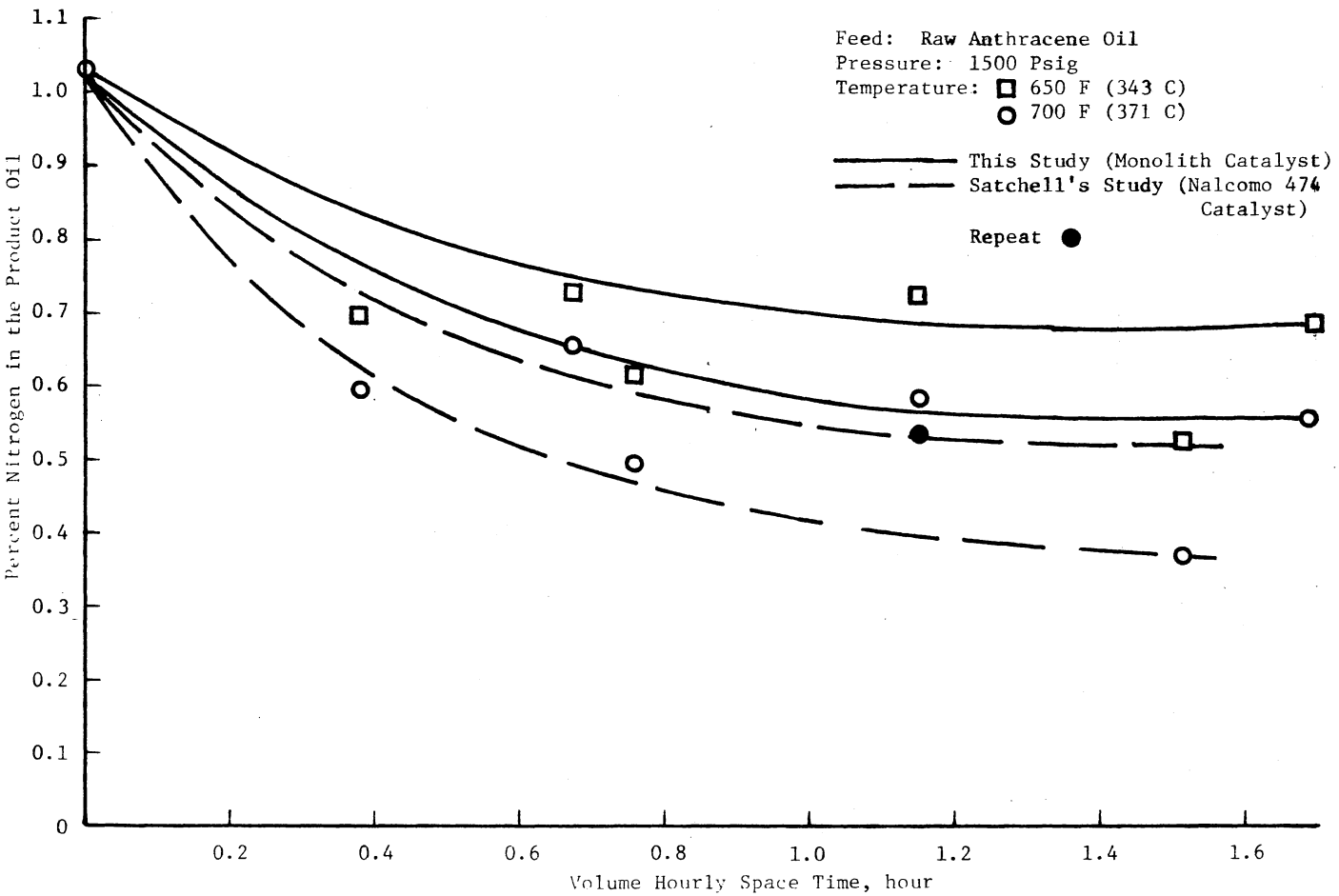

Figure 18. Raw Anthracene Oil Denitrogenation, Comparison of Nalcomo 474 and Monolith Catalysts on Volume Hourly Space Time Basis

this particular feedstock, increasing temperature beyond 800 F may not help much. Figure 16 shows the comparison of the space time and temperature effects between this study and that of Sooter's (26). The shape of the curves is almost alike. However, as pointed out earlier, Nalcomo 474 shows higher activity when compared on a volume hourly space time basis.

Identical studies on nitrogen removal and their comparison with Satchell's (27) work are represented by Figures 17 and 18. Satchell also had the same feedstock, i.e., raw anthracene oil, but the catalyst was Nalcomo 474. Almost the same comments as made on desulfurization apply to denitrogenation. Overall denitrogenation activity of Nalcomo 474 is greater than with the monolith catalyst, but responses to space time, temperature and pressure are similar with both the catalysts.

Run ADC

The objective of this run was to assess the ability of Nalcomo 474 catalyst (reference catalyst) for removing sulfur and nitrogen from a heavy feedstock, Synthoil-1. Properties of this feedstock are given on page 59. This catalyst is a vendor preparation and its properties are given on page 61. The reactor packing and start up were done according to the procedures detailed in Chapter III. The run lasted a total of 105.5 hours and was structured to study the effect of space time, temperature, and pressure.

Figures 19 through 22 depict the results of this run. Figure 19 shows the effect of space time on desulfurization at two temperatures 700 F (371 C) and 800 F(426 C). As can be seen, the effect of space time beyond 0.7 hour is marginal at 700 F (371 C). The behavior at

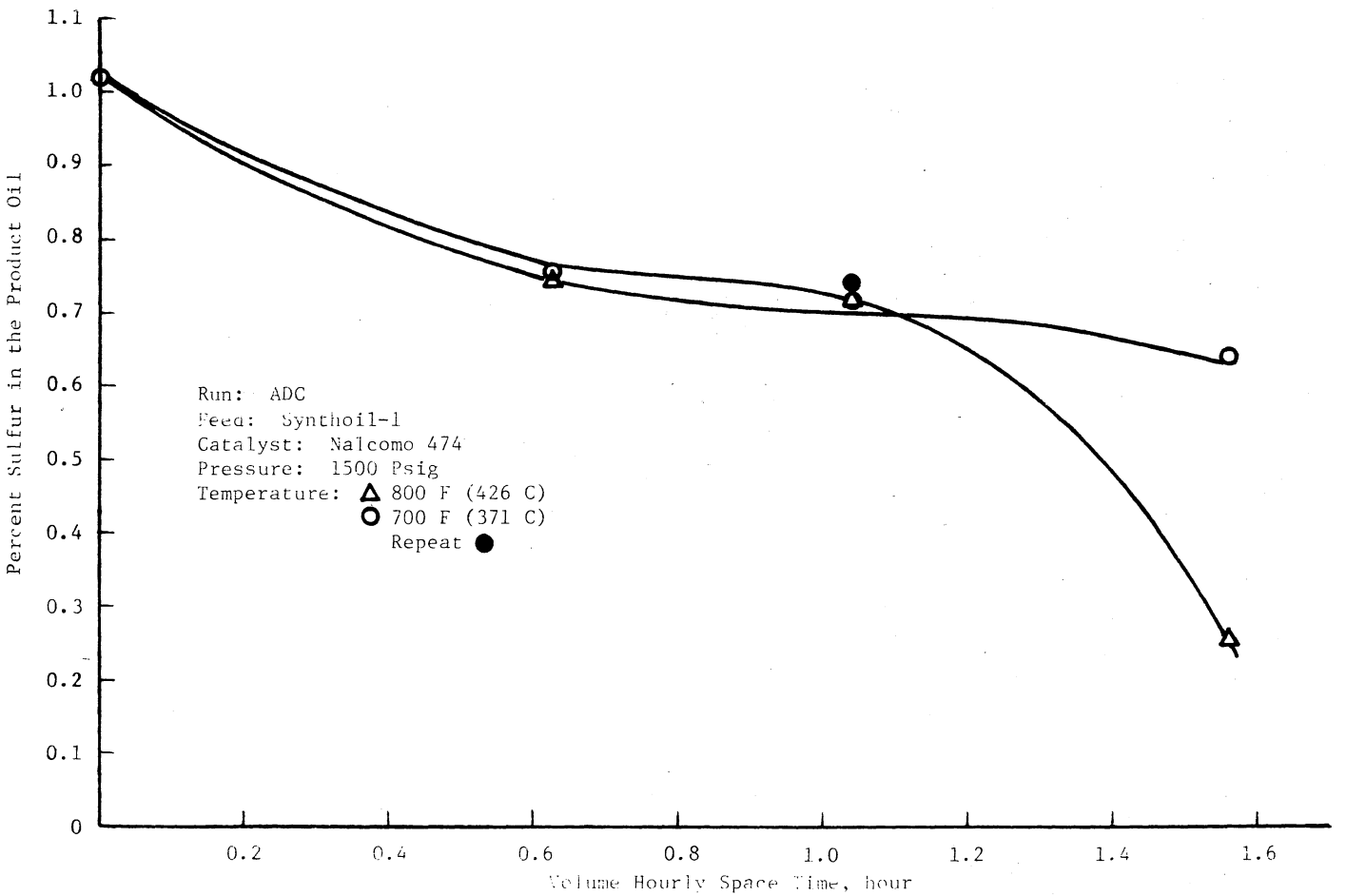

Figure 19. Synthoil-1 Desulfurization Response to Changes in Space Time and Temperature

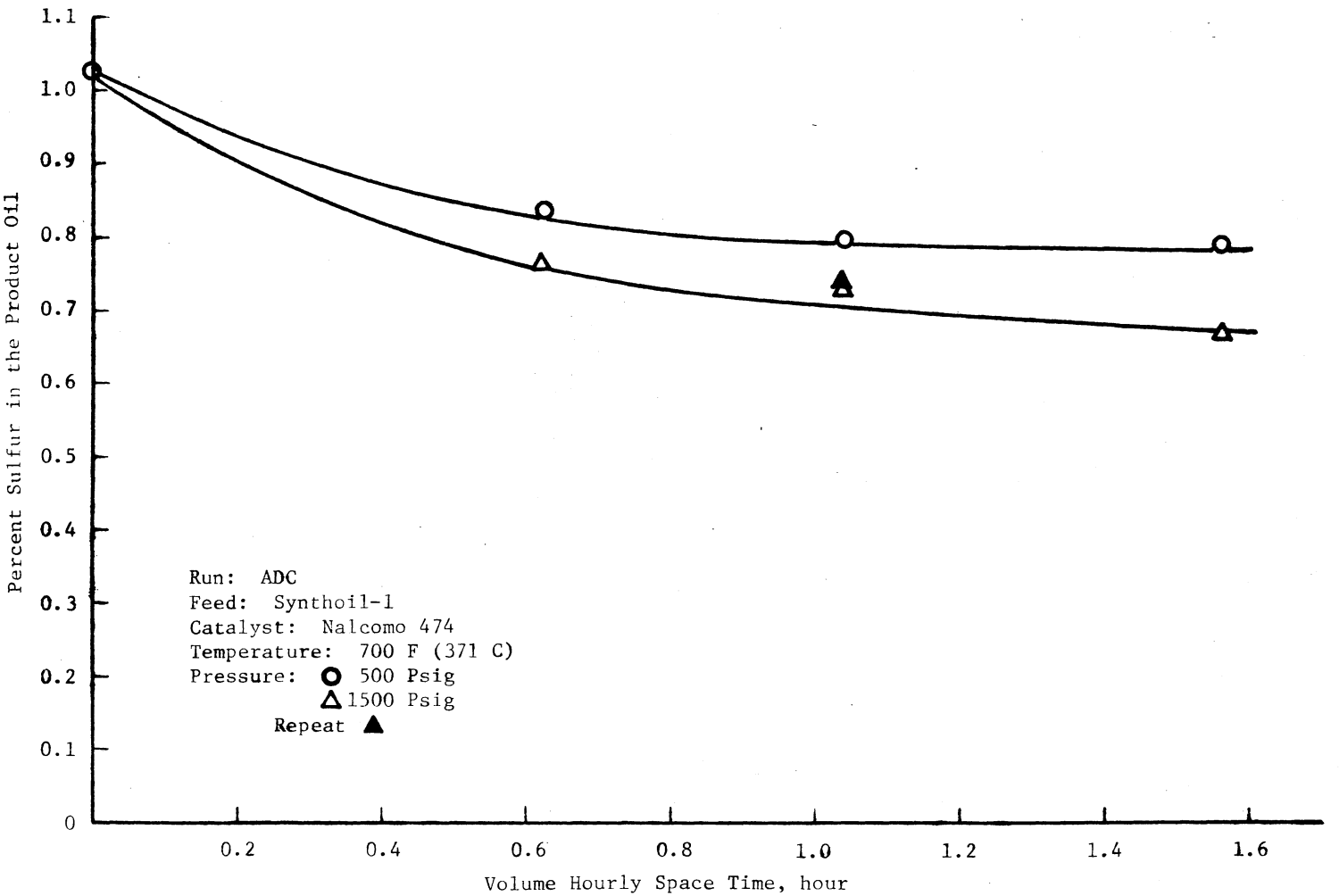

Figure 20. Synthoil-1 Desulfurization Response to Changes in Space Time and Pressure

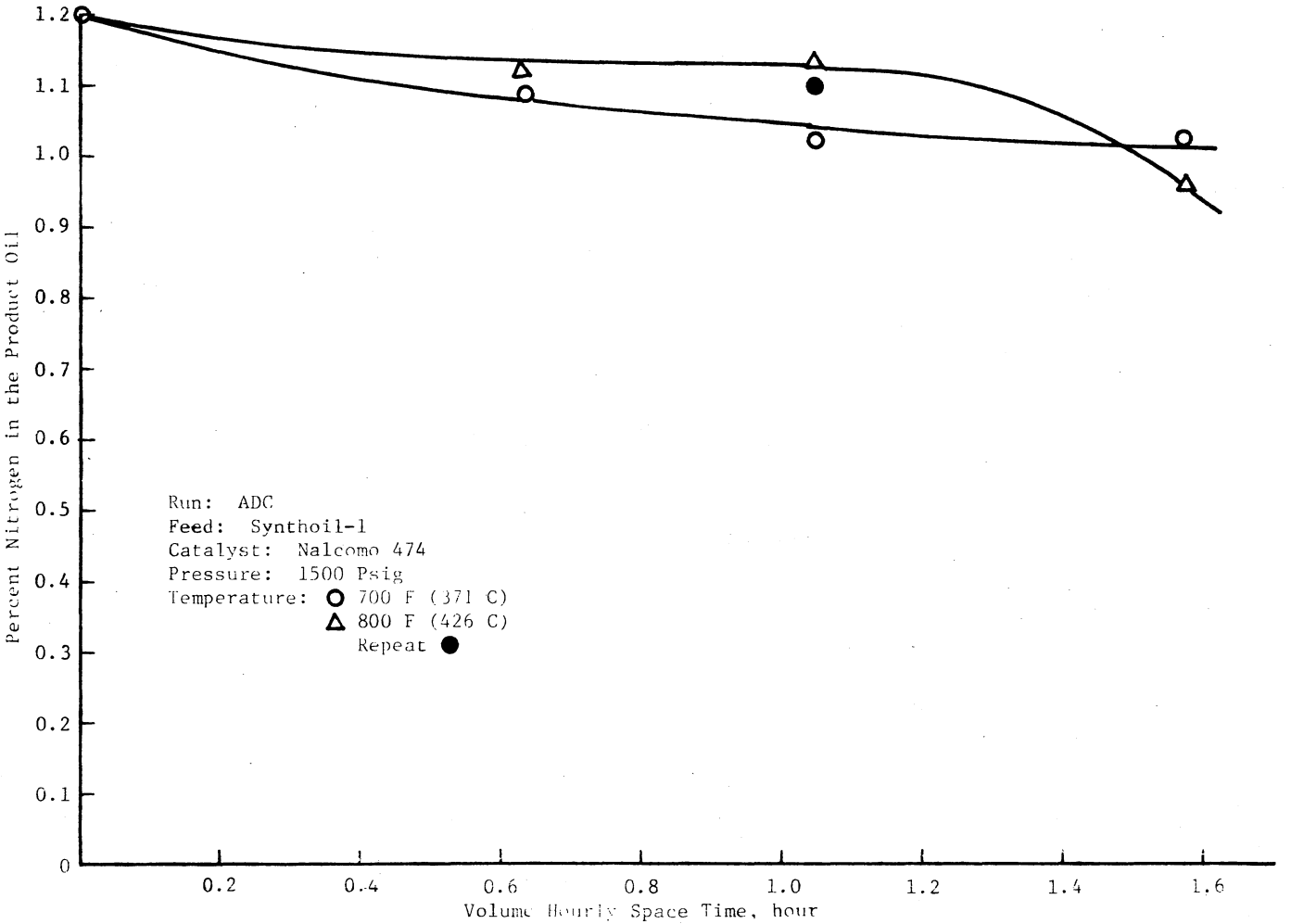

Figure 21. Synthoil-1 Denitrogenation Response to Changes in Space Time and Temperature

800 F is essentially the same until a space time of 1.0 hours. After that there is a steep increase in desulfurization. Sulfur in the product oil reduces, rather suddenly, from about 0.75 to 0.25 percent.

The same figure shows the effect of temperature. There is almost no difference in desulfurization at 700 F (371 C) and 800 F (426 C) up to a space time of 1.0 hour. Beyond this space time the effect of temperature is phenomenal. At a space time of about 1.55, sulfur in the product oil reduces from 0.65 to 0.25 weight percent with increase in temperature from 700 F (371 C) to 800 F(426 C). This behavior is in contrast to that observed while using raw anthracene oil.

Figure 20 shows two curves for pressure effects, one at a pressure of 500 psig and the other at a pressure of 1500 psig. The vertical distance between these two at any point gives the effect of pressure on desulfurization. The difference increases with increase in space time.

Figures 21 and 22 show the effect of space time, temperature and pressure on denitrogenation. A simple look at these figures reveals that Nalcomo 474 has shown practically no ability for denitrogenating Synthoil liquid. However, Figure 21 presents some interesting results. Nitrogen removal is more at 700 F (371 C) than at 800 F (426 C), except at a space time of 1.55 hours when denitrogenation tends to increase at 800 F (426 C). This effect, though not appreciable, is similar to that observed in desulfurization. Apart from this, there is little sensitivity to space time and temperature. The difference between the results at 700 F (371 C) and 800 F (426 C) falls within the scatter of data. Therefore, one can say that essentially there is no difference between nitrogen removal at these two temperatures.

Figure 22 shows the effect of pressure, with the upper curve at 500 psig and the lower at 1500 psig. Denitrogenation is evidently more at 1500 than at 500 psig, but there is little removal at either condition.

Run ADA

The objective of this run was to ascertain the activity of the monolith catalyst towards removing sulfur and nitrogen from Synthoil-1. and to compare its performance with the activity of Nalcomo 474, as shown by the results of Run ADC on the same oil. The monolith catalyst was prepared in the laboratory according to the procedure given in Chapter III. The reactor was loaded and the run started in the same way as the Run ADC. However, there was one difference. The catalyst in Run ADA had to be kept under nitrogen blanket at 650 F (343 C) for about a month. This was because the reactor loading and preparation was done much earlier for a run on Solvent Refined Coal. This run had to be abandoned because of problems with pumping of the Solvent Refined Coal. The inert atmosphere in which the catalyst was kept, would protect the catalyst against any deactivation.

The Run ADA was continuous for 131.5 hours, and toward the end the reactor was returned to start up conditions to check for any deactivation of the catalyst. Variations in space time, temperature and pressure were achieved during this continuous operation. The effects on desulfurization and denitrogenation are represented in Figures 23 through 30. Some of these figures also show the results of Run ADC for comparison.

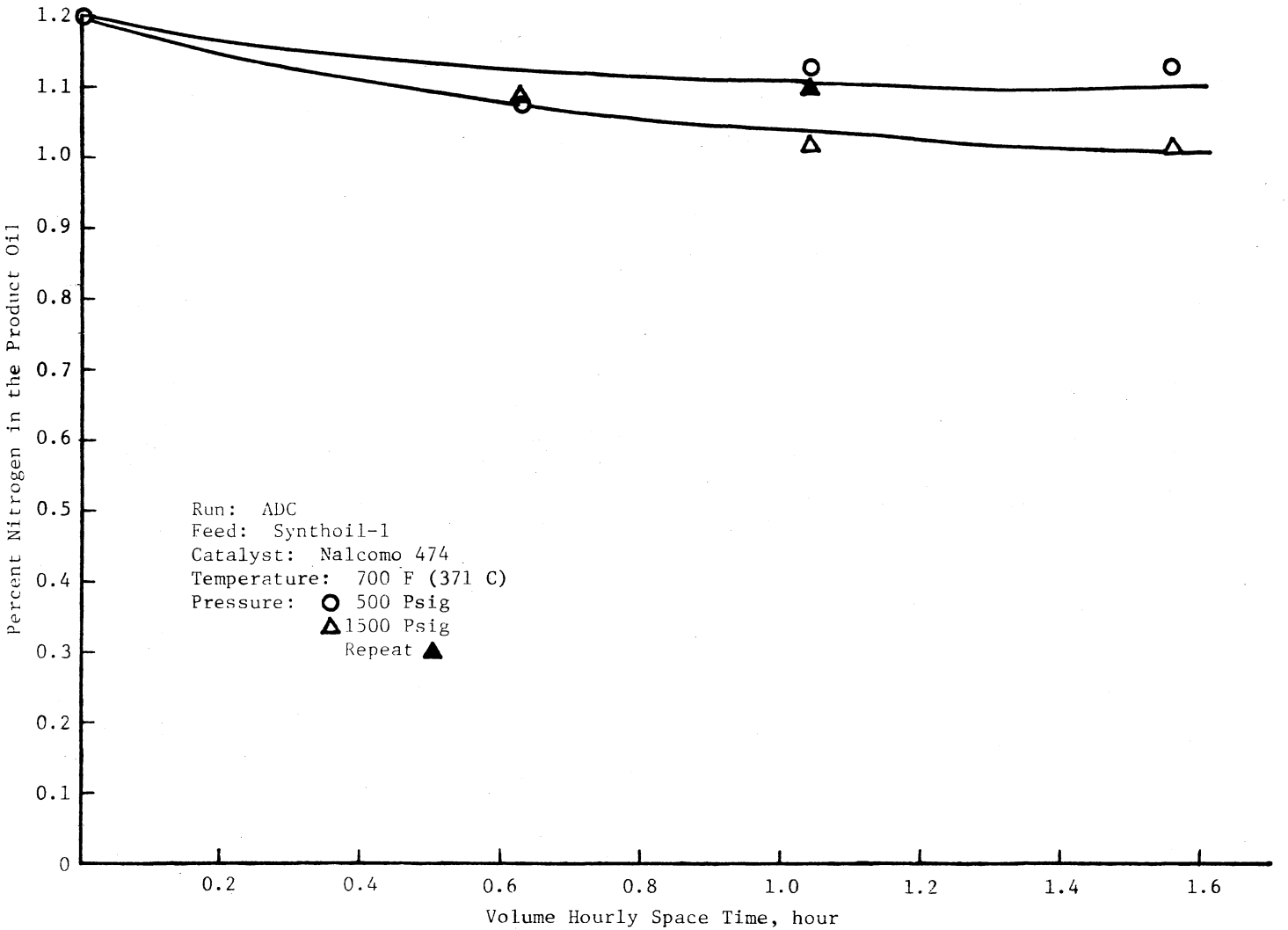

Figure 22. Synthoil-1 Denitrogenation Response to Changes in Space Time and Pressure

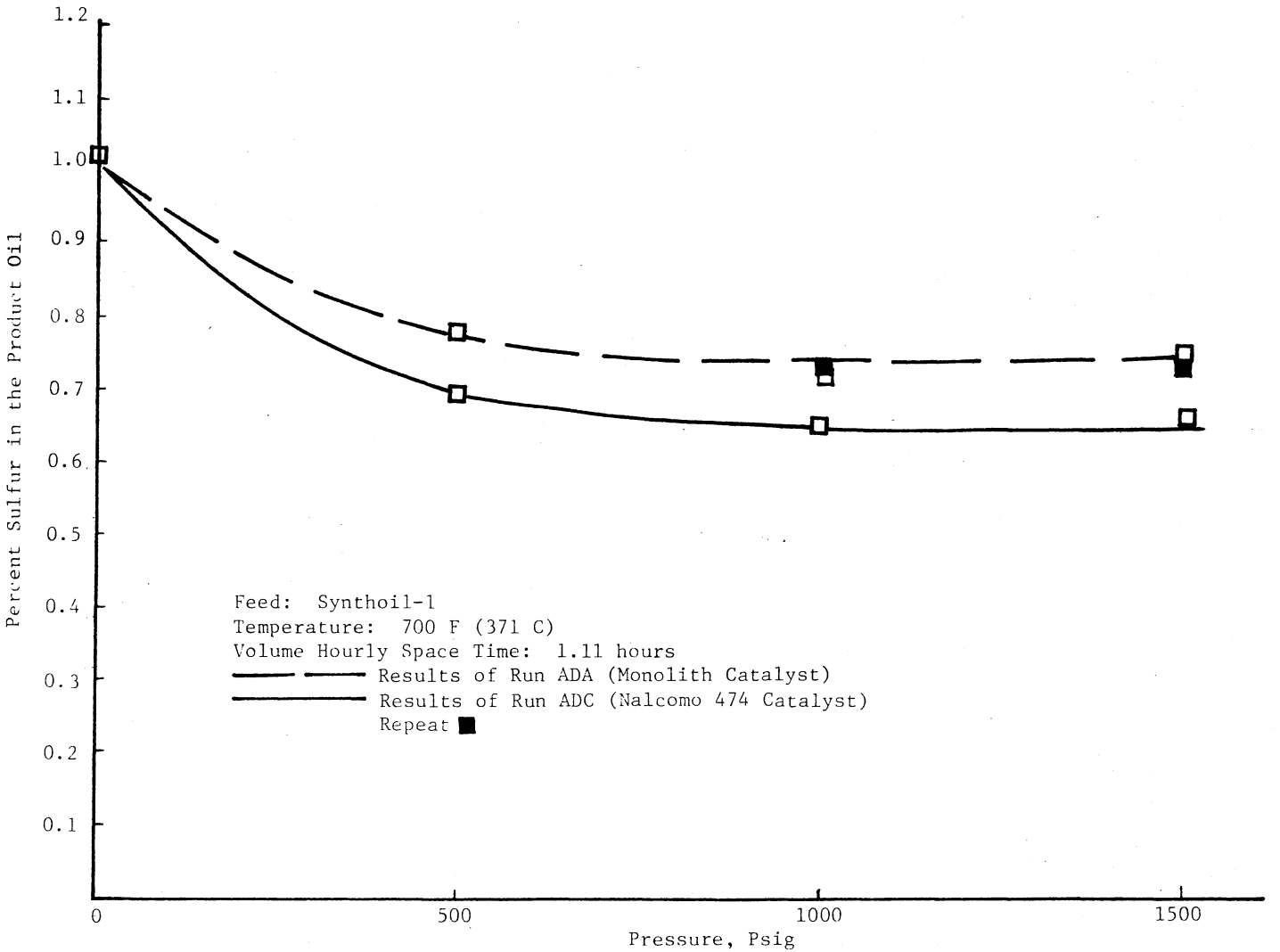

Figure 23: Synthoil-1 Desulfurization Response to Change in Pressure and Comparison of Nalcomo 474 and Monolith Catalysts

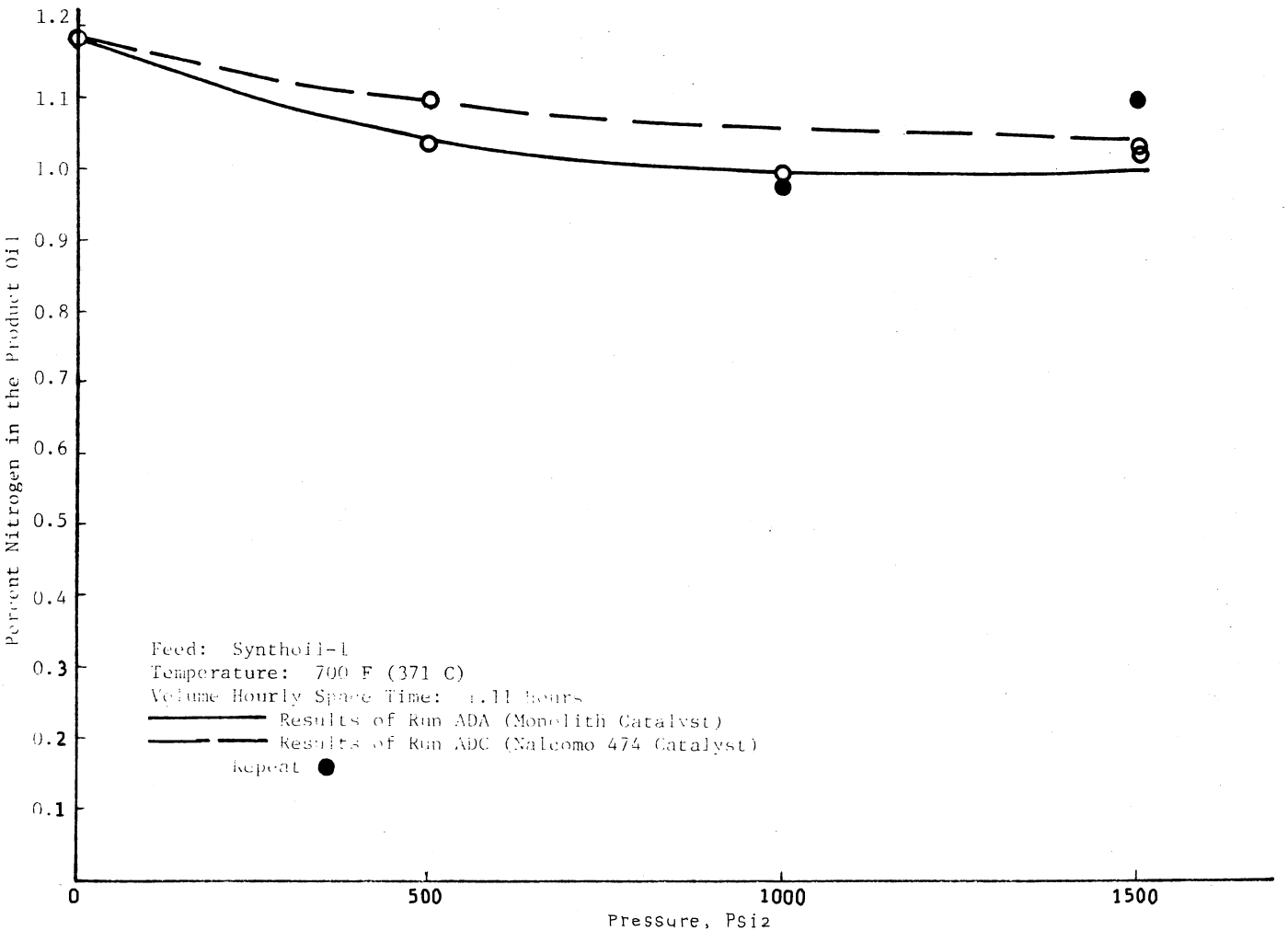

Figure 24. Synthoil-1 Denitrogenation Response to Change in Pressure and Comparison of Nalcomo 474 and Monolith Catalysts

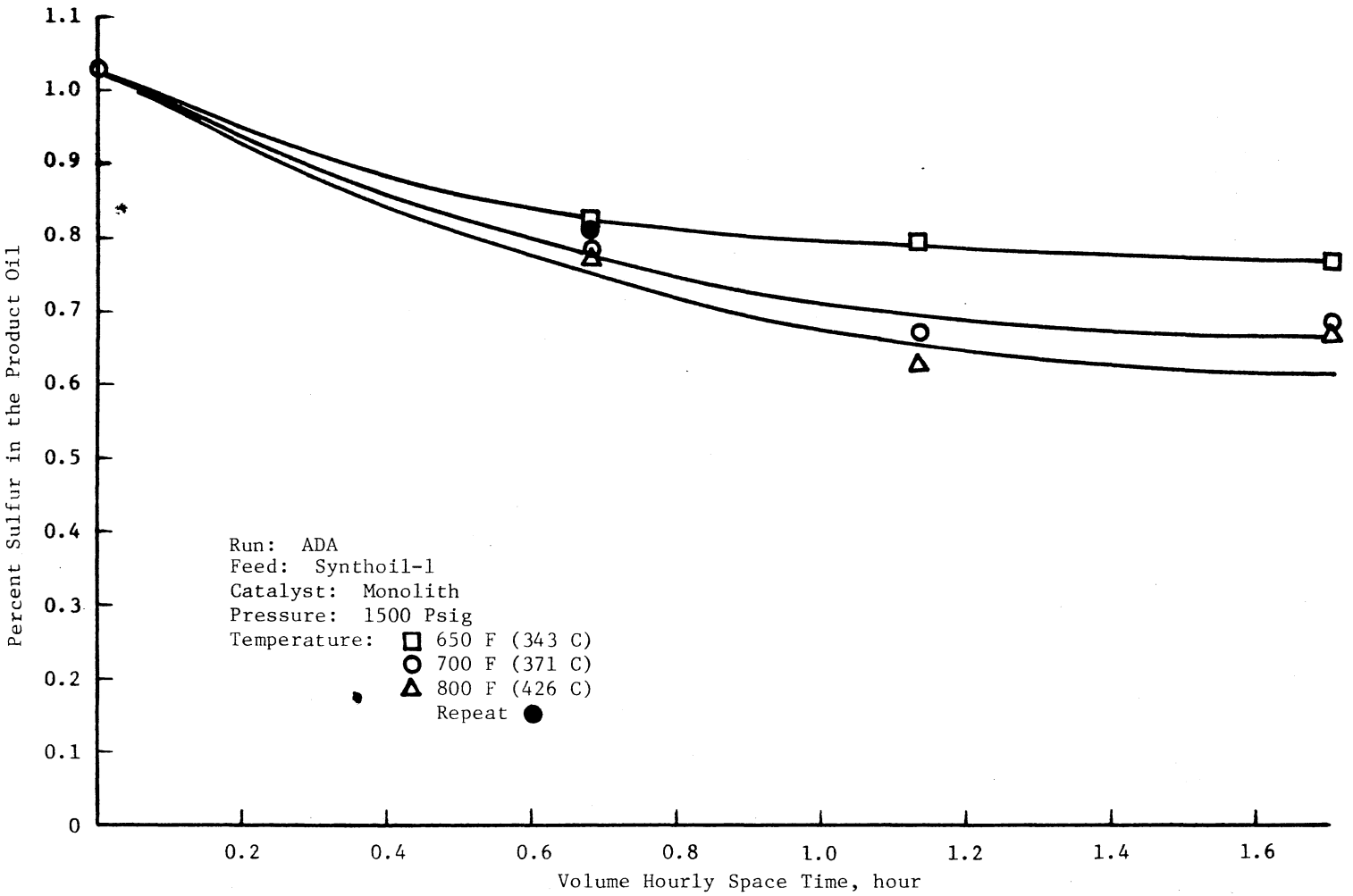

Figure 25. Synthoil-1 Desulfurization Response to Change in Space Time and Temperature

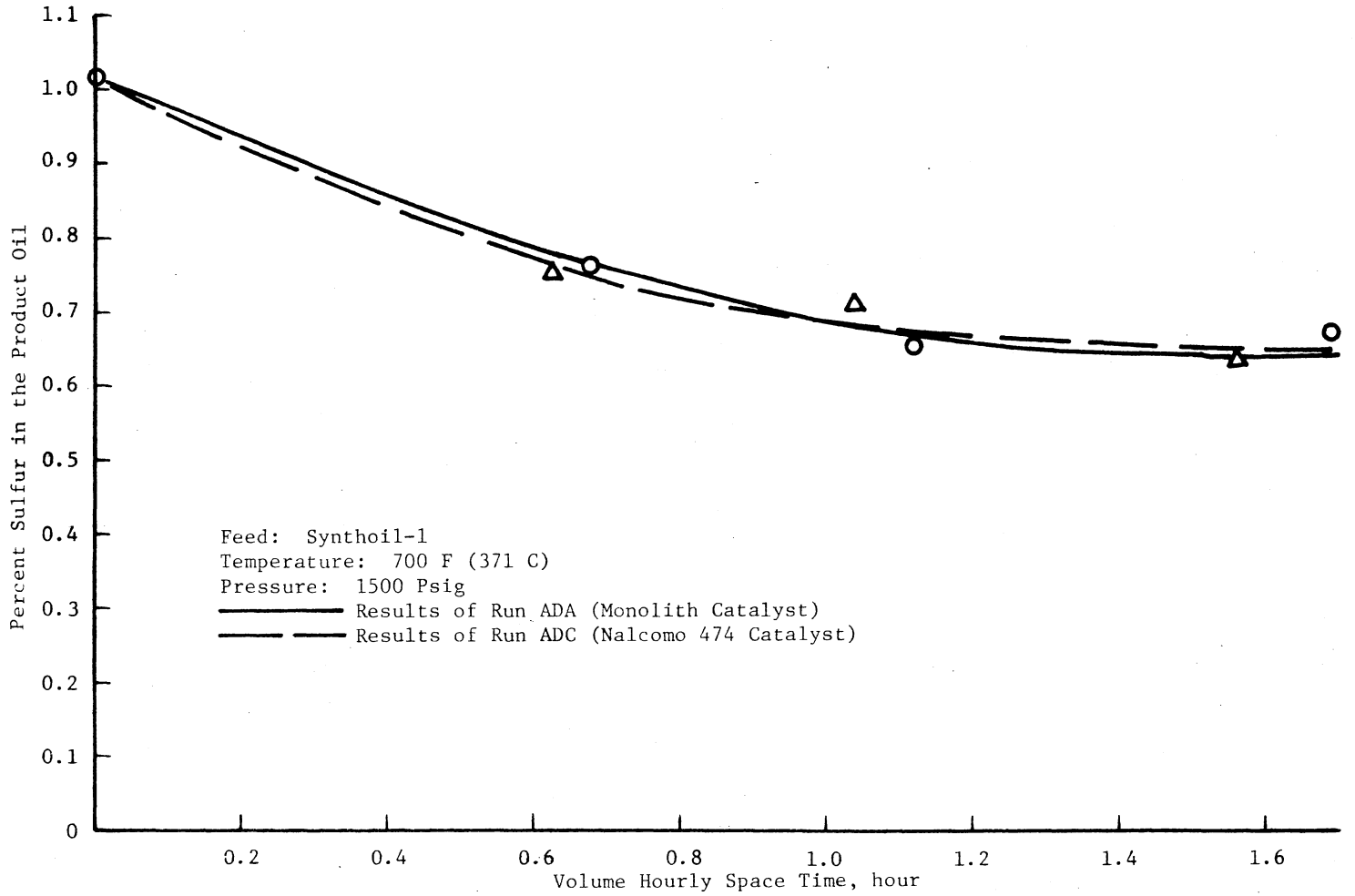

Figure 26. Synthoil-1 Desulfurization, Comparison of Nalcomo 474 and Monolith Catalysts on Volume Hourly Space Time Basis, 700 F (371 C)

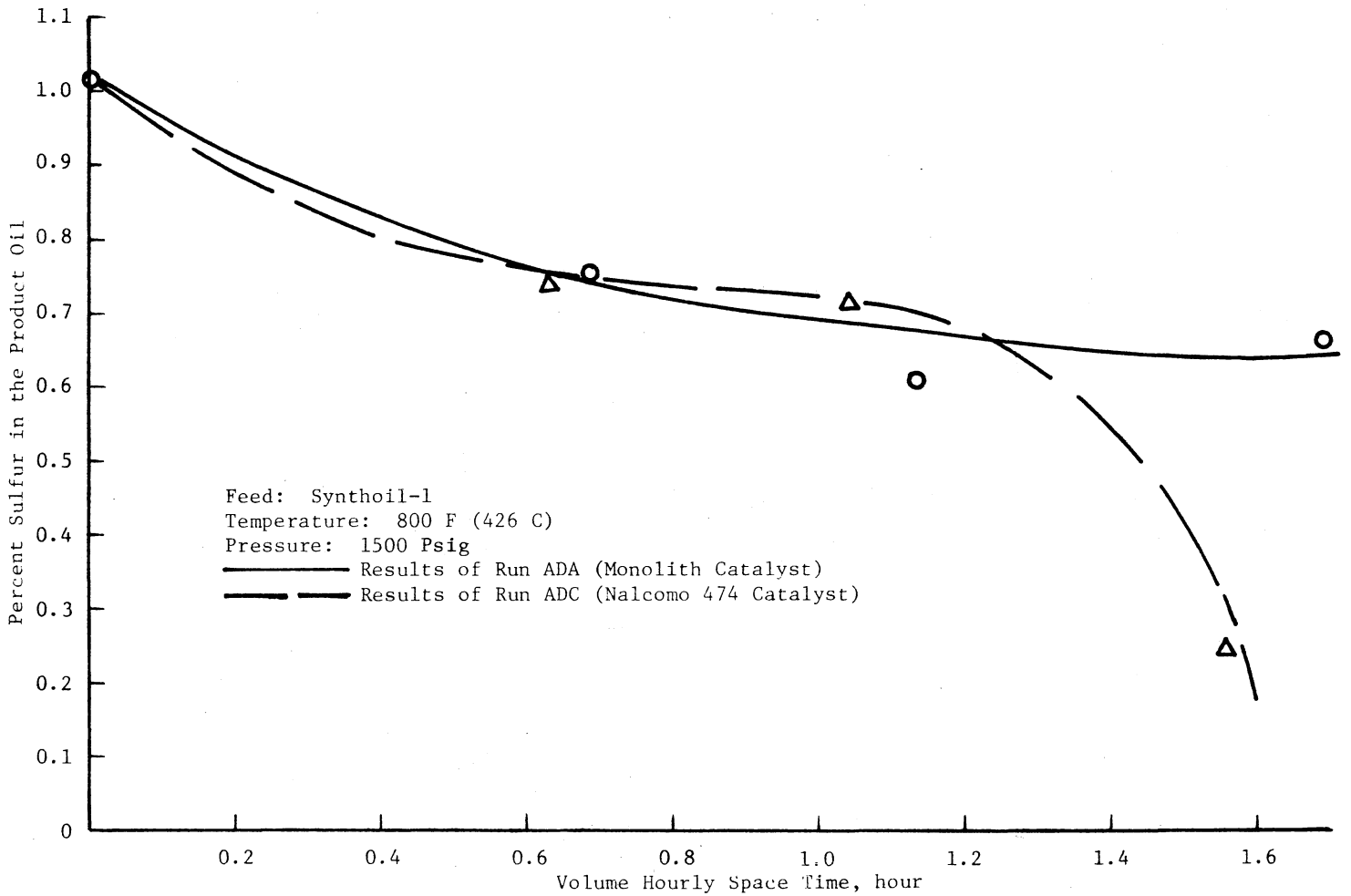

Figure 27. Synthoil-1 Desulfurization, Comparison of Nalcomo 474 and Monolith Catalysts on Volume Hourly Space Time Basis, 800 F (426 C)

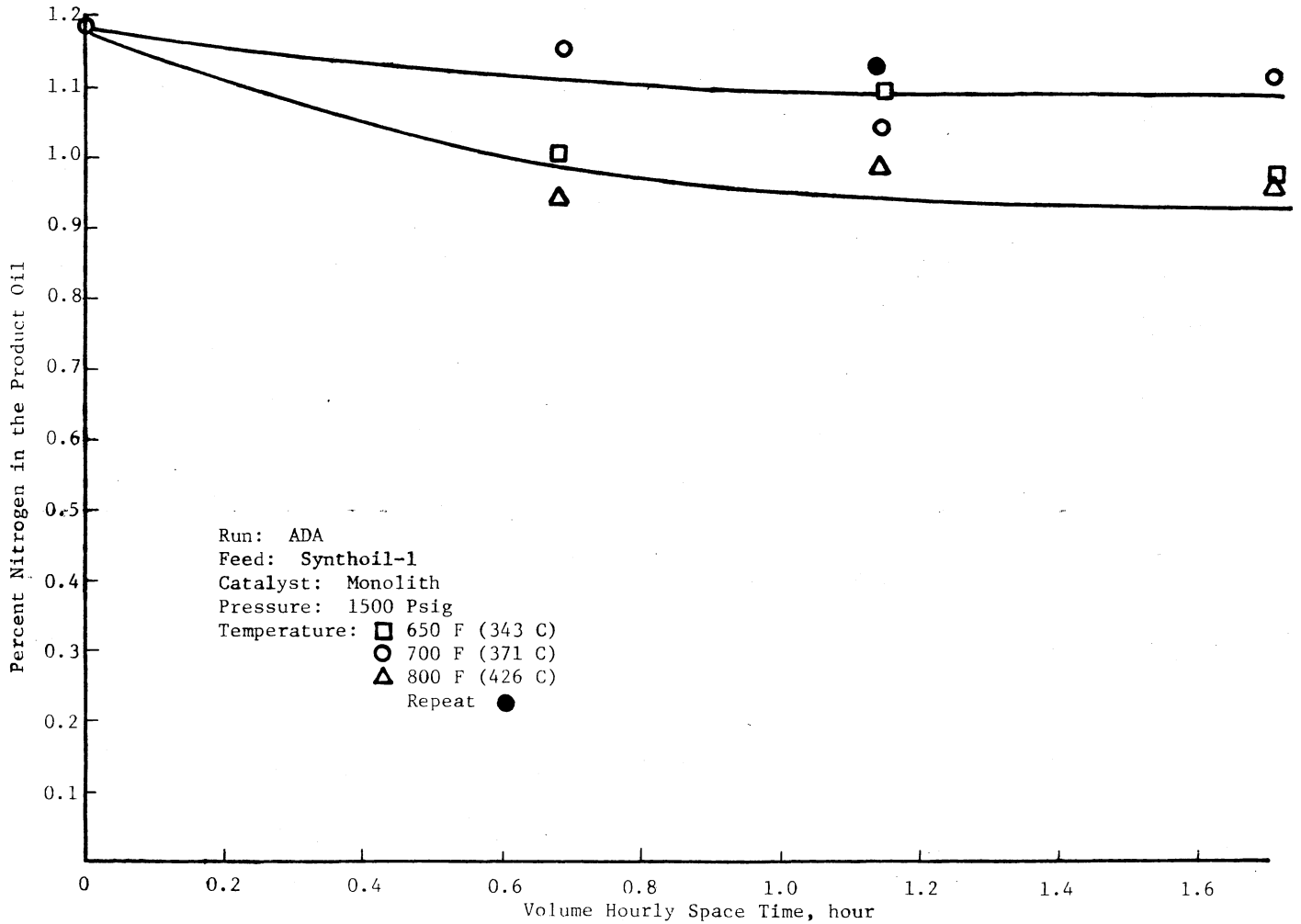

Figure 28. Synthoil-1 Denitrogenation Response to Changes in Space Time and Temperature

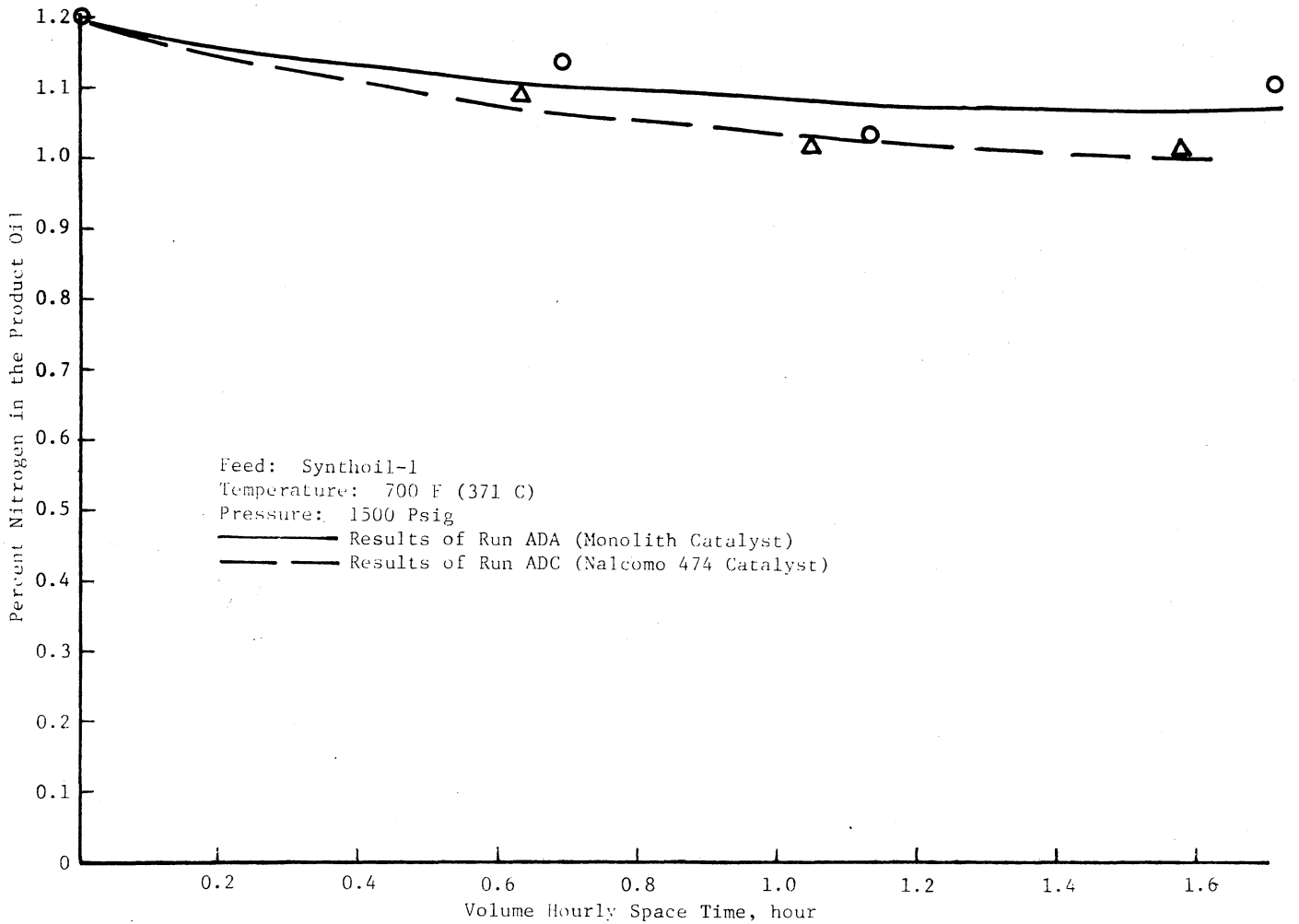

Figure 29. Synthoil-1 Denitrogenation, Comparison of Nalcomo 474 and Monolith Catalysts on Volume Hourly Space Time Basis, 700 F (371 C)

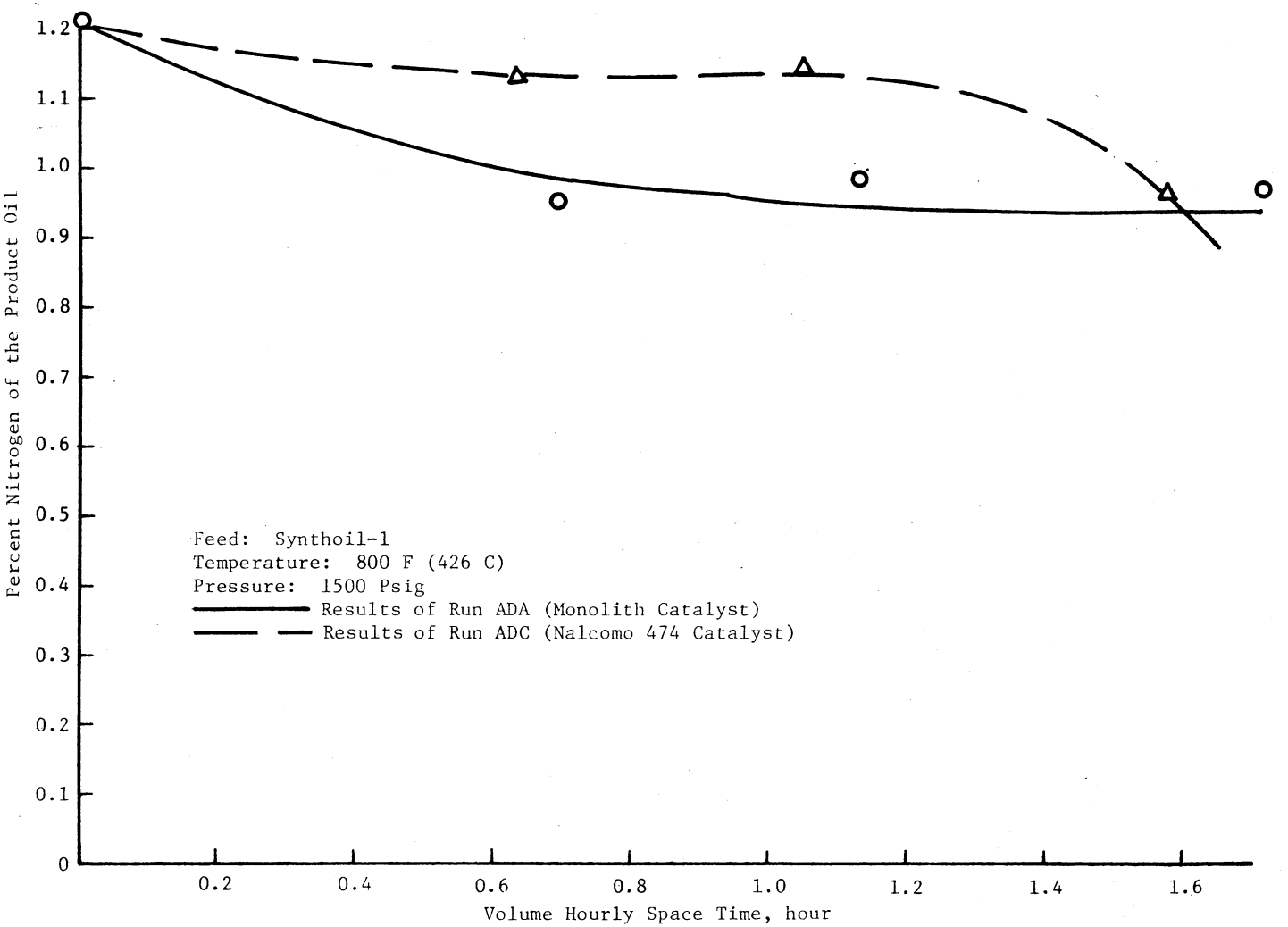

Figure 30. Synthoil-1 Denitrogenation, Comparison of Nalcomo 474 and Monolith Catalysts on Volume Hourly Space Time Basis, 800 F (426 C)

Figures 23 and 24 show the effect of pressure on desulfurization and denitrogenation respectively. This was studied at a space time of 1.11 hour and a temperature of 700 F (371 C). The broken lines in these figures refer to Run ADC which used the Nalcomo 474 catalyst. Both of the figures show that the effect of pressure is significant up to 500 psig. After that, it starts diminishing and beyond 1000 psig, the effect is almost zero. As is obvious, the effect of pressure is the same in both of the Runs, ADA and ADC. But the activity of the Nalcomo 474 catalyst used in Run ADC appears to be somewhat lower than the activity of the monolith catalyst used in Run ADA when compared on a volume hourly basis.

Figure 25 shows the response of desulfurization to changes in space time and temperature. Beyond 1.0 hour, space time has a negligible effect.

There seems to be almost no difference between desulfurization at 700 F (317 C) and at 800 F (426 C). However, temperature increase from 650 F (343 C) to 700 F (371 C) increases desulfurization, especially, at higher space times.

Figure 26 shows the comparison of the results of Runs ADA and ADC. The response of sulfur removal to change in space time at 700 F (371 C) and 1500 psig is the same in both the runs. Figure 27 shows a similar comparison at 800 F (426 C). Here, the influence of space time is the same up to 1.2 hours. Beyond this space time, the difference in results of Run ADA and ADB is very large, indicating increase in activity of Nalcomo 474.

Figure 28 shows the effect of space time and temperature on denitrogenation. Space time beyond 1.0 has almost no effect at all. Denitrogenation increases as temperature is increased from 700 F (371 C) to 800 F (426 C), but at 650 F (341 C), the results show a large scatter in the data.

Figures 29 and 30 show the comparison of the denitrogenation results of Runs ADA and ADC. At 700 F (371 C), the difference between the two is rather marginal, indicating that denitrogenation activity of monolith and Nalcomo 474 catalysts at these conditions is about the same. However, at 800 F (426 C), the results show appreciable difference. The Nalcomo 474 catalyst shows less activity for nitrogen removal up to a space time of about 1.5 hours. Though on Nalcomo 474 there is no data point beyond 1.55 hour, the tendency for denitrogenation to increase beyond 1.5 hour may be important to note. An increase in residence time to 1.8 hour or so, is expected to appreciably increase denitrogenation in the case of Nalcomo 474. This effect is somewhat similar to that observed in desulfurization (refer to Figure 19).

All of the results presented above will be discussed in the next chapter.

The Run on Solvent Refined Coal (SRC)

As mentioned on page 75, an attempt was made to hydroprocess Solvent Refined Coal (SRC) in Reactor-System I. Though this run had to be abandoned due to problems with the pumpability of the feedstock, the experience of working with Solvent Refined Coal will be narrated so that it forms a background for future work on SRC.

The feedstock was received from the Pittsburg and Midway Coal Mining Company. The ultimate analysis of the stock is given in Table VI. The stock was in the form of fragile solid chips which could be easily placed in the feed tank, 27. The heating arrangement on the experimental set up was revamped to provide thorough and uniform heating of the oil feed lines and the pump. Special attention was given to heating around bends, fittings, valves, etc. The temperatures of the feed tank, the pump and the tube line up to the reactor inlet were kept at 450 $\pm$ 50 F (232 $\pm$ 10 C). Even under these conditions the oil did not flow into the pump. Heating was supplemented by wrapping more heating tapes around the tubes to forestall any possibility of cold spots developing anywhere in the system. But all this was of no avail.

Though the stock in the feed tank was seen to have melted, the whole mass looked quite different from usual newtonian liquids. A rod, which was kept in the feed tank for stirring the material, would have SRC rapidly solidifying on it immediately after withdrawing it from the tank. This showed that heat and mass transport properties of the melted SRC were not at all like those of the liquids normally dealt with in these studies. Thinking that the gravitational force (feed method to the pump barrel) may not be sufficient to overcome the viscous resistance to flow, the feeding system was modified so that higher external pressures could be applied to the feed tank.

The modified form of the feed system is shown in Figure 31. It consisted of a one liter stainless steel sampling bomb connected very near to the pump inlet. The bomb was thoroughly wrapped with heating

TABLE VI

PROPERTIES OF SOLVENT REFINED COAL

Carbon*	86.99 wt. %
Hydrogen*	5.61 wt. %
Nitrogen*	2.08 wt. %
Sulfur*	0.78 wt. %
Oxygen*	4.39 wt. %
Ash*	0.15 wt. %
Fusion Point*	335 F

* Analyzed by Pittsburg and Midway Coal Mining Company.

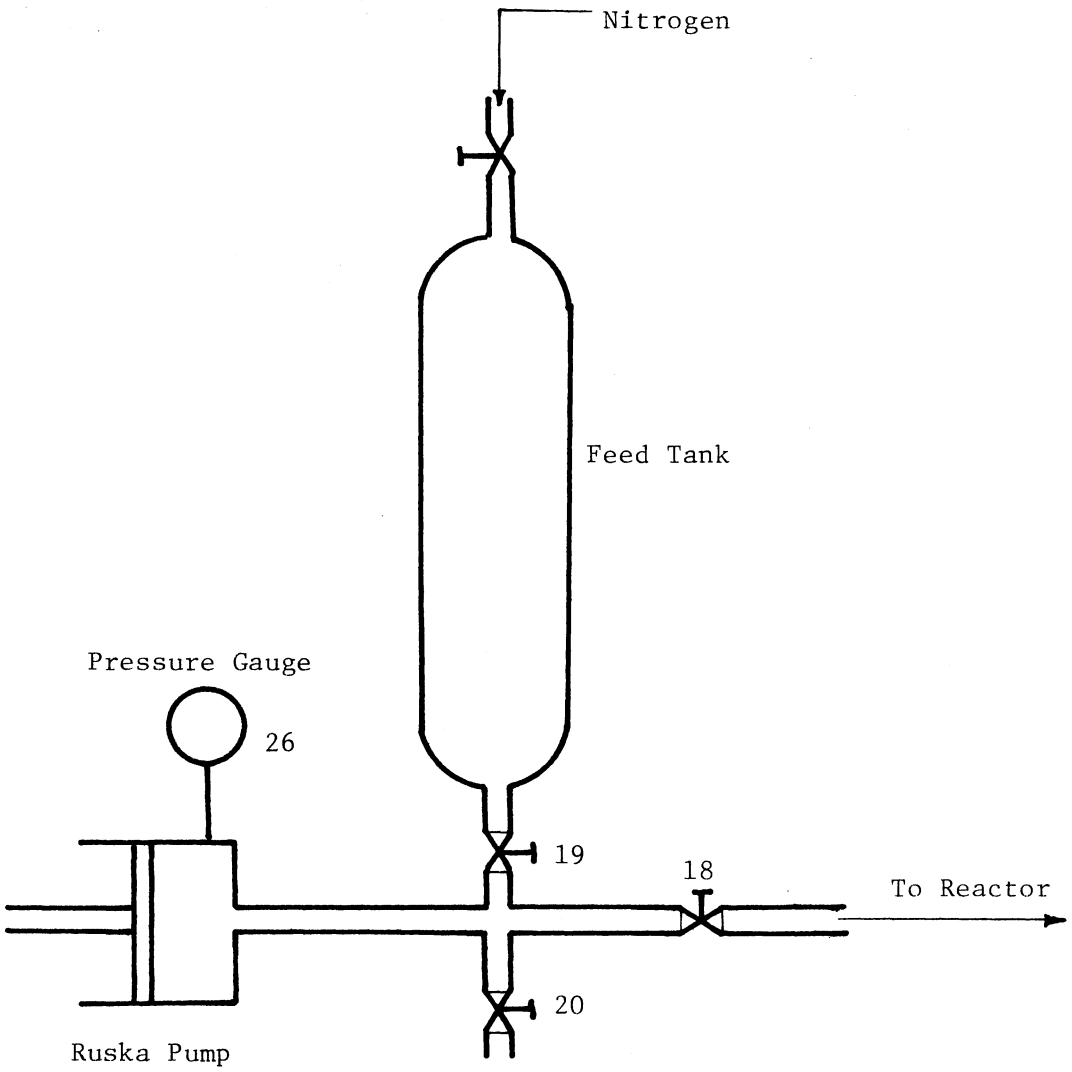

Figure 31. Modified Feed System for Solvent Refined Coal

tapes and then insulated. A provision was made for pressurizing this bomb with nitrogen from the top. The bomb was filled with the feedstock by crushing the feedstock into smaller pieces. It was then heated to 450 ± 50 F (323 ± 10 C) and after a few hours, nitrogen pressure was applied. The liquid started moving into the pump and after filling the pump, nitrogen pressure was removed, valve 19 closed and the pump started. Valve 18 was kept closed for the pressure to build up. When the pressure shown by Gauge 35 was 1500 psig, Valve 18 was opened but 17 (see Figure 2) was kept closed for pressure on Gauge 36 to be 1500 psig. The pump was kept running for sometime for the pressure to build up to this level. But in the meantime, the screw shaft, that drives the plunger of the pump, gave way resulting in shut down of the whole system.

On opening the oil tube, to release the pressure, a surge of dark fumes erupted followed by the flow of the oil. But the oil would solidify immediately after being exposed to the atmosphere. So, to keep the oil flowing, the opening was kept warmed with a heating lamp. The oil from the pump was withdrawn by opening the fitting at the inlet of the pump. The pump and all the tubing system was opened to check for plugging. A lot of solid material was seen sticking to the plunger and the cylinder of the pump. These were cleaned and the pump put back in operation after replacing the broken part. The plugging of the tubes, valves and pressure gauges 35 and 36 could not be removed. These were changed and the Reactor System made ready for a run on a different oil.

The material that plugged the whole feed system was found to have tiny solid particles which looked like free carbon. That might indicate that these solid particles were present, as such, in the melted

feedstock. Also, dark fumes, due to the volatile matter present in the feedstock, were associated with the material that was to flow. Therefore, the entire feed formed a sort of three phase system which changed the viscosity and hence the flow characteristics of the melted feedstock. The pump and the Reactor-System were not designed to process such a material.

Therefore, to run SRC, drastic changes in the Reactor-System would be needed. Even that may not help and one might have to resort to the use of a solvent in which to dissolve the SRC, filter out the solid particles and then hydroprocess the filtered material.

CHAPTER V

DISCUSSION

This chapter will include detailed discussion on the following aspects.

(1) Performance of the trickle bed reactor and its bearing on the results of this study.

(2) Reproducibility and precision of data presented in Chapter IV.

(3) Comparison of the desulfurization and denitrogenation activities of monolith and Nalcomo 474 catalysts on raw anthracene oil.

(4) Similar comparison of the two catalysts on Synthoil-1.

(5) Reasons for the difference in activities of the two catalysts on two different feedstocks.

(6) Reasons for the sharp increase in desulfurization of Synthoil-1 when using Nalcomo 474 catalyst at volume hourly space time of 1.5 hours and temperature of 800 F (426 C).

(7) Space time, temperature and pressure effects on desulfurization and denitrogenation of raw anthracene oil and Synthoil-1.

Performance of the Trickle Bed Reactor

The extensive literature study on reactor engineering presented in Chapter II has made it clear that fluid dynamic conditions in the reactor can deviate much from ideality and thus can adversely affect reactor performance. The non-ideal fluid dynamic conditions

result from maldistirbution of the liquid and axial dispersion. The effect of these variables on conversion or kinetics of a chemical reaction can be accounted by using the correlations of Henry, et al. and Mears (refer to Chapter II). But the objective of this study is not to determine the effect of these factors on sulfur or nitrogen removal. Nevertheless, a discussion of fluid dynamics, in trickle flow, is necessary to have an idea of the importance of the above factors to the present study.

Sivasubramanian (40) in a recent study on denitrogenation of raw anthracene oil using a similar experimental set up as used in this study, observed that a modified Henry and Gilbert (20) relation explains his results best. This suggests that the catalyst was not fully wetted and an account must be made of the ineffective catalyst wetting. In yet another recent work, Ahmed (62) ran Synthoil on the same reactor as used in this study. The catalyst used by him was Ni-Mo-Al_2O_3. But, because of the rather severe operating conditions, the reactor became plugged after 75 hours of operation. To study the plugging and pressure drop, the reactor was removed and cut into four segments. Visual observation of the cross-sections of each segment showed that the plugging was uniform throughout the cross-section. This suggested that the Synthoil had been uniformly distributed over the whole of the reactor cross-section and thus almost all the catalyst was effectively wetted. Figure 32 is a photograph of the cross-section of the reactor showing all parts equally plugged. In previous studies, Sooter (26) and Satchell (27) observed that reducing particle size from 8-10 mesh to 40-48 mesh did not affect desulfurization and denitrogenation of raw anthracene oil. If liquid distribution was important, the reduction

Plugged Material

Catalyst Particle

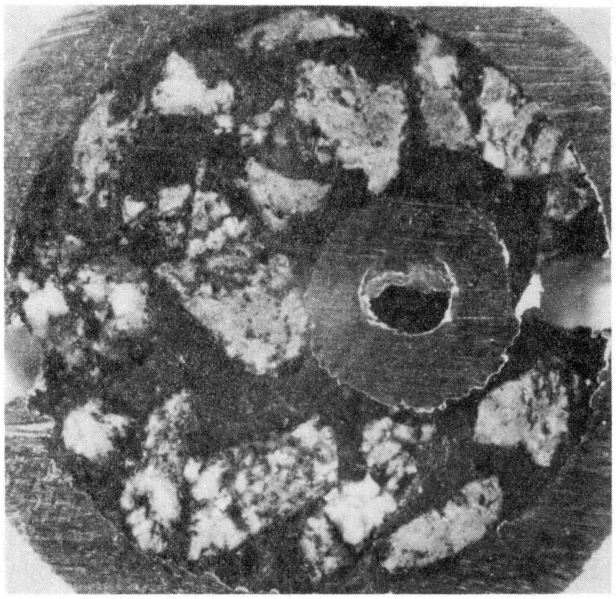

Thermowell

Figure 32. Cross Section of the Plugged Reactor

in particle size should increase conversion by improving liquid distribution. Since this did not happen, they concluded that under the conditions studied, liquid distribution was not a problem in reactors at Oklahoma State University. Wells (29) has argued that the lack of change in conversion on account of reduction in particle size in studies of Sooter and Satchell may be due to cancelling of various effects of particle reduction. But, reduction in particle size introduces two effects, 1) it improves liquid distribution, and 2) it increases the catalyst effectiveness factor. Both of these effects favor increase in conversion if liquid distribution and pore diffusion significantly limit conversion. Since they do not oppose each other, question of their cancelling each other's effect does not arise. Hence the argument of Wells is not tenable. Therefore, in the absence of any other conclusive study, fluid dynamics will be considered to have no or negligible effect on the results of this study.

Regarding axial dispersion, Sooter (26) observed a slight decrease in sulfur removal (88.7 percent to 85.2 percent) when bed height was reduced from 20 inches (50.8 cm) to 10 inches (25.4 cm) at a fixed space time. He attributed this to the effect of axial dispersion at the bed height of 10 inches (25.4 cm). The bed height used in this study was 14 inches (35.56 cm). So, the effect of axial dispersion, if at all present, would be lower than observed by Sooter and for all practical purposes, negligible. Hence fluid dynamics will not be considered to have bearing on the interpretation and analysis of the results of this study.

The foregoing discussion on reactor performance was related to conventional packed beds. But two of the three runs in this study

were conducted with a monolith catalyst which had an entirely different structure. The problems of flow distribution and the pattern of liquid flow through the reactor would, therefore, be different from those in the conventional beds. The major difference between the two beds is in the geometry of the void spaces in them. In the conventional, randomly packed bed these void spaces are irregular in shape and are interconnected with each other. In case of a bed of stacked monoliths, the voidage is in the form of regular channels with no interconnection between them. These channels are enclosed within an outer non-conducting wall. Therefore, the liquid that is likely to flow along the wall of the reactor, due to poor liquid distribution, will have no way to return to the channel. On the other hand, with randomly packed bed, the liquid can flow from the wall to the bed. To guard against this drawback of the monolith bed, three redistributors were provided in the bed (refer to Chapter III, page 48). These distributors were in the form of rings closely fitting inside the reactor tube and were designed to serve as a sealing between the reactor wall and the catalyst bed. Any liquid that would tend to flow along the wall of the reactor would then get redirected back to the center of the catalyst bed. Therefore, the liquid distribution should not affect the results obtained from runs conducted on the monolith catalyst.

Other significant difference between the performance of the two beds can be due to the general flow pattern of the liquid. In the conventional packed beds, the liquid may flow as rivulets through the void spaces in the bed. But the flow of liquid through the regular channels of the monolith bed may either be annular, in which case gas passes as a continuous phase through a moving liquid film on the walls, or slug

like (39). Which of these two types of flow prevades depends on the gas-liquid ratio, physical properties of the fluids, channel size, channel length and on the mode of entrance of the gas and liquid into the channel (39). There is little previous work which can guide one in predicting the type of flow under the operating conditions of the present study. Also, monoliths have never been tried for desulfurization and denitrogenation of petroleum or coal-derived feedstocks under trickle flow conditions. Therefore, one cannot say as to how the flow regime in a bed of stacked monoliths would affect the kinetics of desulfurization and denitrogenation reactions. Experiments in this study were also not designed to gauge these effects in particular. However, one reason for the difference in the observed activities of the two catalysts can be the different fluid dynamic conditions in the two cases. How much these conditions affect the conversion in the two cases cannot be said.

Reproducibility and Precision of Data

The results given in Chapter IV can be imprecise due to irregularities either during reactor operation and sample collection or during analysis of samples for sulfur and nitrogen content. To make a thorough check on the reproducibility of reactor operation, each run should be duplicated from catalyst preparation and reactor loading stage up to the collection of the final samples. Since each run on the reactor required approximately ten days of continuous operation, complete duplication was not considered unless reproducibility should be gravely in doubt. Therefore, no run in this study was duplicated in its entirety. But reproducibility checks must be made so that the results

can be addressed with confidence. The following guidelines were considered sufficient as a measure of the reproducibility of reactor operation:

(1) Many studies have been successfully conducted on the trickle flow reactors at Oklahoma State University. The precision of the experimental set up and the tolerances regarding temperature, pressure and space time have already been established. The variations in these parameters observed during reactor runs for this study would be compared with these established values.

(2) Overall reproducibility of the runs will be checked by comparing the results of two runs on the same feedstock.

(3) Within the same run, duplicate data points were taken at the same conditions of reactor operation after start up stabilization and before shut down. These results would be compared.

An exothermic reaction taking place in a fixed bed reactor calls for precise temperature control. Development of hot spots in any part of the catalyst could trigger undesired side reactions and subsequently deactivate the catalyst. In the present study, the temperature over the catalyst bed varied by $2^{o}F$ ($\pm$ $1^{o}C$) from the desired value. This is the same as observed in the previous studies (26,27). Sooter (26) measured the radial temperature gradient across the catalyst bed and found the maximum value to be 3.1 F (1.7 C) at 750 F (400 C). This variation is considered marginal as compared to the desired value of 750 F (400 C). The above observations regarding temperature precision apply to Run ADC only in which the position of the thermowell was the same as in previous studies, i.e., coaxial through the center of the bed. But as mentioned in Chapter III, in Runs ADA and ADB, the

thermowell could not be put through the center of the bed because of the segmental shape of the monolith catalyst. The thermowell was placed outside the reactor tube i.e., between the reactor tube and the heating blocks. The temperature measured with this thermowell was considered to be the temperature of the reactor. To check as to how much error this introduces in the temperature measurements, Run ADC (which used Nalcomo 474 catalyst in pellet form) was conducted with thermowells in both the above positions, i.e., inside and outside of the reactor. Using the same thermocouple, a maximum difference of 3 F (1.7 C) was observed between measurements with inner and outer thermowells. Generally, the difference was only 2 F (1 C). Therefore, no error beyond the usual would be introduced in the results by placing the thermowell outside the reactor as in Runs ADA and ADB.

A maximum pressure deviation of 20 psig was observed in this study. As discussed in Chapter II, the effect of pressure change on desulfurization and denitrogenation is insignificant when the reactor is operated at high pressures. Therefore, variations of 20 psig in reactor pressure are not likely to introduce any error in the results.

A positive displacement pump was used for pumping oil into the reactor. This would give constant flow rate once flow adjustment has been made, and since the reactor bed volume would also remain constant for a particular run, space time will not vary. Hence, there would be negligible error due to space time. Any time the space time was changed, when the run was in progress, a line out time of about three reactor volumes was allowed before starting collection of a representative sample. This would take care of fluctuations due to change in space time. Sometimes the pump had to be stopped when it needed to

refilled. This can introduce some error in the results. But this error should be small because the pump was stopped only for 5 to 10 minutes while the sample was an average of two hours of reactor operation. However, any error due to this will be considered while analyzing the results.

Figures 13, 14, 16 and 18, given in Chapter IV, show the comparison of the results of Run ADB with the studies of Sooter (26) and Satchell (27) on the same feedstock, i.e., raw anthracene oil. The responses of desulfurization and denitrogenation to changes in space time, pressure and temperature are similar in all three studies. This assures overall reproducibility of Run ADB. The use of different catalyst in this study from that of Sooter and Satchell should not matter because the response of desulfurization and denitrogenation is generally a function of the feed characteristics.

Runs ADA and ADC were conducted with Synthoil. Figures 23, 24, 26 and 29 show that responses of desulfurization and denitrogenation of Synthoil to changs in reactor operating conditions are similar at 700 F (371 C) in both of the runs. This means that the results of Runs ADA and ADC are reproducible at 700 F (371 C). However, at 800 F (426 C) there was a sharp increase in desulfurization of Synthoil in Run ADC (which used Nalcomo 474 catalyst) at space time of 1.5 hours. A similar effect was not there in Run ADA in which the monolith catalyst was used. But the reproducibility of the results of Run ADC at 800 F (426 C) is available in a very recent study of Ahmed (62) who ran Synthoil on Ni-Mo-$\gamma Al_2 0_3$ catalyst. Figure 33 shows his results.

Reproducibility checks made in the same run by sampling reactor product at two similar conditions are shown by solid data points on

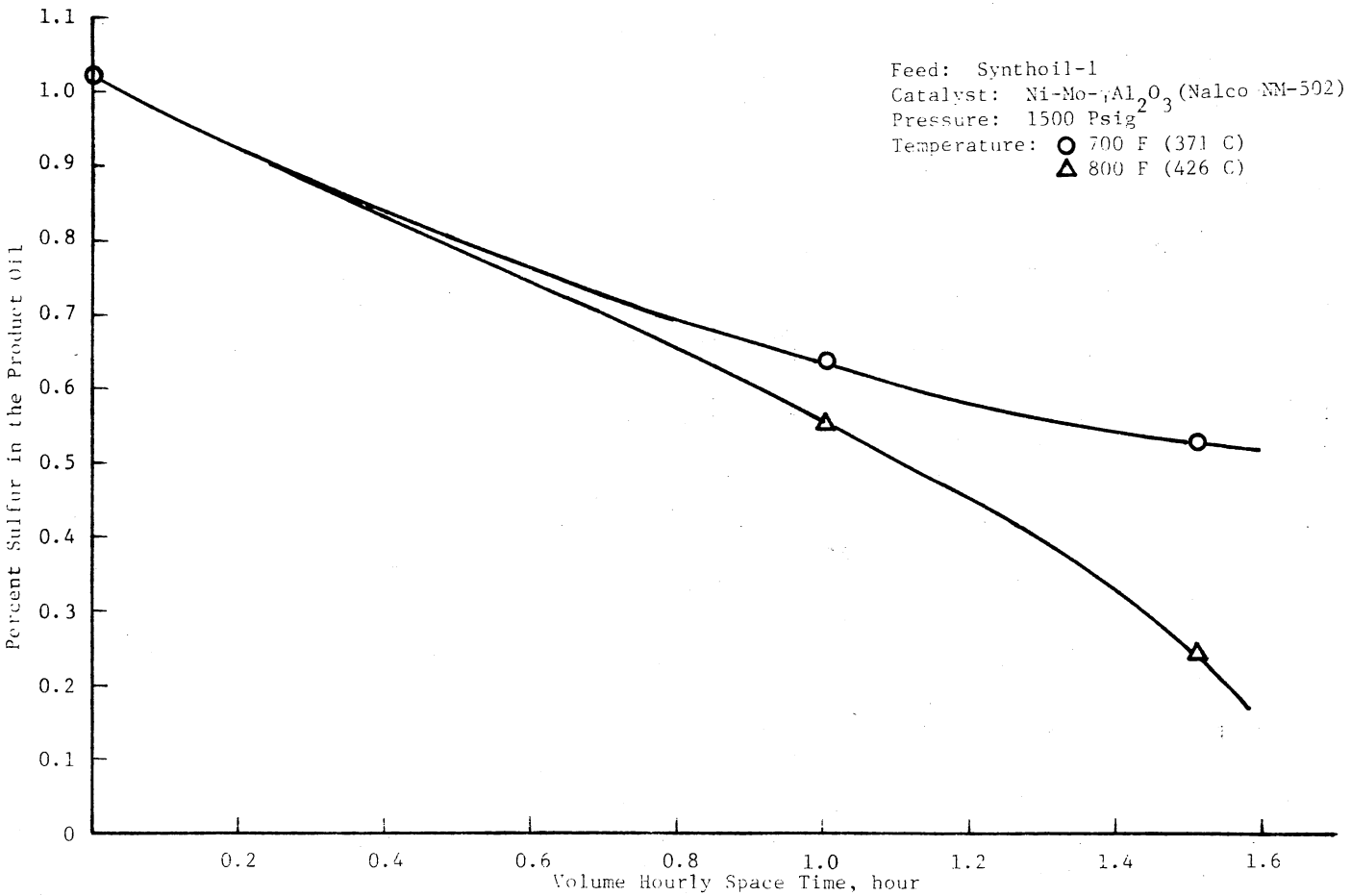

Figure 33. Synthoil-1 Desulfurization Response to Changes in Space Time and Temperature, Results of Ahmed

figures in Chapter IV. However, these points will be true reproducibility checks only if there were no aging or deactivation of the catalyst over the period of the reactor run. Mehta (65) had conducted deactivation studies of Nalcomo 474 catalyst with raw anthracene oil as the feedstock. He observed no deactivation in sulfur removal up to 200 hours of continuous reactor operation. Satchell (27) and Wan (59) also found no appreciable deactivation with respect to nitrogen removal while using the same feedstock over Nalcomo 474 catalyst. Since the catalyst with larger pore size should be more stable in its activity than the catalyst with smaller pore size (refer to page 9), the monolith catalyst in Run ADB will be considered to have maintained its activity. Therefore, the duplicate data points in the Run ADB can be used as reproducibility checks. But the catalyst deactivation studies with Synthoil are not available. This work was also not directed to the study of aging as such. However, the desulfurization data of Run ADC at 800 F (426 C) indicates that there was no significant deactivation of the Nalcomo 474 catalyst over the reactor operating conditions studied. If there was appreciable deactivation of the catalyst, the phenomenal increase in sulfur removal, when space time was increased to 1.5 hours at 800 F (426 C), would not have been there. Therefore, the reproducibility checks made in Run ADC were considered to be valid. For the reasons already given, the monolith catalyst in Run ADA would also be considered to have undergone no significant deactivation or aging. Thus, one can say that in spite of Synthoil being a high-boiling stock and with relatively high percentage of ash in it, this feedstock did not significantly deactivate the catalysts over the operating conditions employed in this study.

Analytical Precision: Samples collected from the reactor run Series ADA, ADB and ADC were analyzed for nitrogen and sulfur contents. An estimate of the precision of nitrogen analysis can be had from the analysis of raw anthracene oil and Synthoil given in Appendix D. Table XXXV in Appendix D shows results of 13 nitrogen analyses of raw anthracene oil. The average value is 1.035 weight percent. The standard deviation is 0.053 which is $\pm$ 5.1 percent of the average value. The ntirogen content in all of the samples analyzed was above 0.263 percent. Smith, et al. (66) have shown that precision of the nitrogen analysis technique employed in this study does not change significantly until the sample nitrogen content is 0.1 wt. percent or lower. Therefore, overall precision of the nitrogen results presented in this study on raw anthracene oil would be $\pm$ 5.1 percent of the nitrogen content. Similarly, nitrogen analyses of eleven samples of Synthoil are given in Table XXXVI of Appendix D. The average value is 1.19 and standard deviation is 0.058. This is $\pm$ 5.1 % of the nitrogen content. Since no sample collected from runs on Synthoil contained nitrogen below 0.1 percent, accuracy of all the nitrogen results on Synthoil will be within $\pm$ 5.1 percent, throughout the range of interest.

Sulfur analyses of seven samples of raw anthracene oil are given in Table XXXVII, Appendix D. The average value is 0.471 and standard deviation is 0.025. Sooter (26) had established precision of sulfur analysis on raw anthracene oil. Table VII below shows comparison of the analytical precision in this study with the precision of the results of Sooter. As is evident, precision obtained in this study is comparable to that obtained by Sooter using the same instrumentation.

TABLE VII

ANALYTICAL PRECISION OF THE SULFUR ANALYSIS

Sample #	This Study			Sooter's Study (26)		
	Wt.%S	Dev.	% Dev.	Wt.%S	Dev.	% Dev.
ADB 15	0.221	0.033	±1.5	0.2	±0.008	±4.0
ADB 6	0.139	0.003	±2.1	0.15	±0.005	±3.5
ADB 17	0.067	0.002	±3.04	0.06	±0.005	±8.2

Table XXXVIII in Appendix D gives results of 14 sulfur analyses of Synthoil. The average value is 1.02 wt. percent and the standard deviation is 0.054. The accuracy is ± 5.3 percent of sulfur content in Synthoil. Since the sulfur content in the samples generally ranged from 0.6 to 0.8 wt. percent, the same precision will be taken for sulfur analyses of the samples from reactor runs on Synthoil. Only three samples contained sulfur content in the range 0.25 to 0.3 weight percent. Establishing different precision levels for this range of sulfur content was not considered necessary.

Performance of the Catalysts on Raw Anthracene Oil

As mentioned in Chapter IV, the activity of the monolith catalyst is lower than that of Nalcomo 474 catalyst if compared on volume hourly space time (VHST) basis. Figures 16 and 18 point out this difference

clearly. However, weight of the monolith catalyst used in this study was different from the weight of Nalcomo 474 catalyst used by Sooter (26) and Satchell (27). Therefore, comparison of the catalysts on weight hourly space time (WHST) basis is not only warranted, but will be a better indicator of the difference in activities of the two catalysts.

Comparison on weight basis: Weight hourly space time (WHST) is defined as:

$$\text{WHST} = \frac{\text{Weight of the Catalyst}}{\frac{\text{Weight of Oil}}{\text{Hour}}}$$

Figures 34 and 35 show the sulfur removal comparison on WHST basis at 650 F (343 C) and 700 F (371 C) respectively. Figures 36 and 37 show similar comparison for nitrogen removal. These figures show that even on weight basis, the activity of the monolith is less than that of Nalcomo 474 catalyst. However, comparisons of Figures 34 and 35 with Figure 16; and Figures 36 and 37 with Figure 18, indicate that the difference in activities is less on weight basis than on volume basis.

To suggest reasons for the difference in the performance of the two catalysts, we have to look at the differences in the two catalysts themselves. There are three main considerations.

(1) Different specific surface areas. Nalcomo 474 has 240 m^2/gram and the monolith has only 66 m^2/gram.

(2) Different pore sizes. The most frequent pore radius of Nalcomo 474 is 33 ^{o}A while that of the monolith is 80 ^{o}A.

(3) Different bulk concentrations of Co and Mo and different Co/Mo ratios. Table XXVI gives these values for both the catalysts.

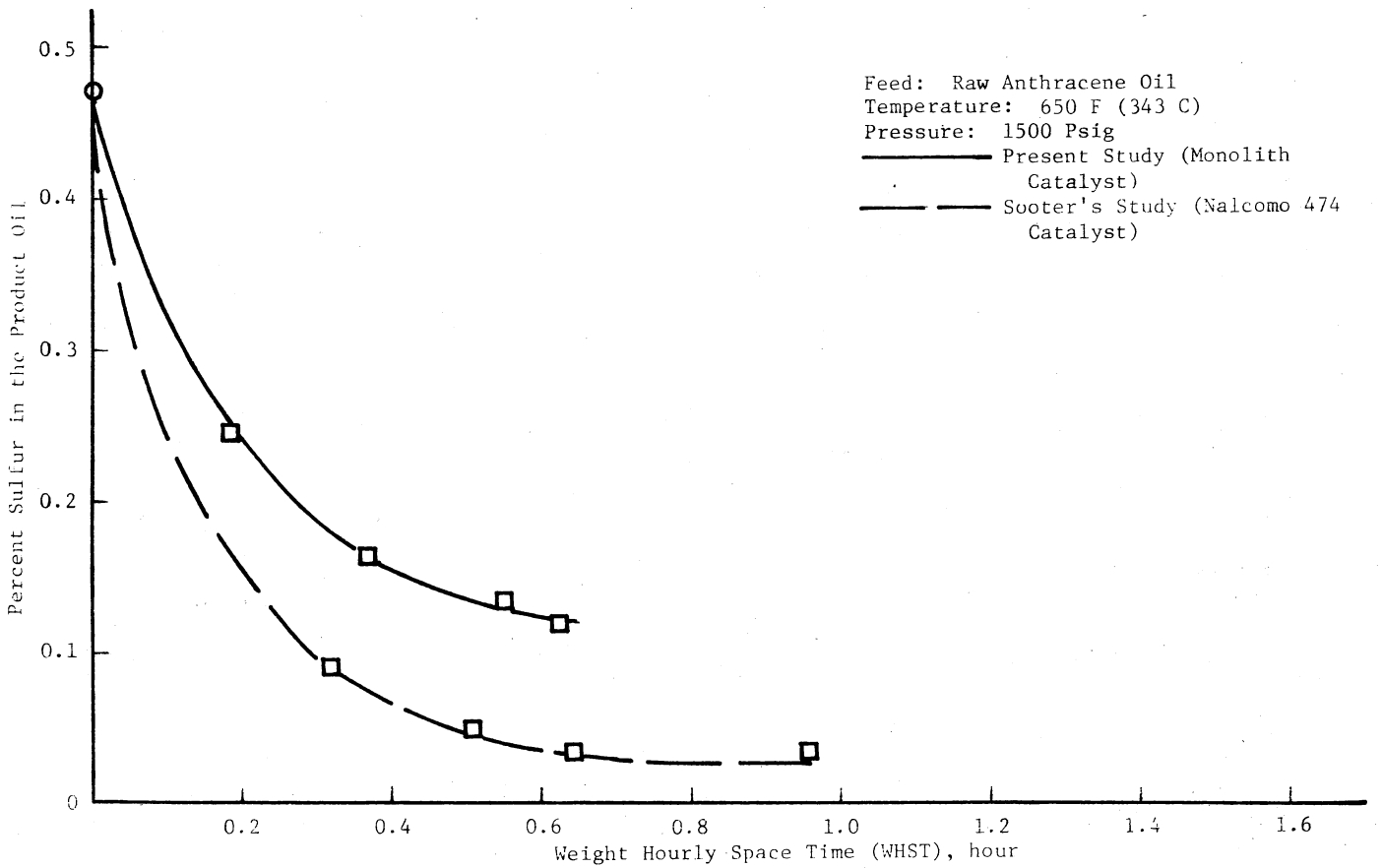

Figure 34. Raw Anthracene Oil Desulfurization, Comparison of Nalcomo 474 and Monolith Catalysts on Weight Hourly Space Time Basis, 650 F (343 C)

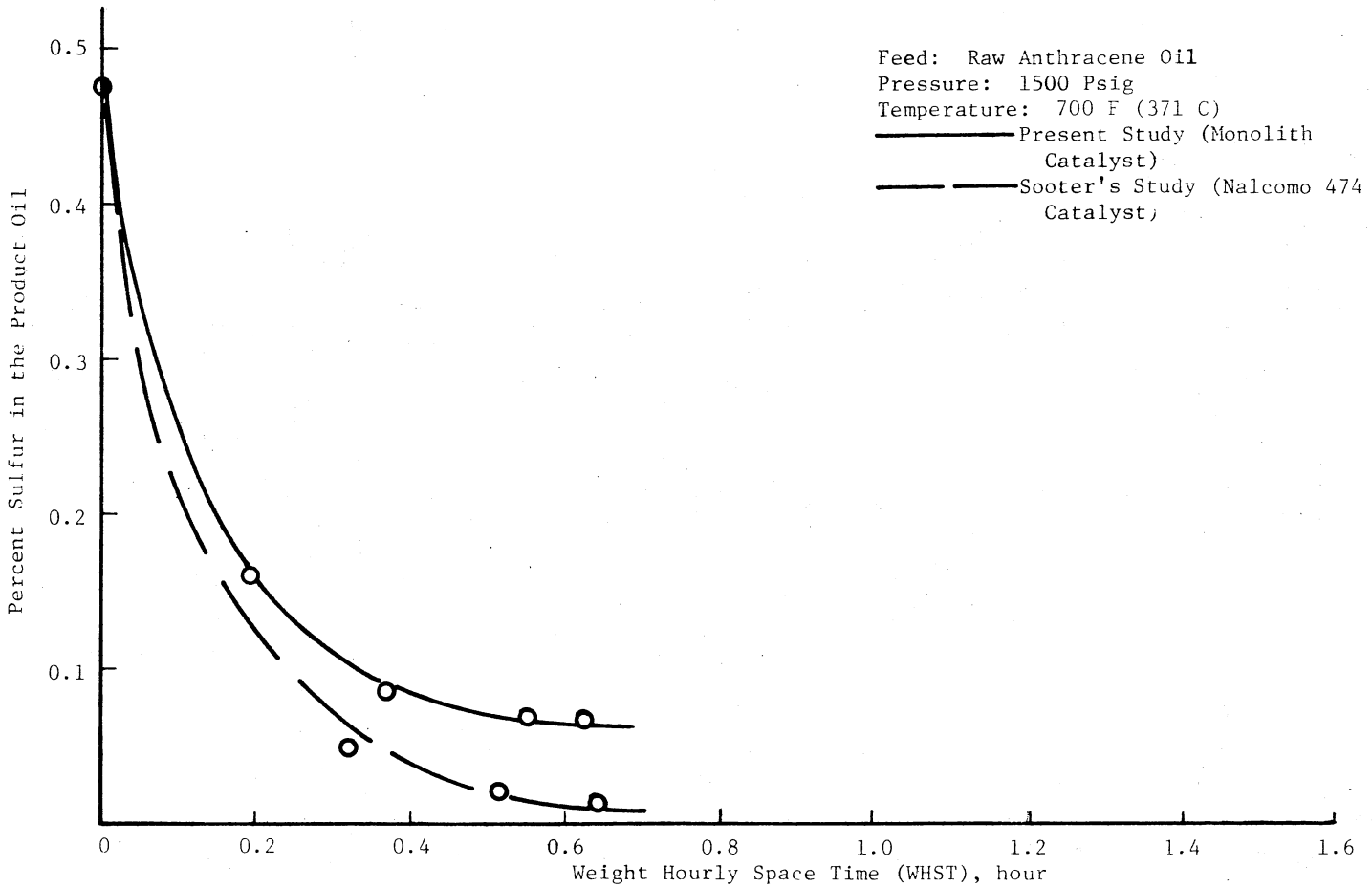

Figure 35. Raw Anthracene Oil Desulfurization, Comparison of Nalcomo 474 and Monolith Catalysts on Weight Hourly Space Time Basis, 700 F (371 C)

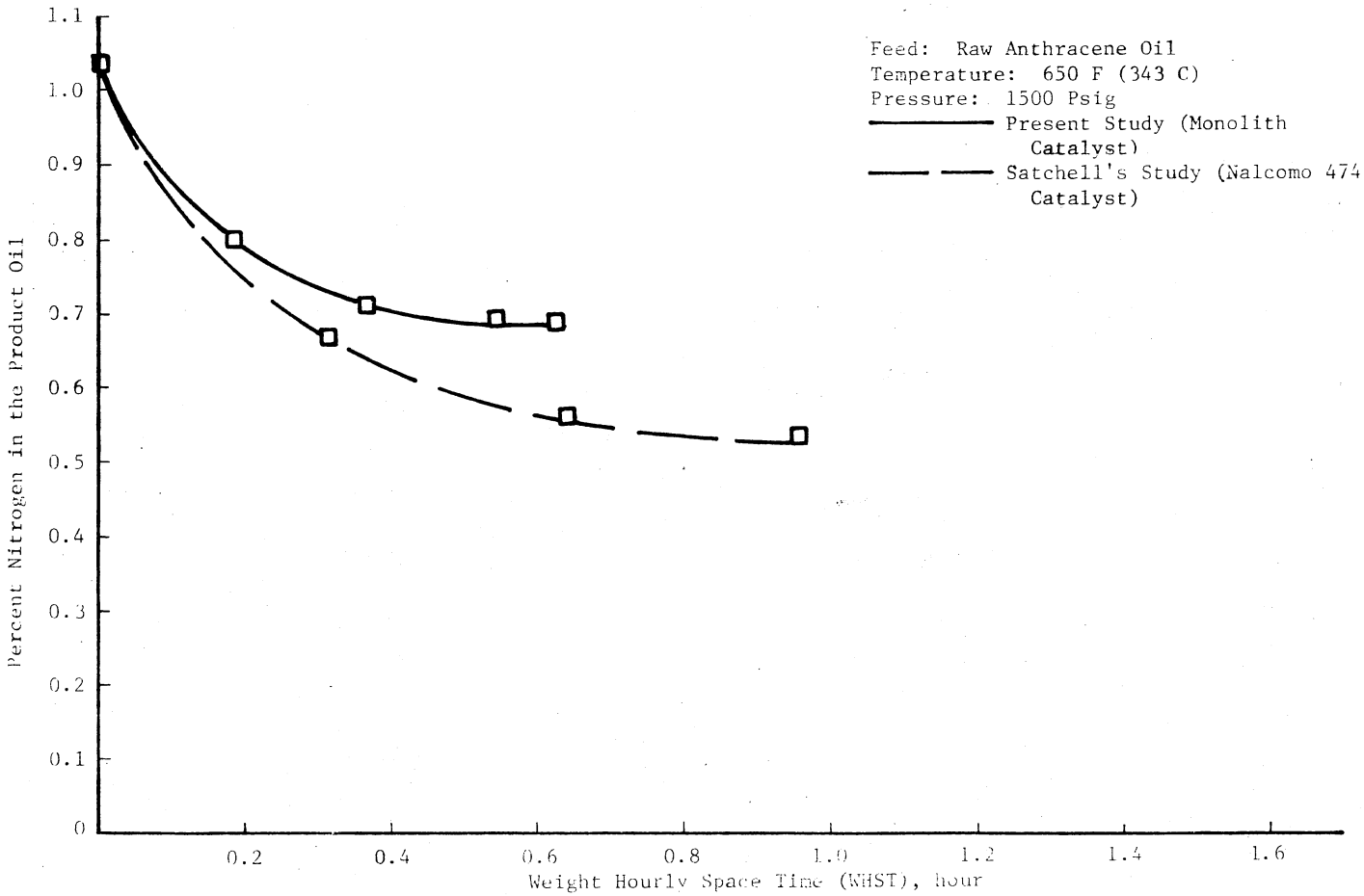

Figure 36. Raw Anthracene Oil Denitrogenation, Comparison of Nalcomo 474 and Monolith Catalysts on Weight Hourly Space Time Basis, 650 F (343 C)

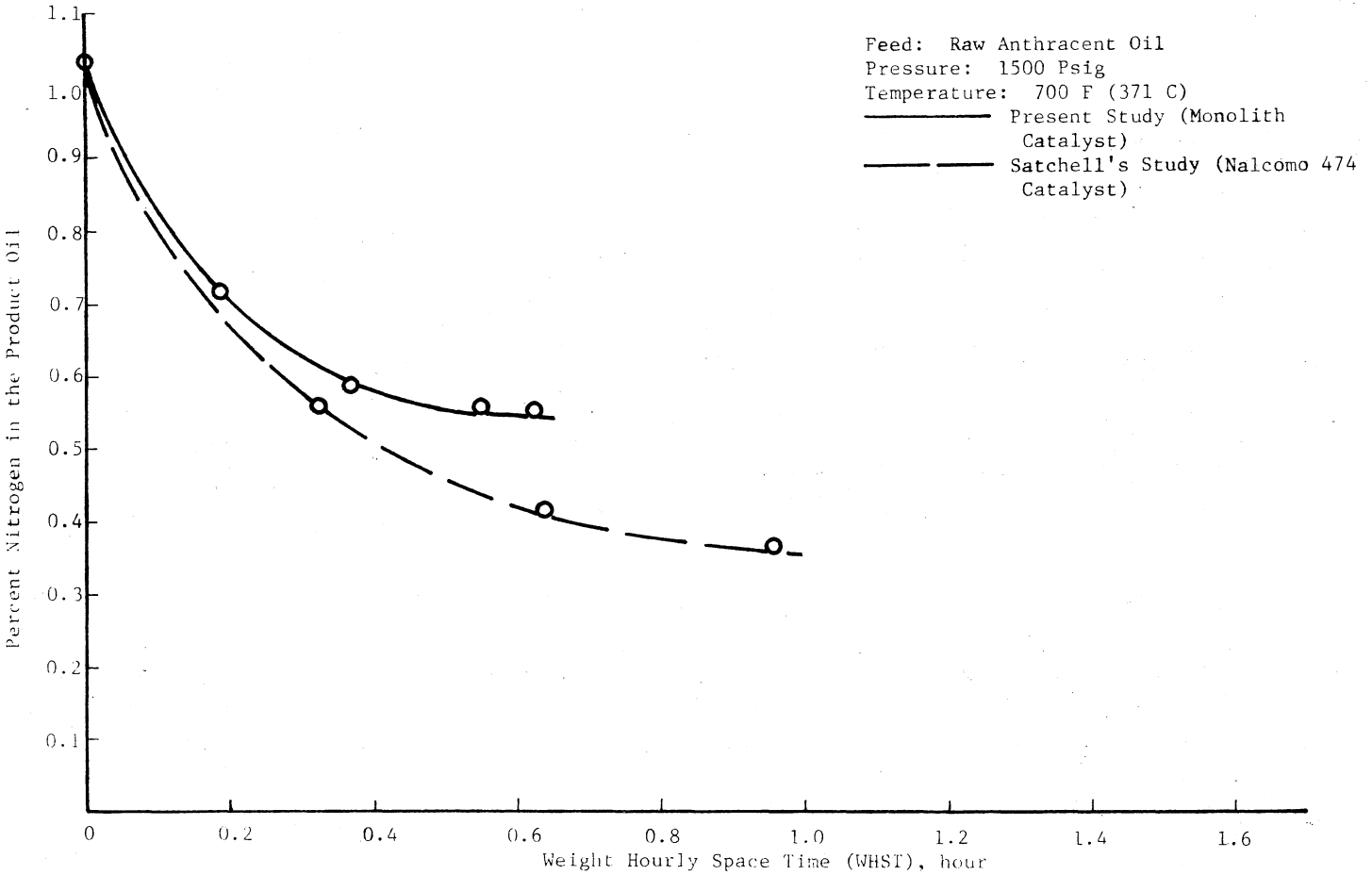

Figure 37. Raw Anthracene Oil Denitrogenation, Comparison of Nalcomo 474 and Monolith Catalysts on Weight Hourly Space Time Basis, 700 F (371 C)

Besides these, the methods of preparation of Nalcomo 474 and the monolith catalysts are also different. Nalcomo 474 is a vendor preparation and is available commercially while the monolith catalyst was prepared in the laboratory here. How far these methods of preparation affect the activities of the two catalysts is not known. This study was also not aimed towards that end. Therefore, the catalysts will be compared, disregarding the effects of methods of preparation on activities of the two catalysts. However, one of the reasons for the difference in the activities could be these factors. This will be discussed again later in this chapter.

Surface Area Effects

Ideally, the number of active sites per gram would be the best measure of catalyst activity. Since the number of active sites are difficult to determine, surface area per gram becomes the next best indicator of catalyst activity. A larger specific surface area would mean a greater number of active sites per gram and hence more activity of the catalyst. Therefore, Nalcomo 474 with more than three times the specific surface area of the monolith would naturally have an advantage over the monolith catalyst in this regard. This advantage shows up in Figures 13 through 30. However, to quantify this superiority of Nalcomo 474 is difficult because to study the effect of increase in surface area, all other properties of the catalysts such as particle size, pore size, pore structure, methods of preparation, etc., should be the same. In the present case, the monolith catalyst has an entirely different pore size and structure. Therefore any attempt

to quantitatively study the effect of increase in surface area from 66 to 240 m^2/gram would be an exercise in futility.

Pore Size Effects

The function of the pores in a catalyst is to increase its surface area and to provide passages for the reactive molecules to reach the active sites of the catalyst. As was discussed in Chapter II, the effect of pore size is a function of the characteristics of the feedstock or to be more specific, the size of the reactive molecules present in the feedstock. Larger molecules would require large pore diameters to diffuse into the particle and thereby utilize the maximum surface area offered by the catalyst. The pore size, therefore, may put diffusion limitations on reactions catalyzed by solids.

To compare the effect of pore size on the activity of the two catalysts, the effects of surface area and the intrinsic activity of the catalyst need be eliminated. The effect of surface area can be accounted by studying the activity based on unit area. But the effect of intrinsic activity is hard to alienate. However, discussion on this point will be taken up when reasons for the difference in activities of the two catalysts are addressed. The comparison based on unit surface area follows:

Comparison based on unit surface area: Figures 38 and 39 show this comparison. These are plots of S/V vs percent sulfur or nitrogen in the product. The abscissa S/V is defined as:

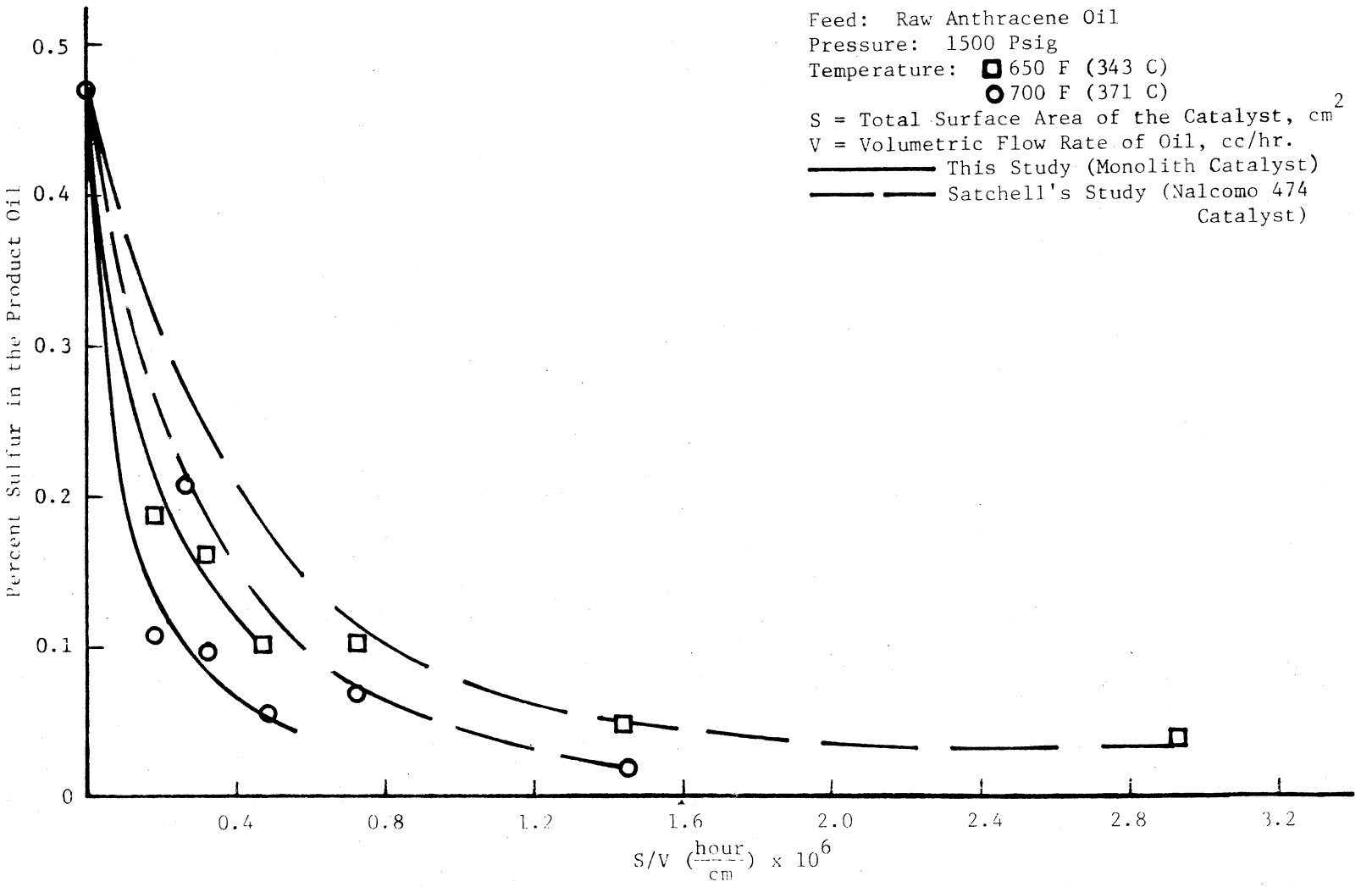

Figure 38. Raw Anthracene Oil Desulfurization, Comparison of Nalcomo 474 and Monolith Catalysts on Surface Area Basis

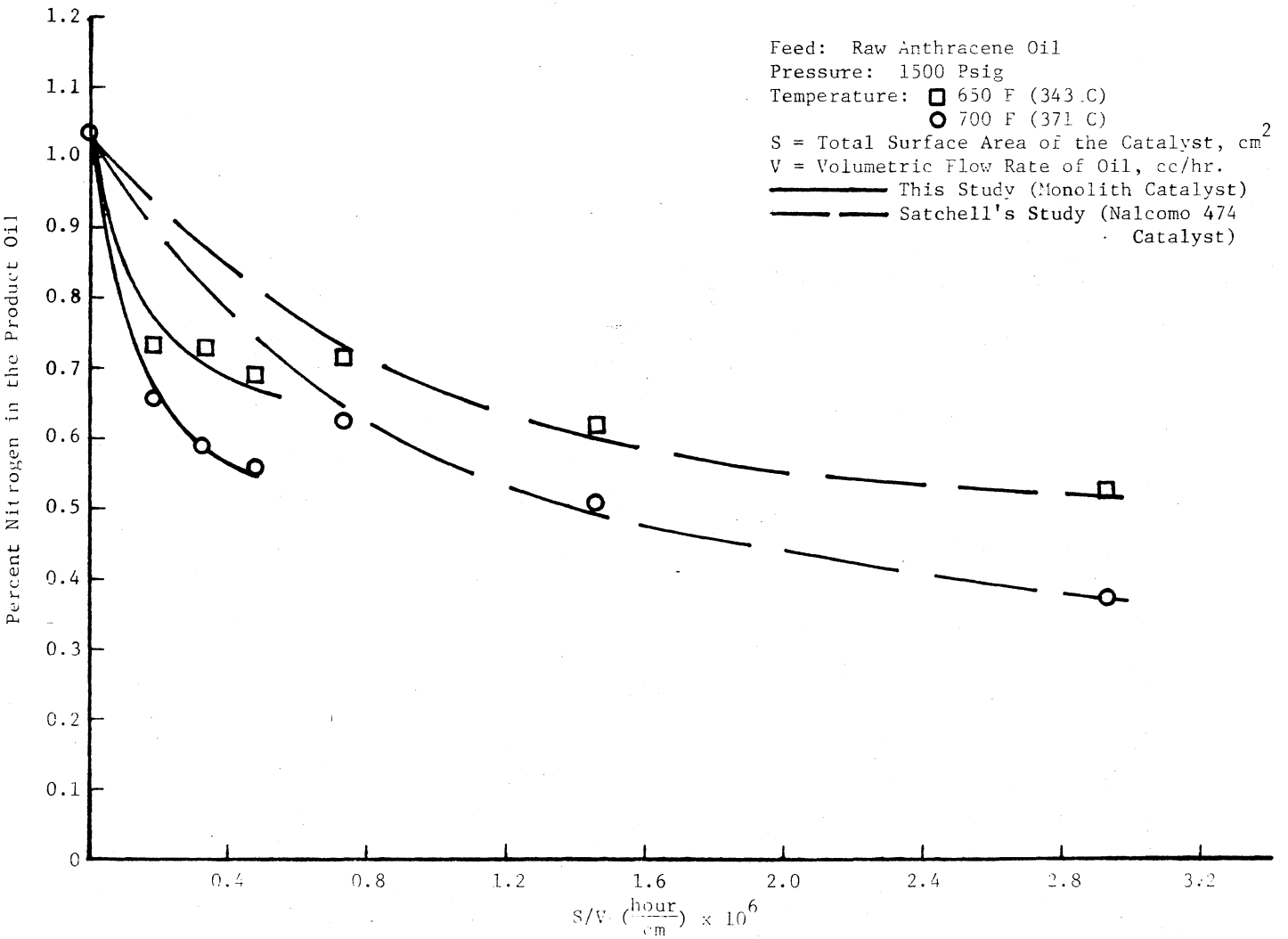

Figure 39. Raw Anthracene Oil Denitrogenation, Comparison of Nalcomo 474 and Monolith Catalysts on Surface Area Basis

$$S/V = \frac{\text{Total Surface Area of the Catalyst in the Reactor}}{\frac{\text{Volume of Oil Treated}}{\text{Hour}}} \qquad \frac{(cm^2)}{(\frac{cm^3}{hour})}$$

This parameter can tell us that for a given conversion and for a given flow rate of oil, how much surface area of a particular catalyst will be required. Figures 38 and 39 show that for the same sulfur or nitrogen removal and for the same flow rate of oil, Nalcomo 474 would require more surface area than the monolith catalyst. This means that the activity of the monolith per unit surface area is more than that of the Nalcomo 474 catalyst.

Another way to compare the activity of the two catalysts based on per unit surface area is to compare the reaction rate constants based on surface area. Determination of these constants follows:

Order of the reaction: The literature study (refer to Chapter II) suggests that the order of desulfurization reaction for petroleum feedstocks is generally one of the following:

(1) Second order, $\frac{1}{C_A} = kt + \frac{1}{C_{AO}}$

(2) Combination of two first order reactions, one for lighter fractions and the other for heavier fractions of the feedstock;

$$\frac{C_A}{C_{AO}} = \alpha e^{-k_1 t} + (1-\alpha)e^{-k_2 t}$$

(3) First order, $\frac{C_A}{C_{AO}} = e^{-kt}$

where

C_A = concentration of reactant (sulfur) at any time, $\frac{\text{gm moles}}{\text{cm}^3}$

C_{AO} = original concentration, $\frac{\text{gm moles}}{\text{cm}^3}$

k = reaction rate constant

α = fraction of the light or heavy component in the feed

t = time, hr.

These models do not include the effects of physical variables such as intraparticle diffusion and fluid dynamics. These three models were tested and the results of non-linear regression analysis of the data are given in Tables VIII through X. As can be seen from these tables, first and second models represent the data at 650 F (343 C) equally well. Therefore, the first model (second order) will be chosen for simplicity. At 700 F (371 C) and 800 F (426 C) the second model represents the data extremely well. But the values of the rate constant, k_2, are zero. This is not reasonable from physical considerations. Therefore, this model will not be considered to represent the desulfurization reaction of 700 F (371 C) and 800 F (426 C). The next best model for the reaction at 700 F (371 C) is the first model (second order). The standard deviation for this model is also much below the value allowable in this study (0.051). Based on the same reasons, the third model (first order) is best for representation of data at 800 F (426 C). Thus, at 650 F (343 C) and 700 F (371 C) desulfurization rate can be represented by second order kinetics in sulfur concentration while at 800 F (426 C) it is best represented by first order kinetics. The literature study on kinetics of desulfurization (refer to Chapter II) showed that desulfurization of pure compounds is a first order reaction. But desulfurization of petroleum feedstocks tends to be of higher order because of the different

TABLE VIII

SECOND ORDER DESULFURIZATION MODEL
FEED: RAW ANTHRACENE OIL

	Monolith Catalyst			Sooter's Data with Nalcomo 474 Catalyst	
	650 F (343 C)	700 F (371 C)	800 F (426 C)	650 F (343 C)	700 F (371 C)
Rate constant, k, $(hour)^{-1}$ $(conc.)^{-1}$	3.77	8.68	20.3	20.3	48.8
Standard Deviation	0.007	0.014	0.047	0.022	0.016
Maximum Deviation	0.012	0.033	0.104	0.049	0.022

TABLE IX

DESULFURIZATION MODEL: $\frac{C_A}{C_{AO}} = \alpha e^{-k_1 t} + (1-\alpha)e^{-k_2 t}$

FEED: RAW ANTHRACENE OIL
CATALYST: MONOLITH

	650 F (343 C)	700 F (371 C)	800 F (426 C)
α	0.647	0.862	0.96
Rate Constant, k_1, $(hour)^{-1}$	2.39	2.88	3.18
Rate Constant, k_2, $(hour)^{-1}$	0.178	Zero	Zero
Standard Deviation	0.0067	0.006	0.003
Maximum Deviation	0.0135	0.0095	0.0046

TABLE X

FIRST ORDER DESULFURIZATION MODEL
FEED: RAW ANTHRACENE OIL

	Monolith Catalyst			Sooter's Data with Nalcomo 474 Catalyst	
	650 F (343 C)	700 F (371 C)	800 F (426 C)	650 F (343 C)	700 F (371 C)
Rate Constant, k, $(hour)^{-1}$	0.98	1.72	2.76	3.0	4.54
Standard Deviation	0.031	0.029	0.009	0.038	0.022
Maximum Deviation	0.051	0.036	0.013	0.058	0.038

reactivities of the wide spectrum of sulfur compounds present in the stock. Therefore, the linearization of the order of the reaction at 800 F (426 C) can result from the increased reactivities of the various compounds, especially those of relatively high activation energies, at this temperature. Besides the higher temperature, the large pore size of the monolith catalyst might have helped the heavier and relatively slow reacting molecules to have easier access to the active sites. Therefore, change in the order of the reaction at 800 F (426 C) is reasonable.

Sooter (26) in his study on the same feedstock, but using Nalcomo 474 catalyst observed that the second model best explains his data at 650 F (343 C) and 700 F (371 C). Table XI given below shows the values of the constants found by him. Values of k_1, at 650 F (343 C) and 700 F (371 C) are 227 $(hour)^{-1}$ and 3110 $(hour)^{-1}$ respectively. But physical considerations dictate that such high exponential values are unlikely. If these values are taken to be true, then more than half (values of α being 0.717 and 0.81) of sulfur compounds should react almost instantaneously. No sulfur compound found in petroleum feedstocks would react so fact. Sooter's model was tested with different values of k_1. A value of k_1 as low as 10 was also found to explain his data as well as a value of 227 found by him. Therefore, a comparison of rate constants found in this study with those of Sooter's study was not considered meaningful. However, comparison of rate constants must be made to get a quantitative idea of the difference in rate of reactions. To achieve this, Sooter's data were subjected to non-linear regression in the same manner as the data of this study. However, as discussed above, the presence of three constants in the

second model introduces a major drawback in that model. There can be many sets of values of these constants which would explain the data equally well and hence these values will not have any physical significance. Therefore this model will not be tested again with Sooter's data. Results of non-linear regression with other two models are given in Tables VIII and X. These results show that the first model is better. Hence a second order desulfurization rate expression will be considered the model that represents Sooter's data. The rate constants between this study and that of Sooter will be compared on this basis.

TABLE XI

VALUES OF THE CONSTANTS FOR THE MODEL OBSERVED BY SOOTER

	600 F (315 C)	650 F (343 C)	700 F (371 C)
α	0.63	0.717	0.81
k_1 $(hour)^{-1}$	5.97	227.0	3110.0
k_2 $(hour)^{-1}$	0.425	0.669	1.1

Comparison of Desulfurization Rate Constants: Second order volumetric rate constants of this study and those calculated with Sooter's data are given in Table XII below.

TABLE XII

COMPARISON OF VOLUMETRIC RATE CONSTANTS BETWEEN THIS STUDY AND THAT OF SOOTER'S

	650 F (343 C)		700 F (371 C)	
	This Study	Sooter's Data	This Study	Sooter's Data
Rate constant k, $(hr.)^{-1}(conc.)^{-1}$	3.77	20.3	8.68	48.8

Clearly, the volumetric rate constants of this study, which used monolith catalyst, are much less than those of Sooter's study, which used Nalcomo 474 catalyst. This is consistent with the volume hourly space time comparison of the two catalysts (see Figure 16). Since the study of activities based on a unit surface area were of interest, the rate constants, k_S, based on unit surface area were determined. The two rate constants are related to each other according to the following equation.

$$k_S = k \frac{V_r}{S}$$

where

k = volumetric rate constant, $\frac{cc}{(hour)(gram\ mole)}$

V_r = volume of the reactor, cc

S = total surface area of the catalyst, cm^2.

Values of k_S calculated for this study and that of Sooter's are given in the following table.

TABLE XIII

COMPARISON OF THE SURFACE AREA RATE CONSTANTS BETWEEN THIS STUDY AND THAT OF SOOTER'S

	650 F (343 C)		700 F (371 C)	
	This Study	Sooter's Data	This Study	Sooter's Data
Rate constant k_S $\frac{(cm)^4}{(hour)(gram\ mole)}$	1300	1170	3182	2400

The rate constants based on surface area are higher for the monolith catalyst than for Nalcomo 474. This again indicates that surface activity of the former is higher than that of the latter. This is consistent with S/V plots.

Comparison of Denitrogenation Rate Constants: To have an idea of the overall activity of the monolith as compared to Nalcomo 474 catalyst, comparison of dentirogenation rate constants is also necessary. Therefore, denitrogenation data in this study were subjected to non-linear regression and the following three models were tested.

(1) First order, $C_A = C_{AO}e^{-kt}$

(2) Second order, $\frac{1}{C_A} = kt + \frac{1}{C_{AO}}$

(3) Pseudo first order, $C_A = C_{AO}e^{-k(t)^x}$

The last model has been recently proposed by Sivasubramanian (40) and incorporates catalyst wetting effects. Tables XIV, XV and XVI give the results of non-linear regression of denitrogenation data. The third model is evidently the best because standard deviation is the lowest. But, since the study by Satchell (27), which is being taken as the reference for comparison, does not suggest this model, the next best is the second model, i.e., a second order rate expression.

Though the model derived by Satchell is also second order, it is based on entirely different considerations. It takes into account relative reactivities of the compounds in different boiling ranges. Therefore, a comparison of the rate constants based on this second order reaction rate will not be correct. Satchell also tried to fit his data by a least square fit and found that a third order rate equation gave the best fit. But, he discarded this model because of the order being very high as compared to first order kinetics exhibited by pure nitrogen compounds.

To overcome the problem regarding comparison, the data by Satchell were tested on a second order model and the results of non-linear regression are given in Table XVII. Comparison with Table XV shows that the standard deviations for the second order model in the two studies are comparable. Values of the rate constants based on surface area are given in Table XVIII.

TABLE XIV

FIRST ORDER DENITROGENATION MODEL
FEED: RAW ANTHRACENE OIL
CATALYST: MONOLITH

	650 F (343 C)	700 F (371 C)
Rate Constant, k, $(hour)^{-1}$	0.38	0.55
Standard Deviation	0.059	0.062
Maximum Deviation	0.09	0.098

TABLE XV

SECOND ORDER DENITROGENATION MODEL
FEED: RAW ANTHRACENE OIL
CATALYST: MONOLITH

	650 F (343 C)	700 F (371 C)
Rate Constant, k, $(hour)^{-1}(conc.)^{-1}$	0.453	0.724
Standard Deviation	0.045	0.038
Maximum Deviation	0.074	0.067

TABLE XVI

POWER LAW DENITROGENATION MODEL: $C_A = C_{AO}e^{-k(t)^x}$

FEED: RAW ANTHRACENE OIL
CATALYST: MONOLITH

	650 F (343 C)	700 F (371 C)
Rate Constant, k, $(hour)^{-1}$	0.386	0.558
x	0.49	0.558
Standard Deviation	0.023	0.027
Maximum Deviation	0.044	0.046

TABLE XVII

SECOND ORDER DENITROGENATION MODEL WITH SATCHELL'S DATA
FEED: RAW ANTHRACENE OIL
CATALYST: NALCOMO 474

	650 F (343 C)	700 F (371 C)
Rate Constant, k, $(hour)^{-1}(conc.)^{-1}$	0.86	1.4
Standard Deviation	0.025	0.021
Maximum Deviation	0.05	0.055

TABLE XVIII

COMPARISON OF SURFACE AREA RATE CONSTANTS BETWEEN THIS STUDY AND THAT OF SATCHELL'S

	650 F (343 C)		700 F (371 C)	
	This Study	Satchell's Data	This Study	Satchell's Data
Rate constant $k_S = \frac{(cm)^4}{(hour)(gram\ mole)}$	166	50	265	81

The surface area constants obtained in this study using monolith catalyst are significantly higher than those obtained from Satchell's data. This shows that surface activity of the monolith with regard to denitrogenation also is higher than that of Nalcomo 474. This is consistent with Figure 39.

Peformance of Catalysts on Synthoil-1

Discussion of the performance of catalysts on Synthoil will be similar to the discussion of the performance of catalysts on raw anthracene oil. Figures 26 and 27 in Chapter IV compare the desulfurization activities of the two catalysts on a volume basis at 700 F (371 C) and 800 F (426 C) respectively. As was mentioned in Chapter IV, there is no difference in sulfur removal between the monolith and Nalcomo 474 catalysts at 700 F (371 C). However, at 800 F (426 C), activities of the two catalysts remain the same only up to a volume

hourly space time of 1.0 hour. Beyond this time, desulfurization with Nalcomo 474 increases sharply. This particular phenomena will be discussed later in this Chapter.

Figures 29 and 30, in Chapter IV, compare the denitrogenation activities of the two catalysts on the same basis at the same temperatures. Nitrogen removal at 700 F (371 C), is somewhat better with Nalcomo 474 than with monolith. But, at 800 F (426 C) monolith removed more nitrogen than Nalcomo 474. However, at this temperature, at high space time, (1.5 hours), denitrogenation activity of Nalcomo 474 tends to be better than that of the monolith catalyst.

Comparison on Weight Basis: Figures 40 through 43 show a comparison on the two catalysts on a weight hourly space time basis. On this basis monolith is far superior to Nalcomo 474, both for desulfurization and denitrogenation. However, at 800 F (426 C) at space time higher than 1.0 hour, the activity of the Nalcomo 474 is better. Comparing with the performance of monolith on raw anthracene oil, one finds that monolith never showed superiority over Nalcomo 474 catalysts on the basis of weight hourly space time. This means that the monolith catalyst behaves much better on a heavier feedstock, such as Synthoil, than on a lighter feedstock such as raw anthracene oil. These observations will be discussed further when reasons for the difference in activities of the two catalysts are taken up.

Comparison on Unit Surface Area Basis: Figures 44 and 45 show the difference in the activities of the two catalysts on surface area basis. The monolith catalyst clearly has more activity per unit surface area than Nalcomo 474. Comparison of these figures with

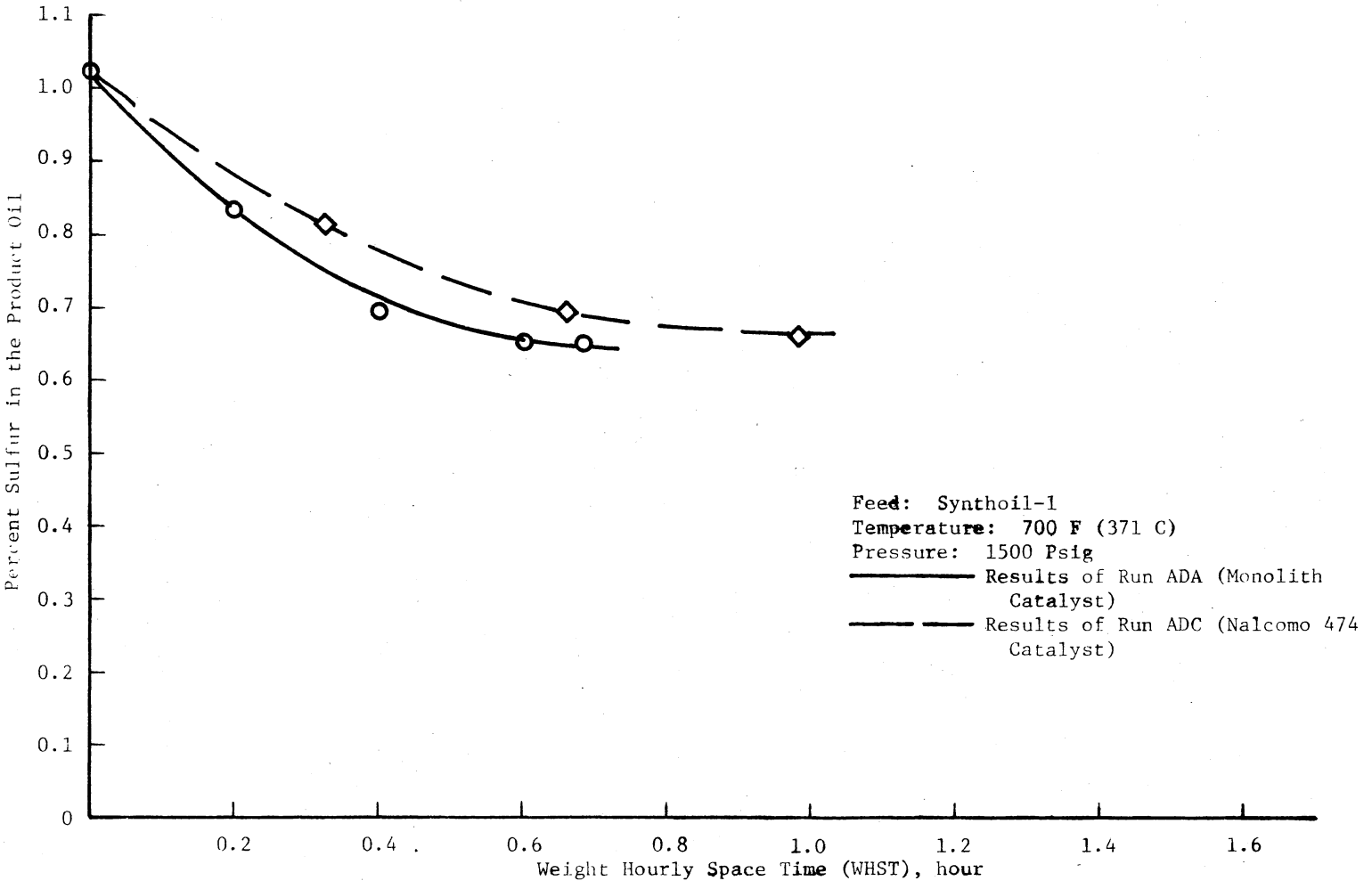

Figure 40. Synthoil-1 Desulfurization Comparison of Nalcomo 474 and Monolith Catalysts on Weight Hourly Space Time Basis, 700 F (371 C)

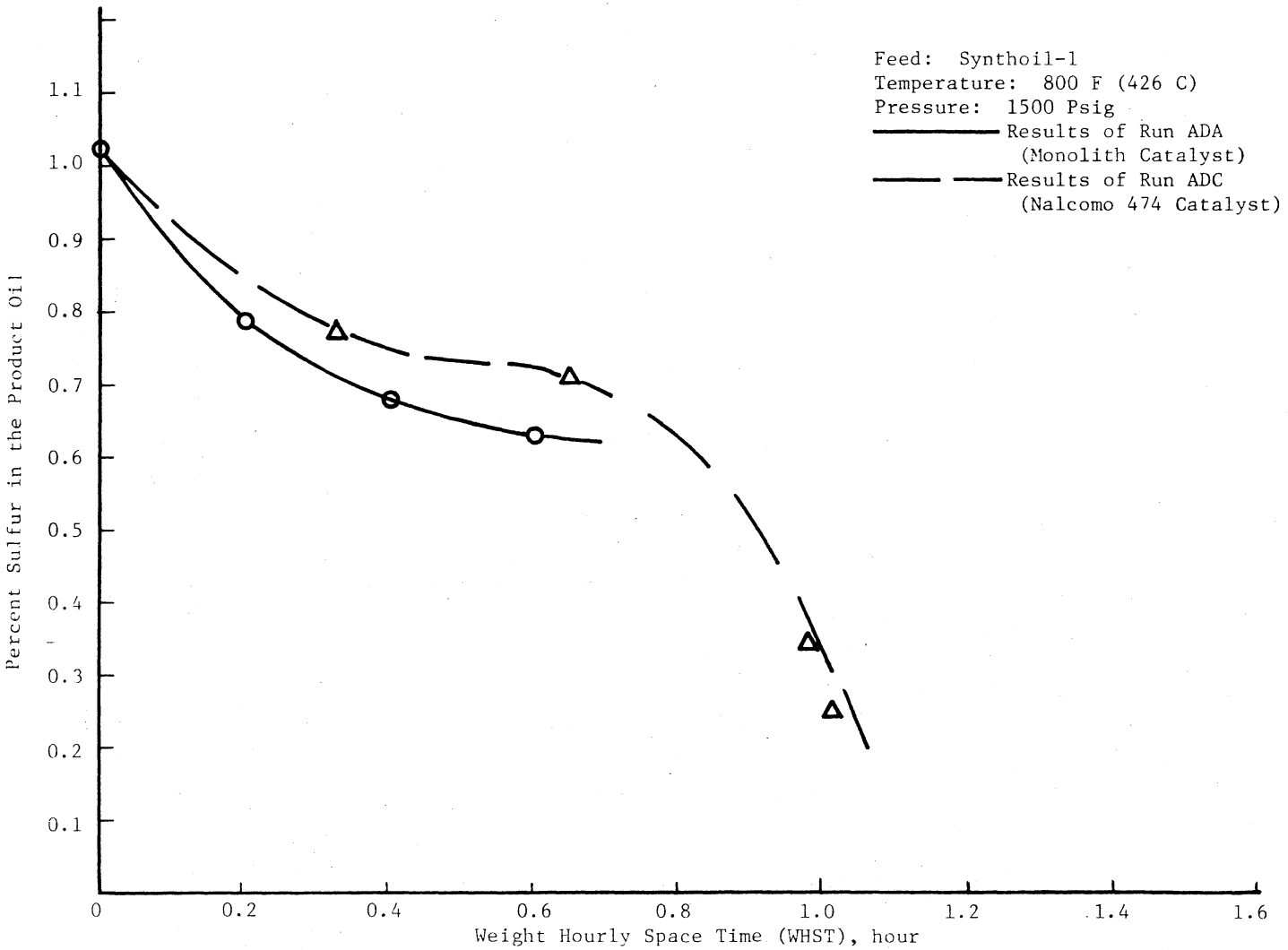

Figure 41. Synthoil-1 Desulfurization Comparison of Nalcomo 474 and Monolith Catalysts on Weight Hourly Space Time Basis, 800 F (426 C)

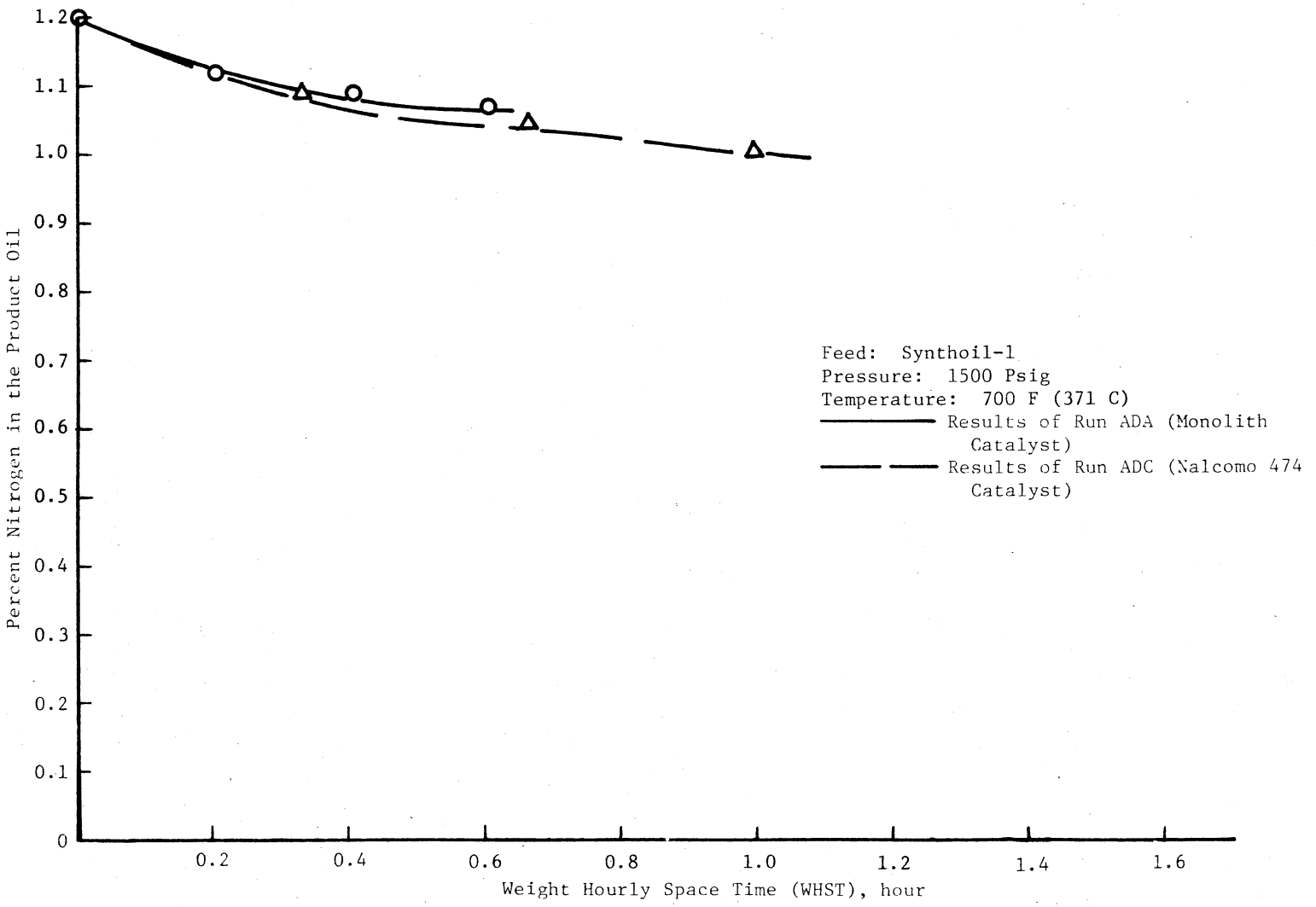

Figure 42. Synthoil-1 Denitrogenation Comparison of Nalcomo 474 and Monolith Catalysts on Weight Hourly Space Time Basis, 700 F (371 C)

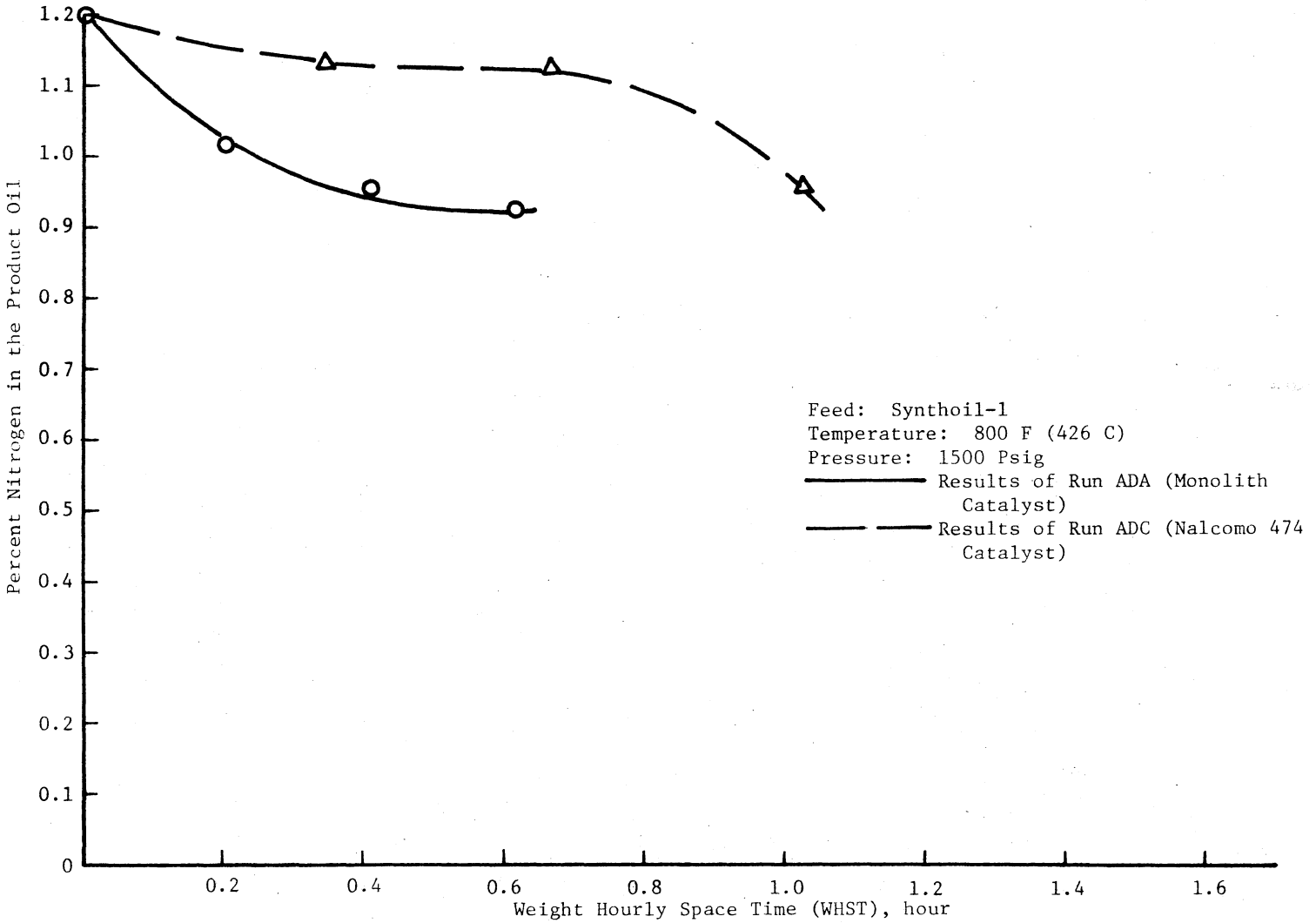

Figure 43. Synthoil-1 Denitrogenation Comparison of Nalcomo 474 and Monolith Catalysts on Weight Hourly Space Time Basis, 800 F (426 C)

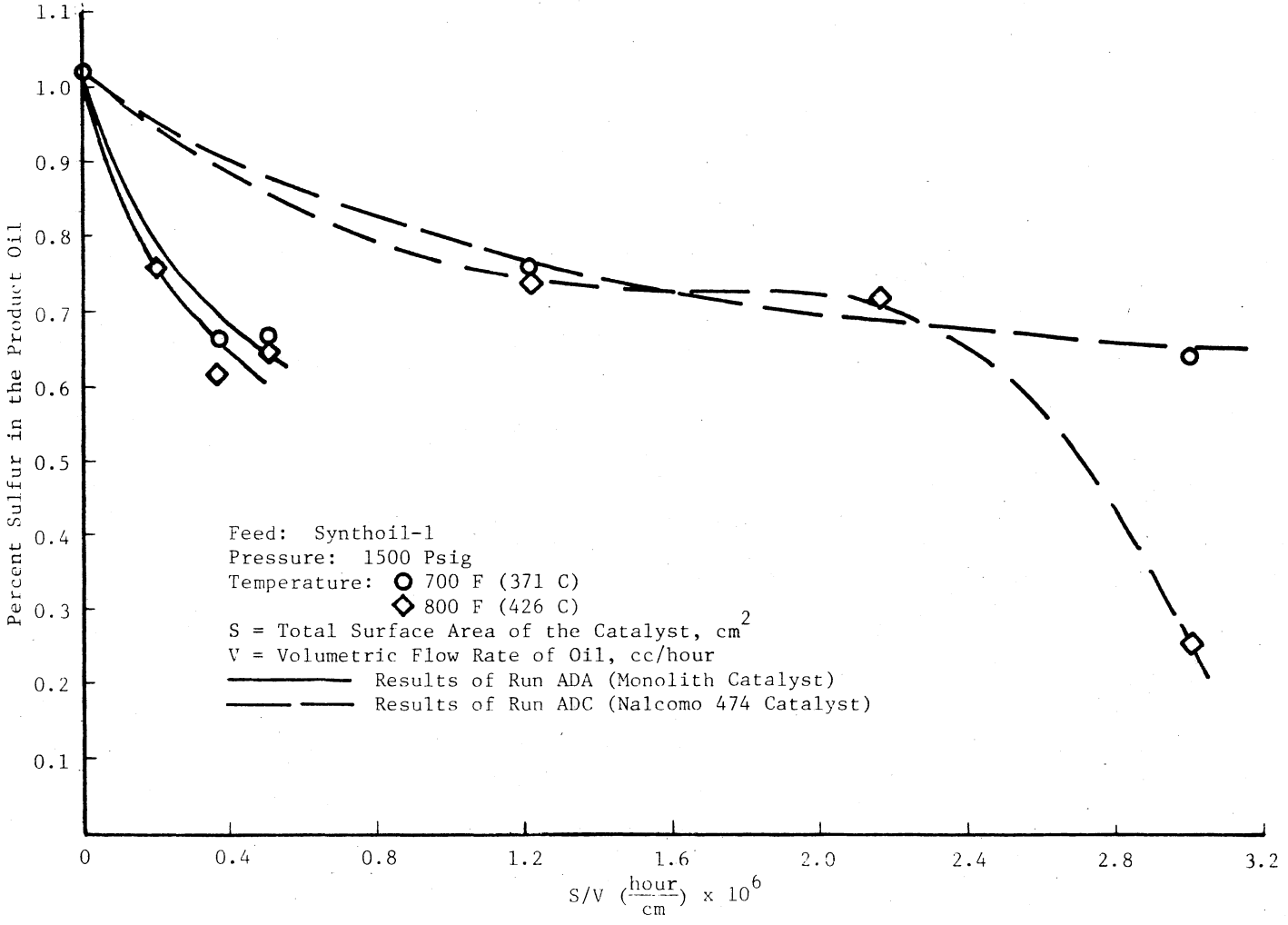

Figure 44. Synthoil-1 Desulfurization, Comparison of Nalcomo 474 and Monolith Catalysts on Surface Area Basis

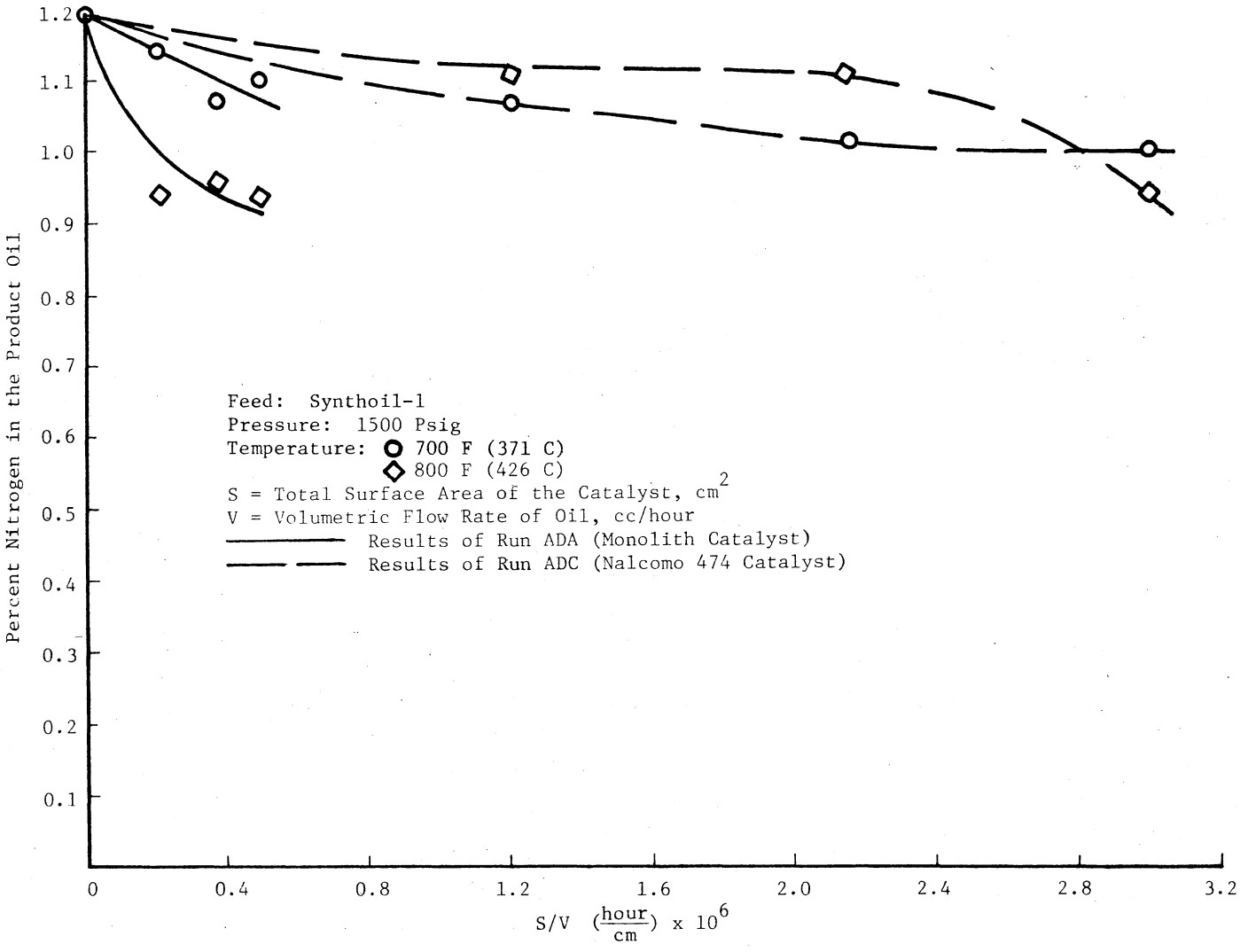

Figure 45. Synthoil-1 Denitrogenation, Comparison of Nalcomo 474 and Monolith Catalysts on Surface Area Basis

Figures 38 and 39 indicates that on unit surface area basis, superiority of the monolith catalyst over Nalcomo 474 catalyst is far less on raw anthracene oil than that on Synthoil. These observations will become more clear when rate constants on surface area basis are compared in the two cases.

Order of the Reaction and Rate Constants: The second model, i.e., combination of two first order rate expressions, will not be tested again for the reasons already given (refer page 120). For the other two models, i.e., second order and first order rate expressions, results of the non-linear regression of data are given in Tables XIX and XX. These tables list the rate constants, for both the catalysts, at 700 F (371 C) and at 800 F (426 C). In the case of the monolith catalyst, the first model, i.e., second order, is better. The standard deviations are below the maximum, i.e., 0.051. Hence the kinetics of desulfurization of Synthoil on monolith catalyst would be considered to be second order in sulfur concentration. The second order volumetric rate constants at 700 F (371 C) and 800 F (426 C) are 0.427 $(\text{hour})^{-1}$ $(\text{conc.})^{-1}$ and 0.468 $(\text{hour})^{-1}$ $(\text{conc.})^{-1}$ respectively. In case of Nalcomo 474, none of the two models adequately explain the kinetics at 800 F (426 C). This may be due to unusual increase in desulfurization after space time of 1.0 hour (Figure 19). However, at 700 F (371 C), the first model, i.e., second order rate expression best represents the data. The rate constant at 700 F (371 C) is 0.431 $(\text{hour})^{-1}$ $(\text{conc.})^{-1}$. The surface area rate constants are given in Table XXI.

TABLE XIX

SECOND ORDER DESULFURIZATION MODEL
FEED: SYNTHOIL-1

	Nalcomo 474 Catalyst		Monolith Catalyst	
	700 F (371 C)	800 F (426 C)	700 F (371 C)	800 F (426 C)
Rate Constant, k, $(hour)^{-1}(conc.)^{-1}$	0.431	0.77	0.427	0.468
Standard Deviation	0.046	0.097	0.017	0.024
Maximum Deviation	0.096	0.153	0.033	0.035

TABLE XX

FIRST ORDER DESULFURIZATION MODEL
FEED: SYNTHOIL-1

	Nalcomo 474 Catalyst		Monolith Catalyst	
	700 F (371 C)	800 F (426 C)	700 F (371 C)	800 F (426 C)
Rate Constant, k, $(hour)^{-1}$	0.35	0.56	0.35	0.377
Standard Deviation	0.057	0.083	0.028	0.038
Maximum Deviation	0.11	0.15	0.048	0.054

TABLE XXI

SYNTHOIL-1 DESULFURIZATION RATE CONSTANTS BASED ON SURFACE AREA, k_S $\frac{(cm)^4}{(gram\ mole)(hour)}$

Nalcomo 474 Catalyst		Monolith Catalyst	
700 F (371 C)	800 F (426 C)	700 F (371 C)	800 F (426 C)
25	44	151	165

Order and Rate Constants for Denitrogenation: Tables XXII through XXIV give the results of non-linear regression of the denitrogenation data for the same three models as tested for denitrogenation of raw anthracene oil. All of the models seem to explain the data well, both for the monolith and Nalcomo 474 catalysts. However, the simpler first order model will be chosen for comparison of rate constants. For monolith, the first order volumetric rate constants at 700 and 800 F are 0.0945 $(hour)^{-1}$ and 0.22 $(hour)^{-1}$ respectively. For Nalcomo 474 these are 0.146 $(hour)^{-1}$ and 0.123 $(hour)^{-1}$. Rate constants, k_S, based on surface area, are given in Table XXV.

Note that the rate constants based on surface area for the monolith catalyst are much higher than the rate constants for Nalcomo 474 catalyst.

The foregoing discussion conclusively proves that the activity per unit surface area is more for the monolith than for Nalcomo 474 catalyst. Also, the monolith catalyst shows far more superiority over

TABLE XXII

FIRST ORDER DENITROGENATION MODEL
FEED: SYNTHOIL-1

	Nalcomo 474 Catalyst		Monolith Catalyst	
	700 F (371 C)	800 F (426 C)	700 F (371 C)	800 F (426 C)
Rate Constant, k, $(hour)^{-1}$	0.146	0.123	0.095	0.22
Standard Deviation	0.019	0.0382	0.017	0.426
Maximum Deviation	0.029	0.071	0.025	0.062

TABLE XXIII

POWER LAW DENITROGENATION MODEL: $\frac{C_A}{C_{AO}} = e^{-k(t)^x}$

FEED: SYNTHOIL-1

	Nalcomo 474 Catalyst		Monolith Catalyst	
	700 F (371 C)	800 F (426 C)	700 F (371 C)	800 F (426 C)
Rate Constant, k, $(hour)^{-1}$	0.15	2.0	0.098	0.233
x	0.768	0.1	0.586	0.56
Standard Deviation	0.014	0.03	0.003	0.017
Maximum Deviation	0.024	0.055	0.005	0.024

TABLE XXIV

SECOND ORDER DENITROGENATION MODEL
FEED: SYNTHOIL-1

	Nalcomo 474 Catalyst		Monolith Catalyst	
	700 F (371 C)	800 F (426 C)	700 F (371 C)	800 F (426 C)
Rate Constant, k, $(hour)^{-1}(conc.)^{-1}$	0.134	0.111	0.084	0.22
Standard Deviation	0.017	0.04	0.016	0.036
Maximum Deviation	0.026	0.071	0.023	0.055

Nalcomo 474 catalyst while treating Synthoil, a heavier feedstock, than while treating raw anthracene oil which is relatively light as compared to Synthoil. Distillation ranges of raw anthracene oil and Synthoil are given on pages 58 and 59 respectively as illustration of these "light" and "heavy" liquids.

TABLE XXV

SYNTHOIL-1 DENITROGENATION RATE CONSTANTS BASED ON SURFACE AREA, k_S $(HOUR)^{-1}(CM)$, FOR BOTH THE CATALYSTS

Nalcomo 474 Catalyst		Monolith Catalyst	
700 F (371 C)	800 F (426 C)	700 F (371 C)	800 F (426 C)
8.5	7.0	33.4	77.4

Before discussing the reasons for the monolith catalyst having higher surface activity, the third major difference between the two catalysts will be addressed.

Different Bulk Cobalt to Molybdenum Ratio: There is abundant proof in the literature (refer to Chapter II) to show that there is an optimum bulk ratio of Co/Mo at which activity of the catalyst is maximum. This optimum ratio is a function of the surface area of the catalyst. However, the maximum value reported in the literature for this ratio is 0.4. But the catalysis being a surface phenomena, surface

concentrations of cobalt and molybdenum and Co/Mo ratio based on surface area are more important. Therefore, comparison of the two catalysts will be based on surface area. However, one uncertainty regarding comparison based on surface area is that the distribution of metallic spieces on surfaces of the two catalysts may be different. Since all the methods for preparation of catalysts try to achieve uniform distribution of metals, it shall be assumed, for the purpose of this study, that cobalt and molybdenum are uniformly distributed over the two catalysts.

Surface concentrations of the two metals and Co/Mo ratio based on the surface area for both the catalysts are given in Table XXVI below.

TABLE XXVI

SURFACE CONCENTRATION OF Co AND Mo AND Co/Mo RATIO IN THE TWO CATALYSTS

Nalcomo 474 Catalyst			Monolith Catalyst		
Co, gm/cm^2 x 10^{-4}	Mo, gm/cm^2 x 10^{-4}	Co/Mo	Co, gm/cm^2 x 10^{-4}	Mo, gm/cm^2 x 10^{-4}	Co/Mo
1.29	4.63	0.28	3.66	7.88	0.465

Though the concentration of the active spieces, i.e., Mo is more in case of the monolith catalyst, the Co/Mo ratio is also very high. As to what is the optimum Co/Mo ratio for the monolith cannot be said unless experimental studies to that end are made. But bulk Co/Mo ratio for the monolith is 0.465 which is more than the highest optimum reported in the literature. This ratio is 1.66 times that of the commercially proven catalyst. Therefore, in all probability, the Co/Mo ratio in the case of the monolith catalyst is on the higher side of its optimum value. This would therefore dampen the activity of the monolith catalyst. The cobalt present in very high concentrations may block the active sites meant for molybdenum (4). Therefore, the difference in Co/Mo ratio goes to the disadvantage of the monolith catalyst. This indicates that surface activity of the monolith catalyst with optimum Co/Mo ratio may be even more than what has been observed in this study.

Reasons for Surface Activity of Monolith Being Higher than that of Nalcomo 474 Catalyst

There can be three main reasons for higher surface activity of the monolith catalyst:

(1) Intrinsic activity of monolith being higher than intrinsic activity of Nalcomo 474 catalyst.

(2) Fluid dynamic effects in monolith give better solid-liquid contacting efficiency.

(3) There are severe diffusional limitations due to which surface area utilization in case of Nalcomo 474, having pore radius of $33^{o}A$,

is very low as compared to surface area utilization in case of the monolith having pore radius of 80^{o}A. To find out as to which of these factors, or which combination of these factors, were responsible for higher observed surface activity of the monolith, is difficult. Experimentation in this study were not designed to differentiate between the effects of the above three factors. However, results of this study do indicate, to some extent, that diffusion limitations played a major part in lowering per unit surface area activity of Nalcomo 474 catalyst, at least, on Synthoil. Figures 38 and 39 show comparison of the activities of the two catalysts on surface area basis with raw anthracene oil as the feedstock. The superiority of the monolith over Nalcomo 474 catalyst seems to decrease with increasing values of S/V. If curves for the monolith are extrapolated, activities of both the catalysts would just about be the same at S/V values of 10^{6} or so and thereafter Nalcomo 474 would show more activity than the monolith. This means that on raw anthracene oil, the monolith catalyst has only a slight edge over Nalcomo 474 catalyst. This is also evident from the difference in surface area rate constants with the monolith and Nalcomo 474 catalysts, (Tables XIII and XVIII).

Figures 44 and 45 show that the monolith is far more superior to Nalcomo 474 when tested on Synthoil. This superiority increases with increasing values of S/V. Table XXI and XXV show that surface area rate constants with the monolith are about 6 to 9 times higher than those with Nalcomo 474 catalyst. Thus the superiority of the monolith catalyst with Synthoil as feedstock differs widely from the superiority of this catalyst with raw anthracene oil as the feedstock.

Now if one considers that the monolith catalyst was intrinsically more active than Nalcomo 474 catalyst, then superiority of the monolith when tested on two different feedstocks should, at least, have the same order of magnitude. Since this is not the case, there is some other factor playing a major role and that might be the intraparticle diffusion limitations. To explain this consider the characteristics of the two feedstocks. Synthoil is very high boiling as compared to raw anthracene oil (refer to Tables II and III). This means that the molecules that constitute Synthoil are much larger on the average than the molecules that consitute raw anthracene oil. The small size of pores in Nalcomo 474 catalyst would, therefore, offer much higher intraparticle diffusion resistance to Synthoil molecules than to raw anthracene oil molecules. This could severly limit the activity of Nalcomo 474 catalyst on Synthoil but not so much as on raw anthracene oil. The pores of the monolith catalyst are approximately three times larger than the pores of Nalcomo 474 catalyst. These will offer much lower diffusional resistance to Synthoil than offered by pores of Nalcomo 474 catalyst. One other factor that can significantly contribute to the difference in diffusional resistance between the two catalysts is the difference in lengths of diffusion paths. As mentioned in Chapter II, the monoliths contain an array of parallel uniform, and non-connecting channels. The thickness of the walls of these channels is about 0.5 mm. Therefore maximum diffusion length in case of monolith catalyst would be 0.025 mm. But, in the case of Nalcomo 474, the maximum length of diffusion path will be about 1 mm, i.e., the radius of the catalyst particle (8 - 10 mesh). Therefore, higher

diffusion path length of Nalcomo 474 would further increase its diffusion resistance. Hence the activity of the monolith on Synthoil would be much higher than the activity of Nalcomo 474 on this feedstock.

On the other hand the higher pore size and lesser diffusion path of the monolith will not matter much when raw anthracene oil is treated because this lighter feedstock does not have significant diffusional problems with Nalcoma 474 catalyst (26,27). Therefore, the activities of the two catalysts on this feedstock will not differ as much as they differ on Synthoil. But some difference in diffusional resistances towards raw anthracene oil will also be there. One fails to comprehend that the pores having a radius of 80^{O}A will have the same resistance as pores having radius 33^{O}A.

Thus we see that if we take diffusional limitations in consideration, we can clearly explain the wide difference in the superiority of the monolith towards Synthoil on one hand and raw anthracene oil on the other. Therefore diffusional limitations likely played a role in showing different activities of the two catalysts.

Higher Desulfurization Rate of Synthoil-1 at 800 F (426 C) and Space Time of 1.5 Hours

Figure 19 shows that the sulfur content of the product oil from reactor reduces rather suddenly from 0.72 percent to 0.25 percent when space time is increased from 1.0 hour to 1.5 hours at temperature of 800 F (426 C). Such an abrupt behavior has generally not been observed. In fact increase in desulfurization has been seen to be marginal when space time is increased from 1.0 to 1.5 hours (26,27,29). Therefore, at first sight one may be tempted to doubt the results for

their accuracy. But the discussion of reproducibility on page 100 has shown that these results are indeed reproducible. Therefore, one must seek a sound explanation of these observations. This explanation must lie in the characteristics of the feedstock because that is where this study markedly differs from the previous ones. Table III gives the distillation range of the Synthoil along with the distribution of sulfur in it. The table shows that 64 percent of the sample remains as residue when distillation is carried out at 50 mm Hg pressure and the vapor temperature increases to 530 F (280 C). This means that more than half of the feed consists of very high boiling compounds. Looking at sulfur distribution we find that more than 80 percent of the total sulfur in the feed is concentrated in this heaviest fraction. This means that for any significant sulfur removal, the heaviest fraction has to take part in the desulfurization reaction. Therefore at 800 F (426 C) and space time of 1.5 hours this fraction must have reacted to give a large sulfur removal. But this could happen only after the heavier compounds had broken down to smaller, more reactive, and less diffusion limited compounds.

In the petroleum industry, high vacuum residuum containing a large fraction of asphaltic sulfur are desulfurized by first subjecting them to a desired degree of hydrocracking (67). The desulfurization rate of this deasphalted feed is seen to be much higher than the desulfurization rate of undeasphalted. Sometimes the same reactor may have the catalyst bed in two stages, one for hydrocracking and the other for desulfurization.

To find out whether hydrocracking had occurred, the samples from the reactor were subjected to ASTM 1160 D distillation. Figure 46

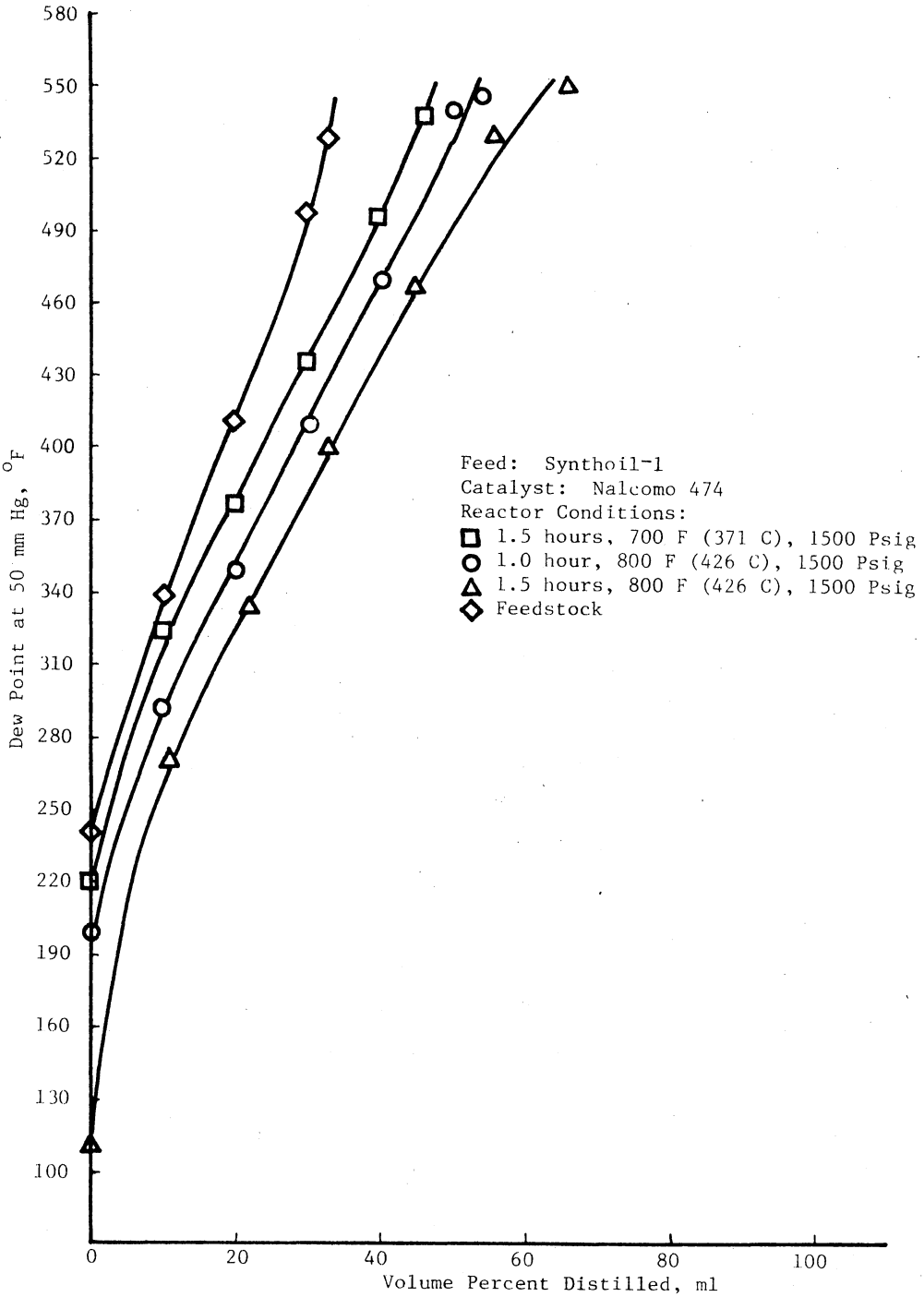

Figure 46. Distillation of Samples from Run ADC

shows distillation curves of the feed and reactor products at three different conditions. Clearly the feedstock had undergone extensive hydrocracking at the reactor conditions of 800 F (426 C), 1500 psig, and space time of 1.5 hours.

Table XXVII gives weight percent sulfur in various distillation fractions of the samples at the three conditions of reactor operation. The sulfur concentration in the bottom fraction of the product from the reactor at 800 F (426 C), 1500 psig., and space time of 1.5 hours is the lowest. That is further evidence of the very high desulfurization of Synthoil at these operating conditions. The weight percent sulfur is also reduced in the bottom fraction of the product oil when the reactor was at same conditions but space time was 1.0 hour. The table also shows the presence of a significant amount of sulfur in the lighter fractions too. This indicates that hydrocracking of the heavier fraction was taking place at a space time of 1.0 hour and due to this the sulfur in the heavier fractions gravitated to the lower fractions. Distillation curves in Figure 46 show the presence of hydrocracking at the above space time. When the space time was increased from 1.0 to 1.5 hours, the sulfur that had transferred to the lower fractions was removed. At a space time of 1.5 hours and reactor conditions of 700 F (371 C) and 1500 psig., sulfur removal was only from the lighter fractions. Sulfur in the bottom fraction of the product at above conditions is almost the same as in the bottom fraction of the feed. This explains the wide difference in desulfurization of Synthoil at 700 F (371 C) and 800 F (426 C) with reactor at 1500 psig. and space time of 1.5 hours in both the cases (Figure 19).

TABLE XXVII

PRODUCT OIL DISTILLATION RESULTS
FEED: SYNTHOIL-1 LIQUID
CATALYST: NALCOMO 474

Product Oil at 1.5 hours, 1500 psig. and 800 F (426 C)			Product Oil at 1.0 hours, 1500 psig. and 800 F (426 C)			Product Oil at 1.5 hours, 1500 psig. and 700 F (371 C)		
Dew Point F	Vol. % Distilled	Wt. % S	Dew Point F	Vol. % Distilled	Wt. % S	Dew Point F	Vol. % Distilled	Wt. % S
270	11	<0.02	292	10	0.071	327	10	<0.02
336	22	0.025	349	20	0.096	377	20	0.035
396	33	0.027	410	30	0.121	436	30	0.024
470	45	0.026	471	40	0.136	697	40	0.088
530	56	0.025	540	50	0.161	540	46	0.124
550	66	0.056	545	54	0.23	---	--	---
Bottoms	34	1.01	---	46	1.31	---	54	1.62

Effect of Space Time, Temperature, and Pressure

Space Time: The discussion on pages 19 and 20 on the order of desulfurization reactions has revealed that desulfurization for coal derived liquids is generally second order in sulfur concentration. That shows a weak dependence of desulfurization on time. The results of this study as discussed on pages 114 through 141 support the above observations except when processing Synthoil at 800 F (426 C) and 1500 psig. As explained earlier, this departure from the generally observed behavior was due to the change in the mechanism of the reaction.

Denitrogenation of petroleum feedstocks or coal-derived liquids also follows the second order reaction, but again, characteristics of the feedstock, and in certain cases, performance of the reactor would influence the order of the reaction.

Temperature: The effect of temperature on desulfurization and denitrogenation can be assessed from the rate constants on Tables VIII through XXV. The second order rate constant of desulfurization of raw anthracene oil, with the monolith catalyst, increases from 3.77 to 20.3 as temperature is increased from 650 F to 800 F. The denitrogenation rate constant increases from 0.453 to 0.724 when temperature is increased from 650 to 700 F. The desulfurization rate constants were plotted against 1/T to see if they follow the Arrhenius law (page 23). Figure 47 is such a plot. The three data points do not fall on a straight line and hence do not agree with the requirement of Arrhenius law. The most probable reason for this is that the desulfurization of coal-derived liquids or petroleum feedstocks involves

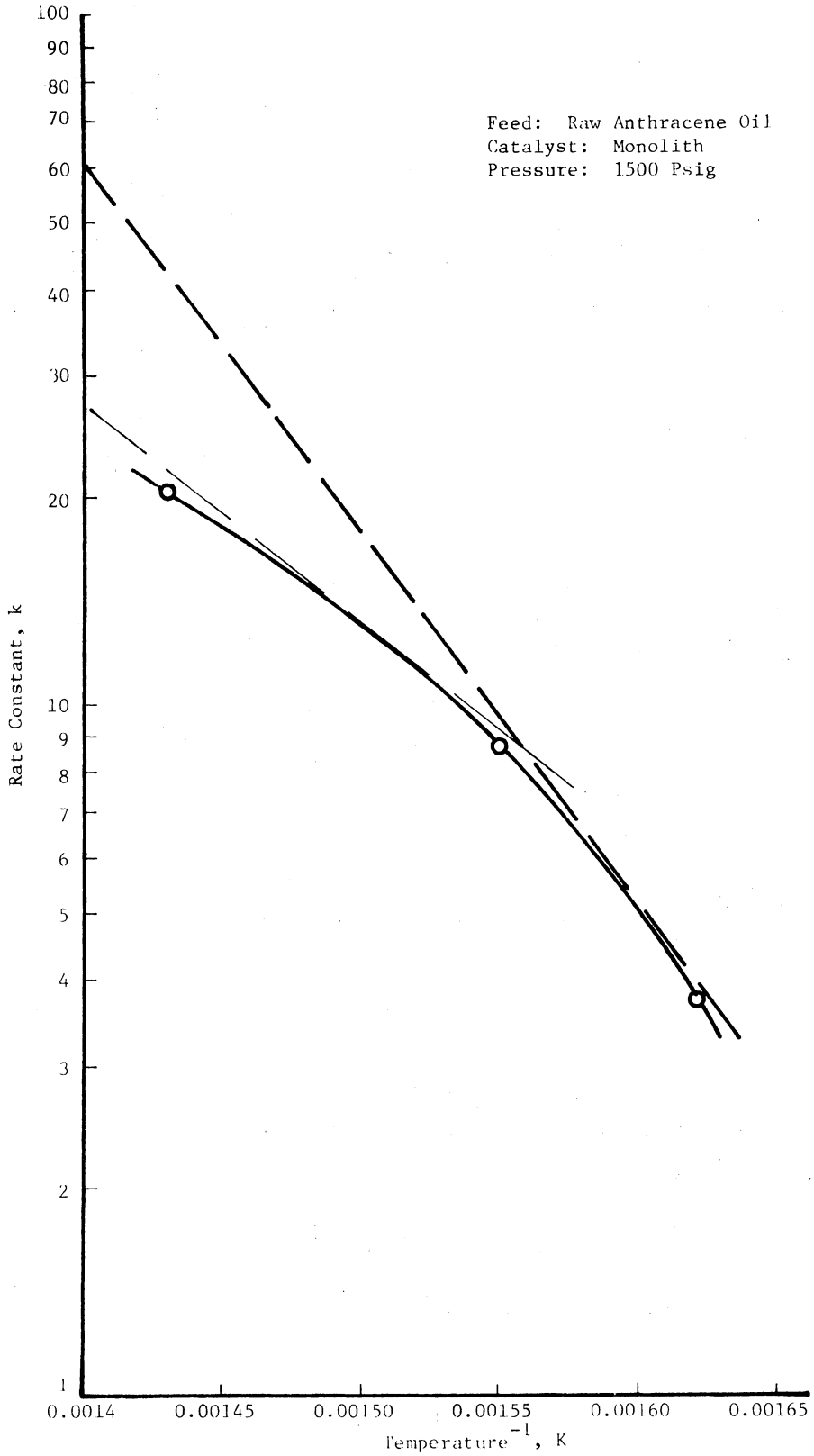

Figure 47. Arrhenius Plot of Second Order Desulfurization Rate Constants

a wide spectrum of compounds with different reactivities. As explained earlier, this may cause a change in the mechanism or the order of the reaction with increase in temperature. Therefore, the departure from Arrhenius law observed in this study is intelligible.

The activation energy for a particular reaction can be determined from the slope of the straight line plot of $\frac{1}{T}$ vs k. This plot being not a straight line in this study, exact calculation of the activation energy is not possible. However, to have an idea of the range of the activation energy for desulfurization of raw anthracene oil, the curved line was considered to consist of two portions over which approximate straight lines could be drawn (refer to Figure 47). From the slopes of these straight lines, the activation energy was calculated to be in the range of 14.5 to 24.5 kcal/gm. mole.

Tables XIX and XXIV give the second order rate constants at 700 F (371 C) and 800 F (426 C) for desulfurization and denitrogenation of Synthoil with two different catalysts. There is not much difference in the rate constants at these two temperatures. In fact the denitrogenation rate constant is less at 800 F (426 C) than at 700 F (371 C) when Nalcomo 474 catalyst is used. This is due to the secondary reactions, like hydrocracking, becoming predominant when temperature was increased from 700 F (371 C) to 800 F (426 C). Figure 46 shows the hydrocracking that took place during Run ADC. Most of the sulfur in Synthoil was concentrated in the heaviest fraction. Therefore, an increase in temperature would not help until this fraction had broken down to provide smaller and more reactive molecules. This happened at a space time of 1.0 hour, 800 F (426 C) and 1500 psig

reactor conditions. After that there was a sharp increase in desulfurization and hence the rate constant.

Pressure. Figures 13 and 14 show the effect of pressure on desulfurization and denitrogenation of raw anthracene oil. Figures 20 and 22 show similar effects on Synthoil. The pressure effects are almost similar in both the cases. There is a sharp increase in desulfurization or denitrogenation with increase in pressure from 500 to 1000 psig, but beyond this pressure, increase is negligible. These effects are in conformity with those observed in previous studies (26,27).

CHAPTER VI

CONCLUSIONS AND RECOMMENDATIONS

Conclusions

The discussion of the results, presented in this study, leads to the following conclusions:

(1) When compared on unit surface area or weight basis, the desulfurization and denitrogenation activity of the Nalcomo 474 catalyst on Synthoil (a heavy feedstock) is lower than the activity of the monolith catalyst. However, on a volume basis the activity of the monolith catalysts is lower.

(2) One of the major reasons for lower surface activity of Nalcomo 474 catalyst is its smaller pore size (33^{o}A). Because of this there are likely to be diffusion limitations when a heavy stock like Synthoil is processed, and so the surface area utilization would be smaller.

(3) When using Nalcomo 474 catalyst at reactor conditions of 800 F (426 C) and 1500 psig, Synthoil undergoes extensive hydrocracking.

(4) The sharp increase in the desulfurization activity of Nalcomo 474 catalyst on Synthoil, at reactor conditions of 800 F (426 C) and 1500 psig and space time of 1.5 hours, is due to the feedstock having hydrocracked and thus becoming lighter and more reactive. Therefore, a certain degree of hydrocracking is essential for desulfurization of

heavier feedstocks, particularly, when the sulfur is concentrated in the heaviest fraction of the stock, which is usually the case.

(5) No sharp increase in desulfurization of Synthoil when using the monolith catalyst, at the above reactor conditions, indicates that this catalyst does not help in hydrocracking the material.

(6) On a lighter feedstock, like raw anthracene oil, the activity of the monolith catalyst is lower than Nalcomo 474 catalyst, both, on a volume and weight basis. But on a surface area basis the activity of the Nalcomo 474 catalyst is lower.

(7) The results of the present study do not show whether the lower surface activity of the Nalcomo 474, on raw anthracene oil, is due to its lower intrinsic activity or due to the effect of smaller pore size. Nevertheless, the large difference in pore sizes (33^{o}A against 80^{o}A) of the two catalysts does suggest that pore size would have been one of the factors responsible for differentiating the activities of the two catalysts.

(8) The response of desulfurization and denitrogenation of the raw anthracene oil to changes in space time, temperature and pressure is the same when using the monolith catalyst as when using Nalcomo 474 catalyst. The sulfur and nitrogen removal increases with the increase in temperature but pressure beyond 1000 psig and space times higher than 1.2 hours or so have minimal effect.

(9) The effect of pressure on removal of sulfur and nitrogen from Synthoil is the same for the two catalysts. There is little increase in desulfurization or denitrogenation beyond a pressure of 1000 psig.

But the effects of temperature and space time differ in the two cases. This is because, Synthoil, when treated on Nalcomo 474,

undergoes extensive hydrocracking at 800 F.

(10) The rate expressions for desulfurization or denitrogenation of coal-derived liquids can be best approximated to second order in sulfur or nitrogen concentrations.

Recommendations

(1) The monolith catalyst should be prepared in such a way that its metallic composition is the same as that of Nalcomo 474 catalyst. To achieve this a method is suggested in Appendix B. After the monolith catalyst has approximately the same composition, its activity should be compared with Nalcomo 474 catalyst.

(2) Experimentation should be carried out to establish optimum Co/Mo ratio for the monolith support as well as other catalysts used for treating coal-derived liquids.

(3) A run should be conducted on the monolith support to assess the activity of the support itself.

(4) Deactivation studies should be carried out on both the catalysts to find out which of them would be better in the long run while processing a Synthoil or a similar liquid.

(5) Distillation of the samples from runs on raw anthracene oil should be done. The sulfur and nitrogen content in the various fractions might indicate whether the difference in intrinsic activities or the difference in pore sizes was the main reason for difference in activities of the two catalysts.

(6) This study has shown that keeping the thermowell outside of the reactor (between the reactor and the heating blocks) is as good

as keeping the thermowell in the center. Therefore future studies should be done by keeping the thermowell outside. This would give better flow distribution.

(7) Since the monolith catalyst is effective for desulfurization and denitrogenation but not so much for hydrocracking of heavy feedstocks, it should be used in combination with a hydrocracking catalyst when some degree of hydrocracking is necessary. For example, the catalyst bed can be in two portions, the upper one containing Nalcomo 474 (or some other hydrocracking catalyst) and the lower one containing the monolith catalyst.

BIBLIOGRAPHY

1. Hagenbach, G., P. H. Courty and B. Delmon, J. Catal., 31, 264 (1973).

2. Phillips, R. W. and A. A. Fote, J. Catal., 41, 168 (1976).

3. De Beer, V. H. J., T. H. M. Van Sint Fiet, et al., J. Catal. 35, 297 (1974).

4. Ratnaswany, P., et al., J. Catal., 38, 19, (1975).

5. Satterfield, C. N., A. I. Ch. E. Journal, 21 #2, 209 March 1975.

6. Mear, D. E., Am. Chem. Soc., Adv. in Chem. Ser., 133, 218 (1974).

7. Wijffels, J. B., et al., Am. Chem. Soc., Adv. Chem. Ser., 133 151 (1974).

8. Mears, D. E., Chem. Eng. Sci., 26, 1361 (1971).

9. Schwartz, J. G. and G. W. Roberts, Ind. Eng. Chem., Process Des. Develop. 12 #3 (1973).

10. Sedriks, W. and C. N. Kenney, Chem. Eng. Sci., 28 #2, 559 (1973).

11. Satterfield, C. N. and P. E. Way, A. I. Ch. E. Journal, 18 #2, March 1972.

12. Ross, L. D., Chem. Engr. Progr., 61 #10, 77 (1965).

13. Satterfield, C. N. and F. A. Ozel, A. I. Ch. E. Journal, 19 #6 1259 (1973).

14. Heineman, H., Catalysis Review, New York: Marcel Dekker, Inc., (1971).

15. Van Santen, R. A. and M. A. M. Boerma, J. Catal., 34, 13 (1974).

16. Trifiro, F. and A. Iannibellow, Chim. Ind. (Milan), 57 #3, 173 March 1975.

17. Furimsky, E. and C. H. Amberg, Can. J. Chem., 53, 2542 (1975).

18. Puranik, S. S. and A. Vogelpohl, Chem. Eng. Sci., 29, 501 (1974).

19. Smith, J. M., Chemical Engineering Kinetics, 2nd ed., New York: McGraw Hill Book Company (1970).

20. Henry, H. C. and J. B. Gilbert, Ind. Eng. Chem., Process Des. Develop., 12, 328 (1973).

21. Montagna, A. A. and Y. T. Shah, Ind. Eng. Chem., Process Des. Develop. 14 #4, 479 (1975).

22. Cecil, R. R., et al., Paper presented at Am. Inst. Chem. Eng. Meeting, Los Angeles (1968).

23. Schuit, G. C. A. and B. C. Gates, A. I. Ch. E. Journal, 19 #3, 417 (1973).

24. Satterfield, C. N., Mass Transfer in Hetrogeneous Catalysis, Cambridge, Mass.: M. I. T. Press (1970).

25. Adlington, D. and E. Thompson, Third European Symp. on Chem. Reaction Eng., 203, Pergamon Press.

26. Sooter, M. C., Ph.D. Thesis, Oklahoma State University (1974).

27. Satchell, D. P., Ph.D. Thesis, Oklahoma State University (1974).

28. Ahmed, M. M., M.S. Thesis, Oklahoma State University (1975).

29. Wells, J. W., M.S. Thesis, Oklahoma State University (1977).

30. Shah, Y. T. and J. A. Paraskos, Ind. Eng. Chem., Process Des. Develop. 14 #4, 368 (1975).

31. Van Zoonen, D. and C. T. Douwes, J. of Pet., 49, 383 (1963).

32. Jones, J. F. and L. D. Friedmann, Office of Coal Research Report No. 56, 383 (1963).

33. Voorhoeve, R. J. H. and J. C. M. Sluiver, J. Catal., 23, 243 (1971).

34. Voorhoeve, R. J. H., J. Catal., 23, 236 (1971).

35. Farragher, A. L. and P. Cossec, Proceedings of the 5th International Congress on Catalysis, 1301, North-Holland, Amsterdam (1973).

36. Minaev, V. Z., et al., Chem. Technol. of Fuel Oils, VII, 436 May-June 1975.

37. Newsom, E., Ind. Eng. Chem., Process Des. Develop., 14 #1, 27 (1975).

38. Eley, D. D., Advances in Catalysis, 24, 82, New York: Academic Press (1975).

39. Satterfield, C. N. and F. Ozel, Paper presented at A. I. Ch. E. Meeting at Chicago, 17C (1976).

40. Sivasubramanian, R., Ph.D. Thesis, Oklahoma State University (1977).

41. Van Deemter, J. J., Third European Symposium on Chemical Reaction Engineering, 215 (1964).

42. McIver, J. M., et al., J. Catal., 2, 485 (1963).

43. Johnson, R. A., et al., Adv. Chem. Ser., Am. Chem. Soc., 127, 105 (1973).

44. Hastings, K. E., et al., Oil and Gas J., 122, June 30, 1975.

45. Callen, R. B., et al., Ind Eng. Chem. Prod. Res. Dev., 15 #4 , 223 (1976).

46. Zinkov, L. M., et al., Int. Chem. Eng., 16 #3, 446, July 1976.

47. Otto, W. and S. Land, Sulphide Catalysts, Their Properties and Applications, Oxford, New York: Pergamon Press (1973).

48. Frye, C. G. and J. F. Mosby, Chem. Eng. Prog., 63 #9, 66 Sept. 1967.

49. Hoog, H. J., Inst. Petrol., 36, 738 (1950).

50. Ohtsuko, T. S., et al., Bull. Japan Petrol. Inst., 2, 13 (1960).

51. Bridge, A. G., et al., Am. Inst. Chem. Engrs., Sym. Ser., 71, 148 (1975).

52. Beuther, H. and B. K. Schmidt, Proc. Sixth World Petroleum Congress, Section III, Frankfurt (1963).

53. Flinn, R. A., et al., Hydro. Process. Pet. Ref., 129 , 129 Sept. 1963.

54. Jones, J. F. and L. D. Friedman, "Char Oil Energy Development Final Report," Office of Coal Research, #56, 25 (1970).

55. Goudriaan, F. H. Gierman and J. C. Vlugter, J. Inst. Pet., 59 #565, 40, Jan. 1973

56. Satterfield, C. N., M. Modell and J. F. Mayer, A. I. Ch. E. Journal, 21 (6), 1100 (1975).

57. Wan, K. T., M.S. Thesis, Oklahoma State University (1973).

58. Chirakaparambil, F. G., M.S. Thesis, Oklahoma State University (1974).

59. Crynes, B. L., "Catalysts for Up-Grading Coal-Derived Liquids," Quarterly Report to Energy Research and Development Administration for Period June 9, 1975 to September 9, 1975.

60. Qader, S. H. and G. R. Hill, Ind. Eng. Chem., Process Des. Develop., 8, 450 (1969).

61. Levenspiel, O., Chemical Reaction Engineering, 2nd ed., New York: John Wiley and Sons, Inc. (1974).

62. Ahmed, M. M., Unpublished work, Oklahoma State University, Stillwater, Oklahoma (1977).

63. _____, Leco Automatic Sulfur Determinator Instruction Manual, Lab Equipment Corporation, 1415 Hilltop Road., St. Joseph, Michigan 49085.

64. _____, Model 240 Elemental Analyzer Instruction Manual, Perkin-Elmer, Norwalk, Conn.

65. Mehta, D. C., Ph.D. Thesis, in preparation, Oklahoma State University, Stillwater, Oklahoma.

66. Smith, A. J., G. Myers and W. C. Slaner, Jr., Microchimica Acts (Wien), 217 (1972).

67. U. S. Patent 2,987,467, June 6, 1961.

68. Crynes, Billy L., Personal Communications, Oklahoma State University.

69. Jones, J. J. and J. F. Jones, Preprints, Div. of Fuel Chem., American Chemical Society (1), 26 (1972).

70. Scotti, L. J., Char Oil Energy Development Interm Report (2), R & D Report No. 73, U. S. Department of Interior, Office of Coal Research (1974).

71. Mamidi, R., Special Report to Dr. B. L. Crynes, Oklahoma State University (1976).

72. Sokolnikoff, I. S. and R. M. Redheffer, Mathematics of Physics and Modern Engineering, New York: McGraw Hill (1966).

APPENDIX A

EXPERIMENTAL PROCEDURE

This appendix will contain details of some of the steps involved in conducting actual experimentation to obtain the required data.

Catalyst Preparation

One of the three reactor runs for this study was conducted with Nalcomo 474 catalyst which is a vendor preparation and available commercially. Properties of this catalyst are given in Table V. For the other two runs the catalyst was prepared according to the procedure suggested by Bruce F. Leach, Research Chemist at Conoco in Ponca City, OK. The procedure is as follows:

(1) The catalyst support is crushed and screened to give the desired mesh size, usually 8-10 mesh.

(2) 3.725 grams of MoO_3 is dissolved in 15 milliliters of distilled water and 5 milliliters of 30 percent aqueous ammonia.

(3) The mixture is heated very gently until MoO_3 has dissolved. If MoO_3 does not dissolve, a little more of NH_3 is added.

(4) The solution is cooled to room temperature and the pH is adjusted to 5.5 with concentrated HNO_3.

(5) Then 10 milliliters of HNO_3 and 4.0548 grams of $Co(NO_3)_3.6H_2O$ are added.

(6) The solution is diluted to 40 ml. with distilled water.

(7) The above solution is poured over 25 grams of catalyst support. This is allowed to set overnight.

(8) The catalyst is dried at 212 F (100 C) and then calcined at 900 F (477 C) for one hour.

However, the above method had to be altered in certain respects in this study. The catalyst support, received from Corning Glass Company, was in the form of Monolith segments as described on page 27. Therefore, the first step in catalyst preparation, i.e, crushing and screening, was omitted. Also, the amount of support used was about 14 grams instead of 25 grams. Therefore, all other quantities, in the catalyst preparation method, were scaled down accordingly. The prepared catalyst was analyzed for cobalt and molybdenum by Atomic Mass Spectrograph in Geology Department of Oklahoma State University.

Normal Operation of the Reactor

Normal operation of the reactor has been described in Chapter III. Table XXVIII gives position of the valves during normal operation of the reactor.

Sampling Procedure

After the reactor was on oil for 32 hours, sampling of the reactor products was started. The line out time of 32 hours was given for the catalyst activity to stabilize. Sampling was done in such a way as not to disturb the normal operation of the reactor. Detailed sampling procedures for the liquid and gaseous products are given below.

TABLE XXVIII

POSITION OF VALVES DURING NORMAL OPERATION

Valve	Position	Valve	Position
1	open	12	open
2	open	13	open
3	open	14	closed
4	closed	15	closed
5	closed	16	closed
6	closed	17	open
7	closed	18	open
8	open	19	closed
9	closed	20	open
10	open	21	open
11	open		

Liquid Sampling: Following steps constitute the total procedure.

(1) The valves 11 and 13 were closed to isolate sample bomb 23.

(2) The valve 9 was opened slowly to depressurize the sample bomb 23.

(3) After pressure gauge 37 showed atmospheric pressure, valves 14 and 15 were opened. This allowed nitrogen to bubble through the

sampling bomb and purge it of H_2S and NH_3. This purging was done for 20 - 30 minutes.

(4) After purging was over, valves 15 and 9 were closed. A bottle was kept below the sampling point and valve 16 was opened. After all the liquid had come in the bottle, valve 16 was closed.

(5) After the sample was collected, valve 12 was closed and valve 15 slowly opened to repressurize the bomb, 23, with hydrogen, to the original pressure.

(6) The valve 15 was then closed and 12 opened.

(7) The valves 11 and 13 were opened to bring the sampling bomb back in line.

Gas Sampling:

(1) Run the liquid nitrogen into the Dewar flask and kept the coil immersed in it.

(2) Opened valves 4, 5, 6, and 7 to let the off-gas pass through the coil. At the same time closed valve 8.

(3) Kept the gas flowing through the coil for the duration the sample was to be taken.

(4) Opened valve 8 and closed valves 4, 5, 6, and 7 to isolate the coil from the system.

(5) A 300 c.c. stainless steel gas bottle with stainless steel valves at both the ends was then hooked to vacuum pump and was evacuated to an absolute pressure of 15 mm Hg. The bottle was heated somewhat to drive out any condensed material inside the bottle.

(6) The bottle was pressurized with nitrogen and re-evacuated to a pressure of 10 mm Hg. The valve between the vacuum pump

and the bottle was then closed and vacuum pump stopped.

(7) The coil was removed from the system and connected to the lower end of the bottle. Figure 48 shows the whole arrangement. The valve between the bottle and the coil was opened to transfer the gas from the coil to the bottle. The coil was heated for 10 - 15 minutes with heating lamp to facilitate the transfer.

(8) The coil was kept connected to the bottle for about one hour so that equilibrium was achieved between the coil and the bottle.

(9) After transferring the gas from the coil to the bottle, the valve between the coil and the bottle was closed and the coil removed.

(10) The bottle was tightly capped at both the ends to prevent any leakage.

(11) The coil was then installed back in the reactor system.

The gas samples collected were sent to the Chemistry Department for analysis.

Analysis of Samples

The product samples from the reactor were analyzed for their sulfur and nitrogen contents. A few samples were distilled. The Synthoil feedstock was also analyzed for its ash content. The procedural details involved in these determinations are described below.

Sulfur Analysis: An automatic sulfur analysis system, supplied by Leco Laboratory Equipment Corporation, was used to determine sulfur content of the samples. The procedure for sulfur analysis, given below, is based on the one given in Leco Bulletin (63). It consists of the following steps:

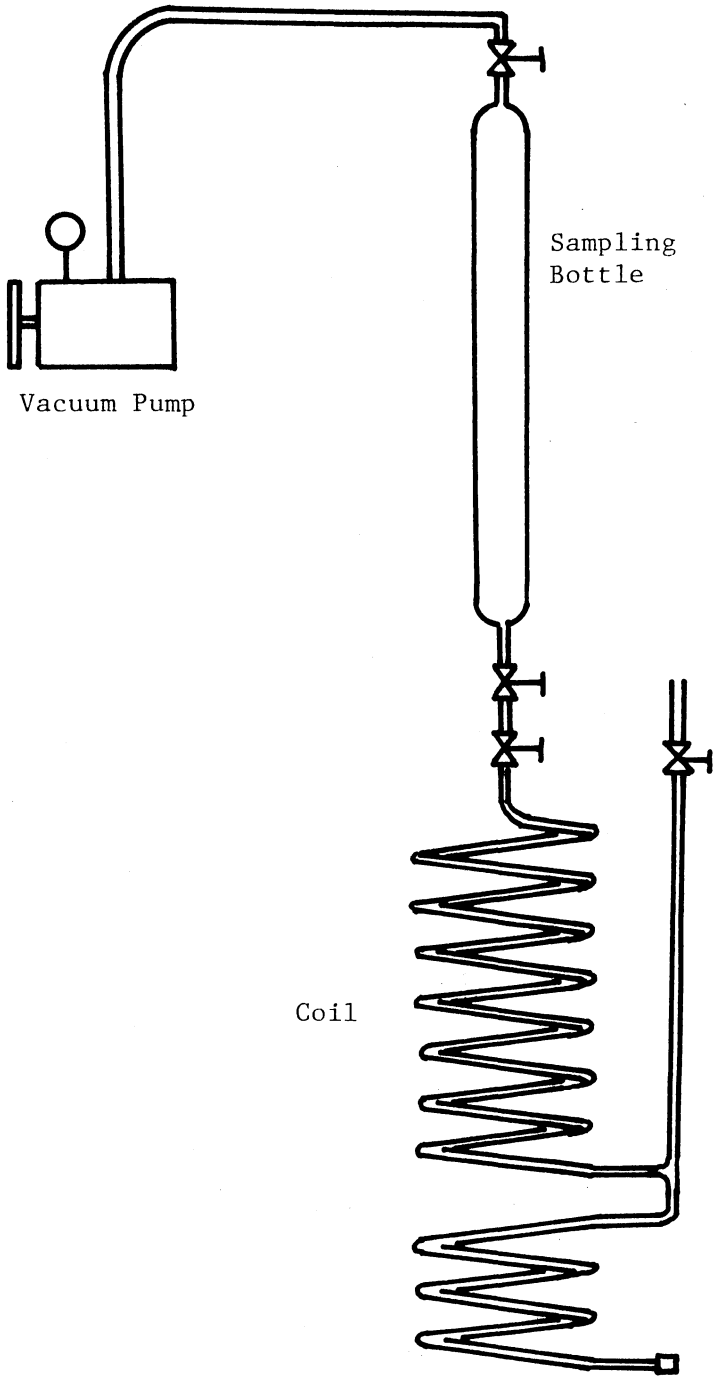

Figure 48. Arrangement for Transferring Gas in the Sampling Bottle

(1) Solution Preparation: Three solutions, i.e., starch, HCl and KIO_3 are needed for sulfur analysis. The starch solution was prepared by adding 2 grams of arrow starch in 50 c.c. of distilled water. This was then poured into 150 c.c. of boiling distilled water. The mixture was boiled for 1 to 2 minutes and then allowed to cool to room temperature. After this, six grams of KI was added to the starch solution and it was stirred vigorously till all the KI dissolved. Fresh starch solution was prepared every day the analyses were done. The HCl solution was prepared by dissolving 10 ml of concentrated HCl in one liter of distilled water. This solution was prepared usually in large quantities. The KIO_3 solution was prepared by dissolving 0.111 grams of KIO_3 in one liter of distilled water. This solution was also made in large quantities.

(2) Machine Warm Up: The combustion tube, the titration vessel, and all other apparatus were cleaned thoroughly with distilled water and allowed to dry. The photocell alignment was then done to see that resistance across the photocell was 30,000 to 50,000 ohms. After this, the furnace and the titrator were turned on and allowed to warm up for 30 minutes. Then HCl solution was taken into the titration vessel up to a predetermined level. The purified oxygen was allowed to bubble through the HCl solution for about 15 minutes to ensure that the gas passage was clear. The resistance heater on the tube, connecting the furnance with the titrator, was also switched on.

(3) Sample Preparation: The sample for analysis was prepared in the following manner:

(a) Added 0.282 ± 0.005 grams of MgO into the crucible supplied by Leco Corporation.

(b) Weighed the crucible and noted the weight.

(c) Added 0.1 ± 0.005 grams of oil sample to MgO. In case of Synthoil the oil sample taken was 0.05 ± 0.005 grams.

(d) Weighed the crucible and noted the weight.

(e) Covered the sample with another layer of 0.282 ± 0.005 grams of MgO.

(f) Added 1.5 ± 0.005 grams of iron chips.

(g) Over the iron chips, put 0.77 ± 0.005 grams of tin accelerator.

(h) Covered the crucible with porous lid supplied by Leco Corporation.

The sample was then considered to be ready for combustion.

(4) Setting the End Point: This was done to establish reference color for the titrator. The titration vessel was filled with HCl solution up to the predetermined level and 2 c.c. of starch solution was added. Oxygen was allowed to bubble through the vessel at a rate of 1.2 liters per minute. The end point control knob was turned to the extreme left position and the double throw switch was switched to end point position. The end point control knob was then slowly turned clockwise till the color of the solution in the titration vessel turned medium blue by automatic addition of KIO_3. The end point control knob was then not disturbed unless resetting of the end point became necessary.

(5) Blank Determination: The sample was prepared exactly in the same way as described in step 3 except that no oil was added. The

titration vessel was filled with HCl up to the marked position. Two milliliters of the starch was added and oxygen bubbling, at rate of 1.2 liters per minute, started. The double throw switch was put at end point. When further addition of KIO_3 solution stopped, the switch was turned to neutral position. Then about 0.7 grams of sodium azide was added in the solution in the titration vessel. This would avoid interference by nitrogen oxides and chlorine. The prepared crucible was then placed in the combustion tube so as to burn it in an atmosphere of oxygen. The double throw switch was then turned to titrate position. The gases produced due to combustion passed through the titration vessel and the SO_2 tended to decolorise the solution by undergoing the following reaction:

$$SO_2 + I_2 + H_2O \longrightarrow H_2SO_4 + 2HI.$$

To maintain the color at the end point setting, necessary amount of KIO_3 solution was added by the titrator. When no more addition took place, titration was considered to be over and the volume of KIO_3 added was noted. This was the blank value and was a measure of the sulfur present in the crucible and chemicals added in the crucible.

(6) Determination of Furnace Factor: To minimize the error due to incomplete combustion, a furnace factor was determined by finding the volume of KIO_3 used when an oil of known sulfur content was analyzed. The reference oil used in this study was a coal-derived liquid supplied by Pittsburg and Midway Coal Mining Company. The sample was prepared according to step 3 and was run in the same way as for blank determination. The furnace factor was calculated in the following manner:

$$\text{Furnace factor, } F = \frac{\text{(weight of sample) (weight percent S)}}{\text{(buret reading-blank reading)}}$$

(7) Analysis of an Unknown Sample: The sample was prepared according to step 3 and was run in the same way as for determining the furnace factor described in step 6. The weight percent sulfur in the sample was calculated as follows:

$$\text{weight percent sulfur} = \frac{F\ \text{(buret reading-blank reading)}}{\text{(weight of the sample)}}$$

A sample was normally analyzed twice. If consistency was not good, the analysis was repeated.

Nitrogen Analysis: A brief description of the working of the nitrogen analysis system, used in this study, was given in Chapter III. The stepwise procedure, for actual running of the samples is given below:

(1) Calibration: The instrument was calibrated, each day the samples were analyzed. This was done by first finding the blank signal with empty platinum boat. The empty boat was placed in the combustion ladel and inserted into the combustion tube. The analysis was started by pressing the start switch of the analyzer. After the analyzer went through full program cycle, it gave two outputs. The first was the zero value and the second the read value. The difference between these two, for each of the three elements, gave the blank signals. The blank runs were repeated till consistent blank values were obtained. Then a calibration standard, i.e., acetanilide, was run. Approximately two milligrams of the acetanilide was carefully weighed into the platinum boat which was then placed in the ladel and inserted

into the combustion tube. The calibration factor for nitrogen was found from the analyzer output in the following way:

$$K_N = \frac{(\text{Read})_N - (\text{Zero})_N - (\text{Blank})_N}{(\text{Weight of Sample})(\text{Percentage of N})}$$

Calibration for other elements could also be found in the same way. The calibration runs were repeated to get consistent values of K_N.

(2) Calibration Check: The calibration was checked by running raw anthracene oil whose nitrogen content was known. This material, being a liquid, was analyzed in aluminum capsules. Therefore the blank values for aluminum capsules with tungsten anhydride (which was used as an oxidant along with the sample) were first established. This was done in the same way as for the empty platinum boat. To analyze raw anthracene oil, the bottle containing the oil was vigorously shaken so that the nitrogen got homogeneously distributed. Then 2 - 3 milligrams of oil was weighed into the aluminum capsule. The capsule was sealed, in an atmosphere of helium, with Perkin-Elmer Capsule Sealer, Model 042-1250. The sealed capsule was placed in the ladel and about 20 mg of tungsten anhydride was put near the capsule in the ladel. The ladel was inserted in the combustion tube and the analyzer started by pressing the start switch. The recorder output was used to find the nitrogen content in the following way:

$$\text{Weight percent nitrogen} = \frac{(\text{Read})_N - (\text{Zero})_N - (\text{Blank})_N}{K_N\ (\text{Weight of the Sample})}$$

If the value calculated above was within about 5 percent of the known value, analysis of the unknown samples was started. Sometimes, when the nitrogen content of the raw anthracene oil was in doubt, calibration was checked with cyclohexanone-2,4- dinitrophenylhydrazone.

(3) Analysis of Unknown Samples: The samples from the runs on Synthoil, i.e., runs ADA and ADC, were analyzed by using platinum boat because these samples being too viscous, could not be put in the aluminum capsules. Therefore, the procedure used was the same as used during calibration with acetanilide except that different blank values, with empty boat and 20 mg. of tungsten anhydride, were established. The samples from run ADB, which was on raw anthracene oil, were, however, analyzed in aluminum capsules. Therefore, the procedure for running these samples was the same as for running the samples of raw anthracene oil during calibration check. Each sample was run 2 to 3 times to get consistent results.

Ash Determination: The method given below is based on the ASTM standard D 482-74. The only difference is that the sample is not ignited before putting it in the furnace, as recommended in the ASTM method. Slow heating in the furnace itself is considered to achieve the same purpose as initial ignition.

(1) Take three porcelain crucibles, with lids and three porcelain dishes. Dishes will be used as containers for the crucibles.

(2) Clean all these thoroughly. If required, rinse with HCl and then wash with water and dry.

(3) Mark the three crucibles as A, B and C.

(4) Put the crucibles in the furnace and let its temperature rise to 1300 - 1400 F (700 - 800 C given in ASTM).

(5) Place the three crucibles in the furnace for 10 minutes or more.

(6) Take out the three crucibles, put them in three china dishes. Cover the crucibles with lids and the china dishes with pieces of paper,

preferably glassline.

(7) Let the crucibles come to room temperature.

(8) Weigh the crucibles to nearest 0.1 mg. and note their weight.

(9) Put oil in each crucible and weigh. The weight of oil should be such as to give up to 20 mg. of ash.

(10) Place the three crucibles in china dishes. Cover the crucibles with lids and the china dishes with pieces of paper.

(11) Reduce the temperature of the furnace to 600 - 700 F.

(12) Put the three crucibles in the furnace and let the samples combust first at this low temperature.

(13) After initial combustion has taken place, start increasing the temperature slowly.

(14) Increase the temperature to 1400 F (775 $\pm$ 25 C given in ASTM method). Keep the samples at this temperature for one hour or more.

(15) Take out the three crucibles into three china dishes. Cover crucible with lids and china dishes with pieces of paper

(16) Let the crucibles come to room temperature.

(17) Weigh the three crucibles to nearest 0.1 mg.

(18) Place the crucibles back into the furnace for 20 - 30 minutes.

(19) Repeat steps 15, 16 and 17.

(20) Repeat the heating and weighing until consecutive weighings differ by not more than 0.5 mg.

Calculations:

$$\text{Ash } \% = \frac{W}{W} \times 100$$

where

w = weight of ash , gram

W = weight of samples , gram

Precautions:

(1) While putting oil into the crucibles, see no oil sticks to the outside of the crucible.

(2) Make sure the tongs are clean before holding the crucible.

(3) Use long tongs and asbestos gloves while taking the crucibles in and out of the furnace.

Distillation: The procedure given below was outlined by Wells (29) and is based on the ASTM D 1160 standard. It consists of the following steps.

(1) Turn on water heater on tank behind the unit.

(2) Connect recorder to temperature read out device. Connect positive to positive and negative to negative.

(3) Set the recorder controls to a slow chart drive speed. Turn off recorder.

(4) Load cold trap with acetone and dry ice.

(5) Assemble distillation unit without sample in flask. Lower safety shield and be sure you are wearing goggles.

(6) Turn on the vacuum pump and powerstat. Set powerstat at 30. Open valve to bypass manostat.

(7) Observe cold trap. If acetone begins to accumulate, do not drop pressure below the point at which the acetone in the cold trap starts to bump.

(8) Turn off vacuum pump, repressurize system with nitrogen and drain cold trap.

(9) Again turn on vacuum pump with no sample present and observe cold trap. If no acetone appears, draw the system down to the lowest possible vacuum. If acetone is present, repeat steps 7, 8 and 9.

(10) Repressurize with N_2. Load distillation flask with the sample and four boiling chips. Reassemble the system.

(11) On the manostat, turn adjustment screw fully counterclockwise.

(12) Turn on vacuum pump and draw a vacuum to the lowest point (20 mm of Hg). Turn off vacuum pump and leak test system by observing system vacuum manometer. It should remain steady.

(13) Repressurize with nitrogen. (This supplies a noncombustible atmosphere.)

(14) Turn on the vacuum pump and draw the pressure down to the lowest point (20 mm Hg).

(15) Close manostat bypass valve, then repressurize with nitrogen to a pressure greater than 50 mm of Hg (70 mm of Hg).

(16) Note final pressure of the system and adjust with adjustment screw on manostat.

(17) Lower face shield and be sure you have your goggles on.

(18) Turn on powerstat, hot cooling water and cold cooling water. Initial setting of powerstat is determined by operator (recommend 90 or higher).

(19) Turn on recorder indicating temperature at this point.

(20) Watch for the vapor reflux line in the distillation flask. Also be careful to avoid extensive bumping. A little bumping is OK as long as it does not cause carry over of the pot sample in distillate or touch the thermocouple.

(21) Record temperature of first drop on recorder output and in logbook.

(22) Collect approximately 10% of total sample in each test tube. Record vapor and pot temperatures when test tube is changed.

(23) Powerstat settings are increased to give a smooth distillation curve on the recorder. Be sure to avoid scallops in the curve. Also it is possible to have excessive variation in distillation curve due to acetone in system.

(24) Continue to increase powerstat settings to maintain a smooth curve. On the last test tube, carefully watch the recorder output. It will begin to level off and drop as thermal cracking begins to occur. At this point shut down the unit. Under no circumstances exceed 750 F (400 C) pot temperature.

(25) Shut down. Turn off vacuum pump and powerstat. Repressurize slowly with nitrogen.

(26) Turn off recorder drive.

(27) Isolate manometer and bleed off nitrogen through manometer - vacuum pump exhaust line.

(28) Allow to cool for 20 - 30 minutes. Raise safety shield.

(29) Collect bottom sample and other sample.

(30) Clean up. Clean up is best accomplished by vacuum distillation of a small amount (20 - 30 ml) of raw anthracene oil, followed by atmospheric distillation of acetone.

(31) De-energize all equipment.

APPENDIX B

METHOD RECOMMENDED FOR PREPARING THE MONOLITH CATALYST

This appendix contains guidelines for preparing the monolith catalyst so that its composition is nearly the same as that of Nalcomo 474 catalyst. Exact details of the method may have to be worked out at the time of preparation of the catalyst. When the catalyst is prepared for the first time, some trial and error may become necessary. This can be done by first preparing a single monolith segment as described in the following steps:

(1) Prepare a solution of MoO_3 as described in Appendix A. The volume of the solution should be just sufficient to wholly cover the monolith segment.

(2) The monolith alumina segment should be weighed and kept in the solution overnight. It should then be taken out and completely dried in an oven at 212 F (100 C).

(3) Weigh the dried monolith segment and find the amount of Mo deposited on it.

(4) If the weight of Mo deposited per unit weight of the support is less than that in Nalcomo 474 catalyst, prepare another solution of MoO_3 and place this segment again in that solution. Remove it after some time, dry, weigh and find total quantity of Mo deposited. By repeating this, the amount of Mo on monolith alumina can be adjusted.

(5) After the Mo deposited is somewhat more than that in Nalcomo 474 catalyst, prepare cobalt solution as described in Appendix A. Put the dried monolith alumina segment, on which Mo was deposited, in this solution and keep it overnight.

(6) Remove the segment, dry and weigh to find the quantity of Co deposited on it.

(7) If Co is less than desired, prepare another cobalt solution and put the segment in it.

(8) Repeat steps 6 and 7 until desired amount of Co deposits. If amount of Co absorbed becomes more than required, repeat all over again. By conducting the above experiment once or twice, the concentrations of the solutions and the time for which the segment should be kept in them, can be established such that the composition of the monolith catalyst is approximately the same as that of Nalcomo 474 catalyst.

Once the above objective has been achieved, the catalyst can be prepared with a number of monolith alumina segments, as required for a particular reactor run, in the same way as described for a single monolith segment but using the established values of the solutions concentrations and the time of treatment.

The cobalt and molybdenum solutions, left after treating the monolith alumina supports, should be dried and the quantity of Mo and Co salts left should be found. This information can serve as a check to the amount of Mo and Co deposition already calculated. The prepared catalyst can also be analyzed for concentration of the metallic species in the Geology Department of Oklahoma State University.

APPENDIX C

EXPERIMENTAL DATA

The data obtained from the three experimental runs ADA, ADB and ADC, are listed in this appendix. The feedstock, the catalyst and the reactor conditions employed are also listed. The temperatures, pressures and hydrogen flow rates shown are nominal. The deviations of these parameters from their nominal values have been discussed in Chapter V. The catalyst bed height in each run was 14 inches (35.5 cm).

TABLE XXIX

RESULTS OF RUN ADA, REACTOR I

Catalyst: Monolith Alumina Impregnated with Co and Mo
Weight of the Catalyst: 12.93 grams
Volume of the Catalyst: 30.3 c.c.
Feedstock: Synthoil-1

Sample Number	Temp[a] (F)	Pressure (psig)	Space Time[b] (Volume hrly)	Hydrogen (SCF/BBL)	Hours[c] on oil	%S[d]	%S[e] Removal	%N[d]	%N[e] Removal
ADA 1	700	1000	1.11	1500	36	0.815	21	1.038	13
ADA 2	700	1000	1.11	1500	38	0.646	37	0.988	17
ADA 3	700	1000	1.11	1500	40	0.66	35	0.997	16
ADA 4	700	500	1.11	1500	45	0.805	21	1.05	12
ADA 5	700	500	1.11	1500	47	0.701	31	1.039	13
ADA 6	700	500	1.11	1500	49	0.685	33	1.05	12
ADA 7	700	1500	1.11	1500	53	0.854	16	1.00	16
ADA 8	700	1500	1.11	1500	55	0.69	32	1.025	14
ADA 9	700	1500	1.11	1500	57	0.638	38	1.06	11
ADA 10	700	1500	0.666	1500	60	0.755	26	1.155	3
ADA 11	700	1500	0.666	1500	61	0.781	23	1.2	-
ADA 12	700	1500	0.666	1500	62	0.786	23	1.06	11
ADA 13	700	1500	1.665	1500	68	0.733	28	1.09	8

TABLE XXIX (Continued)

Sample Number	Temp[a] (F)	Pressure (psig)	Space Time[b] (Volume hrly)	Hydrogen (SCF/BBL)	Hours[c] on oil	%S[d]	%S[e] Removal	%N[d]	%N[e] Removal
ADA 14	700	1500	1.665	1500	70	0.687	33	1.154	3
ADA 15	700	1500	1.665	1500	72	0.62	39	1.053	12
ADA 16	700	1500	1.11	1500	75	0.741	27	1.14	4
ADA 17	700	1500	1.11	1500	76.5	0.756	26	1.084	9.
ADA 18	700	1500	1.11	1500	78	0.683	33	1.16	3
ADA 19	650	1500	1.11	1500	83.5	0.779	24	1.24	-
ADA 20	650	1500	1.11	1500	85	0.77	25	1.09	8
ADA 21	650	1500	1.11	1500	86.5	0.80	22	1.17	2
ADA 22	650	1500	1.665	1500	92	0.827	19	0.942	21
ADA 23	650	1500	1.665	1500	94	0.755	26	0.958	20
ADA 24	650	1500	1.665	1500	96	0.759	26	0.969	19
ADA 25	650	1500	0.665	1500	99	0.778	24	1.044	12
ADA 26	650	1500	0.665	1500	100	0.818	20	0.976	18
ADA 27	650	1500	0.665	1500	101	0.826	19	0.953	20
ADA 28	800	1500	0.665	1500	106	0.846	17	0.956	20
ADA 29	800	1500	0.665	1500	107	0.646	37	0.903	24

TABLE XXIX (Continued)

Sample Number	Temp[a] (F)	Pressure (psig)	Space Time[b] (Volume hrly)	Hydrogen (SCF/BBL)	Hours[c] on oil	%S[d]	%S[e] Removal	%N[d]	%N[e] Removal
ADA 30	800	1500	0.665	1500	108	0.783	23	0.931	22
ADA 31	800	1500	1.665	1500	113	0.732	28	0.97	18
ADA 32	800	1500	1.665	1500	115	<0.02	-	0.945	21
ADA 33	800	1500	1.665	1500	117	0.604	41	0.915	23
ADA 34	800	1500	1.11	1500	120.5	0.607	41	1.0	16
ADA 35	800	1500	1.11	1500	122	0.636	38	0.965	19
ADA 36	800	1500	1.11	1500	123.5	0.607	41	0.94	21
ADA 37	700	1000	1.11	1500	128.5	0.665	35	0.932	22
ADA 38	700	1000	1.11	1500	130.0	0.776	24	0.997	16
ADA 39	700	1000	1.11	1500	131.5	0.768	25	1.035	13

a Nominal Reactor Temperature
b This is a volume hourly space time (volume of catalyst/volume of oil per hour)
c Total hours which the catalyst has been contacted with oil at reaction conditions.
d Percent of sulfur or nitrogen in liquid product.
e % Removal = (raction in feed less fraction in product)/(fraction in feed.)

TABLE XXX

RESULTS OF RUN ADB, REACTOR II

Catalyst: Monolith Alumina Impregnated with Co and Mo
Weight of the Catalyst: 12.52 grams
Volume of the Catalyst: 30.3 c.c.
Feedstock: Raw Anthracene

Sample Number	Temp[a] (F)	Pressure (psig)	Space Time[b] (Volume hrly)	Hydrogen (SCF/BBL)	Hours[c] on oil	%S[d]	%S[e] Removal	%N[d]	%N[e] Removal
ADB 1	700	1000	1.118	1500	36	0.142	70	0.645	38
ADB 2	700	1000	1.118	1500	38	0.136	71	0.604	42
ADB 3	700	1000	1.118	1500	40	0.114	76	0.610	41
ADB 4	700	500	1.118	1500	45	0.143	70	0.720	30
ADB 5	700	500	1.118	1500	47	0.142	70	0.745	28
ADB 6	700	500	1.118	1500	49	0.141	70	0.760	27
ADB 7	700	1500	1.118	1500	53	0.098	79	0.591	43
ADB 8	700	1500	1.118	1500	55	0.127	73	0.556	46
ADB 9	700	1500	1.118	1500	57	0.099	79	0.632	39
ADB 10	700	1500	0.67	1500	60	0.099	79	0.644	38
ADB 11	700	1500	0.67	1500	61	0.094	80	0.702	32
ADB 12	700	1500	0.67	1500	62	0.144	69	0.615	41
ADB 13	700	1500	1.677	1500	68	0.056	88	0.578	44
ADB 14	700	1500	1.677	1500	70	0.065	86	0.498	52

TABLE XXX (Continued)

Sample Number	Temp[a] (F)	Pressure (psig)	Space Time[b] (Volume hrly)	Hydrogen (SCF/BBL)	Hours[c] on oil	%S[d]	%S[e] Removal	%N[d]	%N[e] Removal
ADB 15	700	1500	1.677	1500	72	0.44	-	0.608	41
ADB 16	700	1500	1.118	1500	75	0.059	87	0.529	49
ADB 17	700	1500	1.118	1500	77	0.068	86	0.574	44
ADB 18	700	1500	1.118	1500	78.5	0.125	73	0.588	43
ADB 19	650	1500	1.118	1500	84	0.175	63	0.756	27
ADB 20	650	1500	1.118	1500	85.5	0.159	66	0.706	32
ADB 21	650	1500	1.118	1500	87	0.17	64	0.883	15
ADB 22	650	1500	1.677	1500	93	0.089	81	0.670	35
ADB 23	650	1500	1.677	1500	95	0.125	73	0.67	35
ADB 24	650	1500	1.677	1500	97	0.092	80	0.745	28
ADB 25	650	1500	0.67	1500	100	0.190	59	0.616	40
ADB 26	650	1500	0.67	1500	101	0.184	61	0.743	28
ADB 27	650	1500	0.67	1500	102	0.196	58	0.817	21
ADB 28	800	1500	0.67	1500	107	0.074	84	0.53	49
ADB 29	800	1500	0.67	1500	108	0.076	94	0.51	51

TABLE XXX (Continued)

Sample Number	Temp[a] (F)	Pressure (psig)	Space Time[b] (Volume hrly)	Hydrogen (SCF/BBL)	Hours[c] on oil	%S[d]	%S[e] Removal	%N[d]	%N[e] Removal
ADB 30	800	1500	0.67	1500	109	0.05	88	0.39	62
ADB 31	800	1500	1.677	1500	114	<0.02	>96	0.333	68
ADB 32	800	1500	1.677	1500	116	<0.02	>96	0.345	33
ADB 33	800	1500	1.677	1500	118	<0.02	>96	0.263	25
ADB 34	800	1500	1.118	1500	121.5	0.023	95	0.435	58
ADB 35	800	1500	1.118	1500	123	0.041	91	0.54	48
ADB 36	800	1500	1.118	1500	124.5	0.018	96	0.48	46
ADB 37	700	1000	1.118	1500	129.5	0.100	79	0.7	68
ADB 38	700	1000	1.118	1500	131	0.087	81	0.805	22
ADB 39	700	1000	1.118	1500	132.5	0.101	79	0.635	39

[a] Nominal Reactor Temperature
[b] This is a volume hourly space time (volume of catalyst/volume of oil per hour)
[c] Total hours which the catalyst has been contacted with oil at reaction condition.
[d] Percent of sulfur or nitrogen in liquid product.
[e] % Removal = (fraction in feed less fraction in product)/(fraction in feed.)

TABLE XXXI

RESULTS OF RUN ADC, REACTOR I

Catalyst: Nalcomo 474
Weight of the Catalyst: 14.8 grams
Volume of the Catalyst: 27.5 c.c.
Feedstock: Synthoil-1

Sample Number	Temp[a] (F)	Pressure (psig)	Space Time[b] (Volume hrly)	Hydrogen (SCF/BBL)	Hours[c] on oil	%S[d]	%S[e] Removal	%N[d]	%N[e] Removal
ADC 1	700	1500	1.03	1500	35.5	0.635	38	0.995	16
ADC 2	700	1500	1.03	1500	37.0	0.703	31	1.1	8
ADC 3	700	1500	1.03	1500	38.5	0.735	28	1.02	14
ADC 4	700	1500	0.62	1500	41.5	0.681	33	1.08	9
ADC 5	700	1500	0.62	1500	42.5	0.753	26	1.08	9
ADC 6	700	1500	0.62	1500	43.5	0.753	26	1.07	10
ADC 7	700	1500	1.545	1500	49.5	0.621	39	1.02	14
ADC 8	700	1500	1.545	1500	51.5	0.741	27	0.994	16
ADC 9	800	1500	1.545	1500	53.5	0.668	35	1.03	14
ADC 10	800	1500	1.545	1500	60	0.263	74	0.915	23
ADC 11	800	1500	1.545	1500	62	0.345	66	1.00	16
ADC 12	800	1500	1.545	1500	64	0.248	75	0.911	23
ADC 13	800	1500	0.62	1500	67	0.737	28	1.15	3
ADC 14	800	1500	0.62	1500	68	0.729	29	1.08	9

TABLE XXXI (Continued)

Sample Number	Temp[a] (F)	Pressure (psig)	Space Time[b] (Volume hrly)	Hydrogen (SCF/BBL)	Hours[c] on oil	%S[d]	%S[e] Removal	%N[d]	%N[e] Removal
ADC 15	800	1500	0.62	1500	69	0.782	23	1.1	8
ADC 16	800	1500	1.03	1500	73.5	0.729	29	1.1	7
ADC 17	800	1500	1.03	1500	75	0.755	26	1.13	5
ADC 18	800	1500	1.03	1500	76	0.72	29	1.13	5
ADC 19	700	500	1.03	1500	81.5	0.782	23.4	1.12	6
ADC 20	700	500	1.03	1500	83.0	0.778	23.8	1.12	6
ADC 21	700	500	1.03	1500	84.5	0.80	23.6	1.14	4
ADC 22	700	500	1.545	1500	90.5	0.773	24.2	1.11	7
ADC 23	700	500	1.545	1500	92.5	0.762	25.3	1.15	3
ADC 24	700	500	1.545	1500	94.5	0.803	21.3	1.1	8
ADC 25	700	500	0.62	1500	97.5	0.812	20.4	1.09	8
ADC 26	700	500	0.62	1500	98.5	0.846	17.1	1.04	13
ADC 27	700	500	0.62	1500	99.5	0.831	18.6	1.08	9
ADC 28	700	500	1.03	1500	103.5	0.72	29.4	1.08	9

TABLE XXXI (Continued)

Sample Number	Temp[a] (F)	Pressure (psig)	Space Time[b] (Volume hrly)	Hydrogen (SCF/BBL)	Hours[c] on oil	%S[d]	%S[e] Removal	%N[d]	%N[e] Removal
ADC 29	700	500	1.03	1500	104.5	0.73	28.5	1.14	4
ADC 30	700	500	1.03	1500	105.5	0.77	24.5	1.19	-

[a] Nominal Reactor Temperature
[b] This is a volume hourly space time (volume of catalyst/volume of oil per hour)
[c] Total hours which the catalyst has been contacted with oil at reaction conditions.
[d] Percent of sulfur on nitrogen in liquid product.
[e] % Removal = (fraction in feed less fraction in product)/(fraction in feed.)

APPENDIX D

STANDARD DEVIATIONS OF SULFUR AND NITROGEN ANALYSES

Tables XXXII through XXXV give analyses of sulfur and nitrogen on a large number of samples of Synthoil and raw anthracene oil. An estimate of standard deviation was found from sample variance by using the following equation (72):

$$s^2 = \frac{1}{n} \quad \Sigma \ (x - \bar{x})^2$$

where

s^2 = sample variance

n = number of independent observations

x = independent observations of variance

$\bar{x}$ = mean of the x

$\sigma^2 = \frac{n}{n-1} s^2$

and

σ^2 = unbiased estimate of the variable

σ = unbiased estimate of standard deviation

TABLE XXXII

NITROGEN ANALYSIS OF RAW ANTHRACENE OIL

x	$(x-\bar{x})$	$(x-\bar{x})^2$	$\Sigma(x-\bar{x})^2$
0.98	0.055	0.0038	
1.08	0.097	0.0094	0.0132
1.08	-0.037	0.00136	0.01456
0.962	-0.037	0.00136	0.0159
1.12	0.08	0.0064	0.022
1.046	-0.077	0.0059	0.0282
1.047	0.0035	0.000012	0.0282
1.07	-0.005	0.000025	0.0282
1.02	-0.027	0.000072	0.0283
1.05	0.022	0.00048	0.0288
1.06	-0.0075	0.000056	0.02886
0.974	-0.0175	0.0003	0.02916
0.964	0.068	0.0046	0.03376

$\bar{x} = 1.034$

$\sigma^2 = \frac{0.03376}{12} = 0.0028$

Standard Deviation $\sigma = \pm 0.053$

Accuracy = $\pm$ 5.1%

TABLE XXXIII

NITROGEN ANALYSIS OF SYNTHOIL-1

x	$(x-\bar{x})$	$(x-\bar{x})^2$	$\Sigma(x-\bar{x})^2$
1.27	0.079	6.2×10^{-3}	
1.235	0.044	1.93×10^{-3}	8.13×10^{-3}
1.167	-0.023	5.29×10^{-4}	8.659×10^{-3}
1.155	-0.035	1.22×10^{-3}	9.88×10^{-3}
1.11	-0.08	6.4×10^{-3}	16.28×10^{-3}
1.14	-0.05	2.5×10^{-3}	18.78×10^{-3}
1.12	-0.07	4.9×10^{-3}	23.68×10^{-3}
1.188	-0.002	4.0×10^{-6}	23.683×10^{-3}
1.24	-0.049	2.4×10^{-3}	26.083×10^{-3}
1.22	-0.029	8.4×10^{-4}	26.923×10^{-3}
1.25	-0.059	3.48×10^{-3}	30.403×10^{-3}

$\bar{x} = 1.19$

$\sigma^2 = \frac{0.034}{10} = 0.0034$

Standard Deviation $\sigma = \pm 0.058$

Accuracy = $\pm$ 5.1%

TABLE XXXIV

SULFUR ANALYSIS OF RAW ANTHRACENE OIL

x	$(x-\bar{x})$	$(x-\bar{x})^2$	$\sum(x-\bar{x})^2$
0.467	0.004	0.16×10^{-4}	
0.47	0.001	0.01×10^{-4}	0.17×10^{-4}
0.472	0.002	0.04×10^{-4}	0.21×10^{-4}
0.470	0.001	0.01×10^{-4}	0.22×10^{-4}
0.477	0.006	0.036×10^{-4}	0.256×10^{-4}
0.478	0.007	0.049×10^{-4}	0.305×10^{-4}
0.468	0.003	0.09×10^{-4}	0.395×10^{-4}

$\bar{x} = 0.471$

$$\sigma^2 = \frac{0.039\times10^{-4}}{6} = 0.0658\times10^{-4}$$

Standard Deviation $\sigma = 0.0025$

Accuracy = $\pm$ 0.53 percent

TABLE XXXV

SULFUR ANALYSIS OF SYNTHOIL-1

x	$(x-\bar{x})$	$(x-\bar{x})^2$	$\Sigma(x-\bar{x})^2$
1.063	0.042	1.76×10^{-3}	
1.049	0.028	0.784×10^{-3}	2.544×10^{-3}
1.055	0.034	1.156×10^{-3}	3.7×10^{-3}
1.072	0.051	2.6×10^{-3}	6.3×10^{-3}
1.044	0.023	0.529×10^{-3}	6.829×10^{-3}
0.938	-0.083	6.889×10^{-3}	13.718×10^{-3}
1.135	0.114	12.996×10^{-3}	26.714×10^{-3}
0.94	-0.081	6.56×10^{-3}	33.274×10^{-3}
1.01	-0.011	0.12×10^{-3}	33.395×10^{-3}
0.987	-0.034	1.156×10^{-3}	34.55×10^{-3}
0.984	-0.037	1.369×10^{-3}	35.95×10^{-3}
0.974	-0.047	2.2×10^{-3}	38.12×10^{-3}
1.016	-0.005	0.025×10^{-3}	38.145×10^{-3}
1.027	0.006	0.036×10^{-3}	38.181×10^{-3}

$\bar{x} = 1.021$

$\sigma^2 = \frac{0.03818}{13} = 0.00293$

Standard Deviation $\sigma = \pm 0.054$

Accuracy = $\pm$ 5.3%

APPENDIX E

PORE SIZE DISTRIBUTION CURVES

Figures 49 and 50 give the pore size distribution and pore volume curves for the monolith support. These curves are drawn on the basis of the porosimeter analysis provided by the vendor. Table 36 gives data calculated for plotting the above curves. Following equation (19) was used in these calculations.

$$\text{Radius, R} \quad (^{o}\text{A}) = \frac{8.75 \times 10^{5}}{p(\text{psi})}$$

Figures 49 and 50 also give similar curves for the Nalcomo 474 catalyst. These are taken from previous studies (26,28).

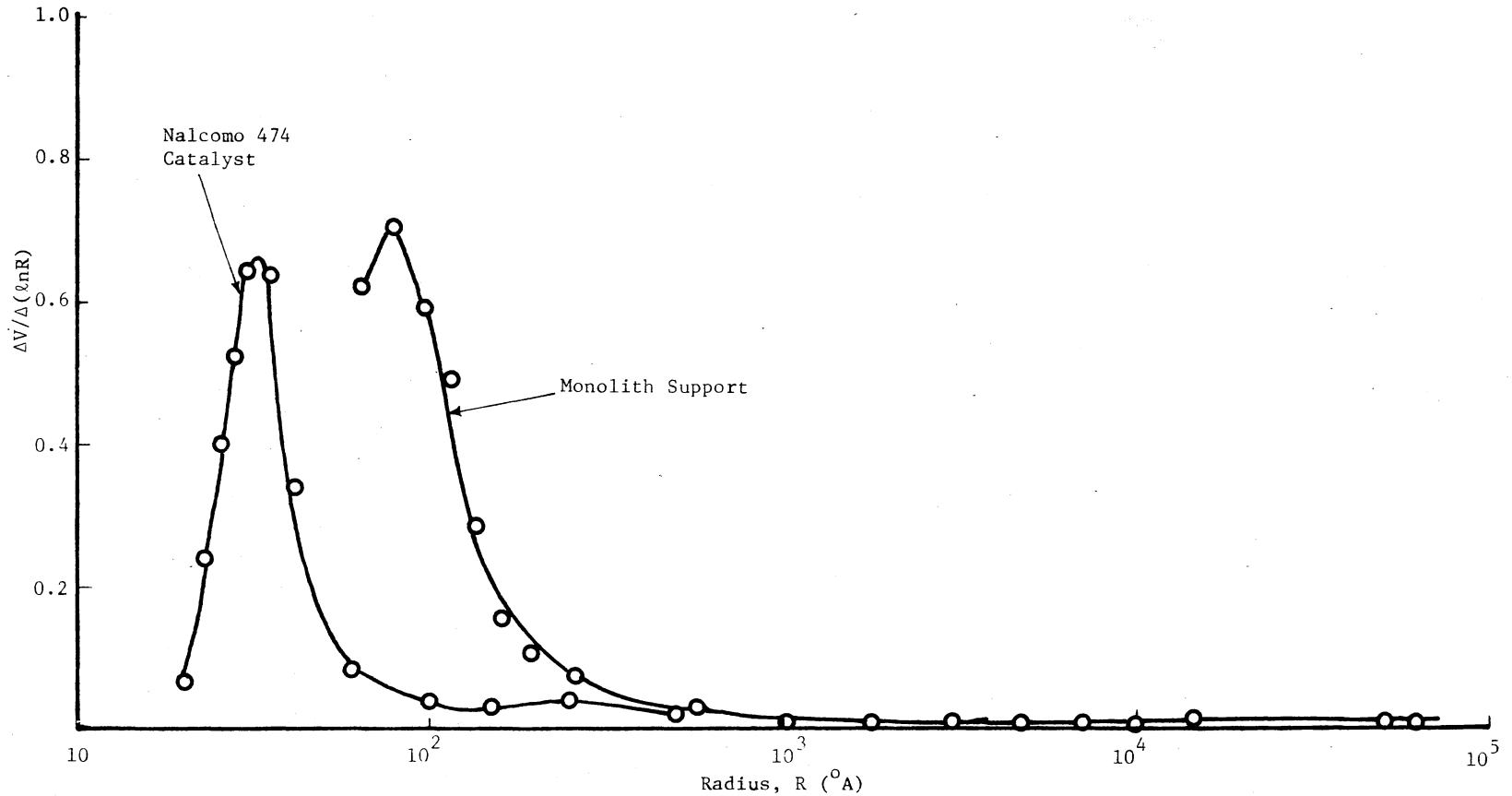

Figure 49. Catalysts Pore Size Distribution

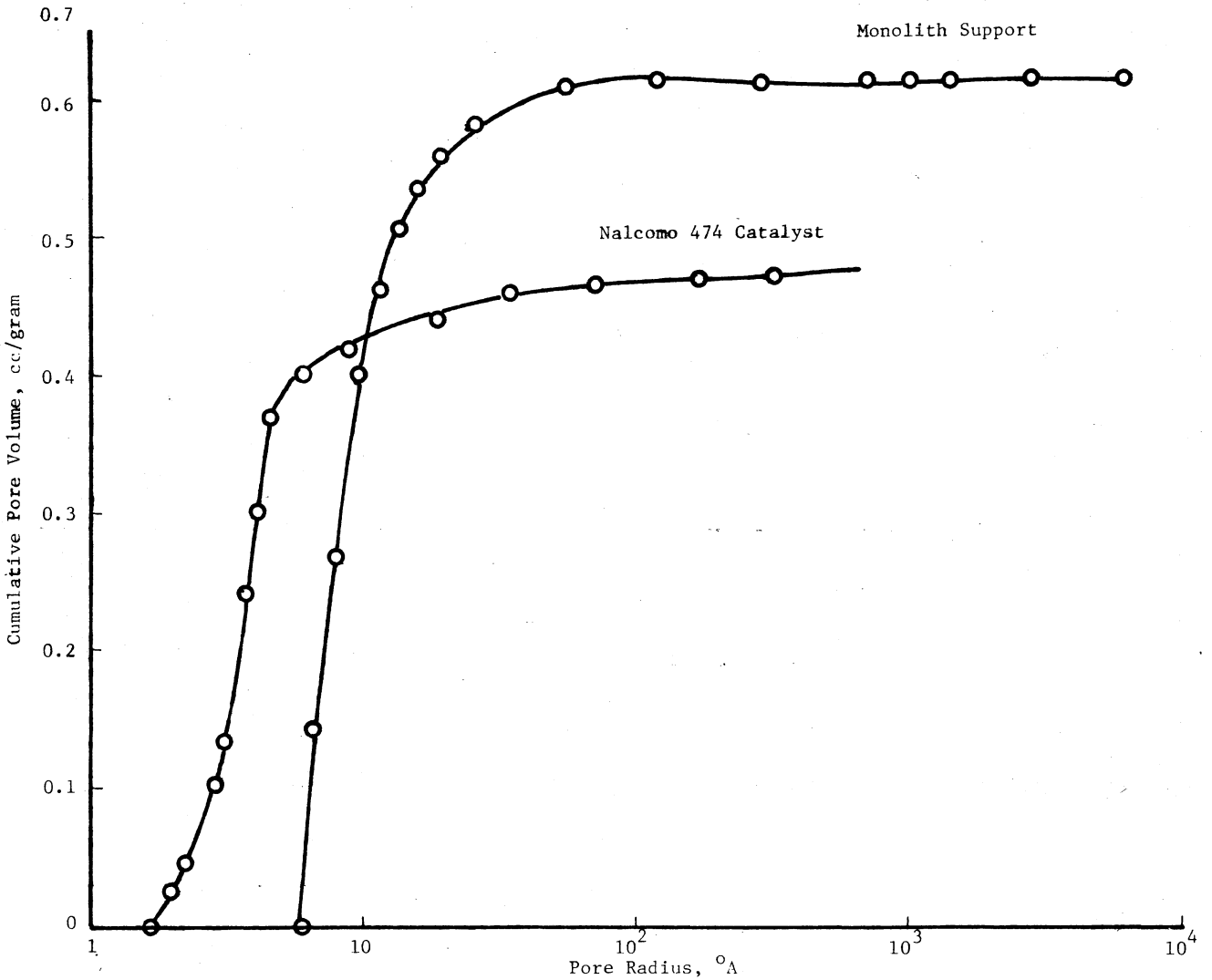

Figure 50. Dependence of Pore Volume on Pore Radius

TABLE XXXVI

CALCULATIONS FOR PORE SIZE DISTRIBUTION CURVE

v Cummulative	Δv	R	ln R	Δ ln R	$\frac{\Delta v}{\Delta \ln R}$
0.62		8.1×10^4	11.3		
	0.002			0.66	0.003
0.618		4.2×10^4	10.64		
	0.003			0.89	0.0033
0.615		1.722×10^4	9.75		
	0.001			0.35	0.0028
0.614		1.235×10^4	9.40		
	0.0			0.332	0.0
0.614		8.68×10^3	9.068		
	0.0			0.468	0.0
0.614		5.44×10^3	8.600		
	0.001			0.27	0.0037
0.613		4.15×10^3	8.33		
	0.0			0.89	0.0
0.613		1.71×10^3	7.44		
	0.001			0.68	0.00147
0.612		8.65×10^2	6.76		
	0.034			1.09	0.031
0.578		2.90×10^2	5.670		
	0.02			.286	0.07
0.558		2.18×10^2	5.386		
	0.023			0.224	0.102
0.535		1.74×10^2	5.160		
	0.029			1.984	0.152
0.506		1.45×10^2	4.976		
	0.044			0.156	0.282
0.462		1.24×10^2	4.820		
	0.063			0.13	0.484
0.399		1.09×10^2	4.69		

TABLE XXXVI (Continued)

v Cummulative	Δv	R	ln R	Δ ln R	$\frac{\Delta v}{\Delta \ln R}$
	0.132			0.224	0.59
0.267		0.87×10^2	4.466		
	0.126			0.179	0.70
0.141		0.728×10^2	4.287		
	0.141			0.227	0.62
0.0		0.58×10^2	4.060		

VITA

Dalip Singh Soni

Candidate for the Degree of

Master of Science

Thesis: A COMPARISON OF THE DESULFURIZATION AND DENITROGENATION ACTIVITIES OF MONOLITH ALUMINA IMPREGNATED WITH COBALT AND MOLYBDENUM AND NALCOMO 474 CATALYST

Major Field: Chemical Engineering

Biographical:

Personal Data: Born in Mighiana (Punjab), India, October 14 1944 to Nand Kaur and S. Nihal Singh.

Education: Attended Khalsa High School at Amritsar, India; received the degree of Bachelor of Science, physical sciences, from Punjab University, Chandigarh, India, in June, 1963; received the degree of Bachelor of Science in Chemical Engineering from Punjab University, Chandigarh, India, July, 1974. Completed the requirements for the degree of Master of Science in Chemical Engineering at Oklahoma State University in July, 1977.

Professional Experience: Foreman, Shriram Chemical Industries, Kota, India, 1963 - 1970; Engineering Traineee, Gujarat Fertilizers and Chemicals, Baroda, India, summer 1973; Process Design Engineer, Chemical and Metallurgical Design Co., New Delhi, India, March, 1975 to August, 1975.

Membership of Professional Societies: American Institute of Chemical Engineers.